

**PROOF OF CONCEPT DESIGN FOR PRECISE SINGLE DIMENSION
POSITION DETERMINATION USING PASSIVE RFID**

by

Timothy D. Carey

BS, University of Pittsburgh, 2004

Submitted to the Graduate Faculty of
The School of Engineering in partial fulfillment
of the requirements for the degree of
Master of Science

University of Pittsburgh

2006

UNIVERSITY OF PITTSBURGH
SCHOOL OF ENGINEERING

This thesis was presented

by

Timothy D. Carey

It was defended on

May 9, 2006

and approved by

Steven Levitan, John A. Jurenko Professor, Department of Electrical and Computer Engineering

Heung No Lee, Assistant Professor, Department of Electrical and Computer Engineering

Joseph W. Schaad, Senior Consulting Engineer - EMC, Union Switch & Signal

Thesis Co-Advisor: James T. Cain, Professor,

Department of Electrical and Computer Engineering

Thesis Co-Advisor: Marlin H. Mickle, Nickolas DeCecco Professor,

Department of Electrical and Computer Engineering

Copyright © by Timothy D. Carey

2006

**PROOF OF CONCEPT DESIGN FOR PRECISE SINGLE DIMENSION
POSITION DETERMINATION USING PASSIVE RFID**

Timothy D. Carey, MS

University of Pittsburgh, 2006

Position determination in RFID systems is a very useful aspect in tracking and managing items, to which a tag device is attached. Knowing the precise location of an item, relative to its environment, allows accurate mapping and control of the item with respect to those people, or things, that use the item's services. Current methods employ zone based localization, triangulation, or tag response time calculation. These methods are not very accurate, and are all reader side solutions. A tag side solution has been developed at the University of Pittsburgh to precisely determine the position of a tag, or reader, using passive RFID technology. Using the electromagnetic field intensity created by a reader, a tag that passes through this field will experience more excitation when parallel to and at the center of the field. Translating this action into DC voltage, a bell shaped voltage curve is apparent. Identifying the peak of this curve, therefore, directly relates to identifying the moment when the tag and reader are parallel and centered. Transmission of an ID, or location, at that moment, then, precisely describes its position. With the described motion in a known, single dimension, the item can be controlled to an even greater degree. One application is that of unmanned transit control. Using multiple tags, a transit car can be slowed and precisely stopped at an approaching station platform. The research contained within proves the existence of the voltage peak, develops an algorithm to find the peak, and creates a tag that can transmit the position ID using harvested RF energy.

TABLE OF CONTENTS

PREFACE	XII
1.0 INTRODUCTION	1
1.1 BACKGROUND	3
1.2 CURRENT RFID SOLUTIONS	5
1.3 PROBLEM STATEMENT	7
1.4 PASSIVE COUPLING THEORY	8
1.5 REQUIREMENTS AND SPECIFICATIONS	12
1.5.1 Overview	12
1.5.2 System Functionality	12
1.5.3 Phase I: Proof of Concept	13
1.5.4 Phase II: Beta Prototype	14
2.0 STAGE 1: GETTING STARTED	15
2.1 THE SYSTEM	15
2.2 PROBLEM ANALYSIS	18
2.2.1 Tag Components	18
2.2.2 System Motion	19
2.2.3 System Power	20
2.3 SYSTEM DESIGN	21
2.3.1 Tag Solution	21
2.3.2 Temporary Reader Solution	23
2.4 TESTING AND INTEGRATION	25
2.4.1 Tag Testing	25
2.4.2 Motion Testing	27
2.4.3 Power Testing	28

2.5	RESULTS	29
2.5.1	Tag A Testing Results.....	29
2.5.2	Train Motion Testing Results	31
2.5.3	TI Power Testing Results	31
2.5.4	Conclusion	33
3.0	STAGE 2: VOLTAGE CURVE VERIFICATION.....	34
3.1	TAG ANTENNA DESIGN.....	34
3.1.1	Antenna Design Method.....	34
3.1.2	Antenna Simulations.....	36
3.1.3	Antenna Simulation Inductance Results.....	40
3.1.4	Verification of Simulation Results.....	40
3.2	VOLTAGE CURVE METHOD.....	42
3.2.1	Method Devised.....	42
3.2.2	Tag Design	43
3.2.3	Testing Procedure	48
3.2.4	Voltage Curve Results	49
4.0	STAGE 3: TAG RANGE INCREASE.....	52
4.1	NEW READER SOLUTION.....	52
4.1.1	Reader Design.....	53
4.1.2	Reader Verification.....	53
4.2	TUNING FOR DISTANCE	55
4.2.1	Tuning Theory.....	55
4.2.2	Antenna-Circuit Analysis.....	57
4.2.3	Tag Design	58
4.2.4	Tag Distance Testing.....	60
4.2.5	Tuning Results.....	61
5.0	STAGE 4: PEAK DETERMINATION ALGORITHM.....	63
5.1	COMMUNICATION SOLUTION	63
5.1.1	Tag Side Communication.....	64
5.1.2	Reader Side Communication	65
5.2	CIRCUIT DEVELOPMENT.....	66

5.2.1	Voltage Regulation.....	66
5.2.1.1	The Voltage Regulator	66
5.2.1.2	The Voltage Divider.....	67
5.2.2	Transmitter Circuit Design.....	68
5.2.3	Transmitter Testing.....	73
5.2.4	Transmitter Results	76
5.3	PEAK ALGORITHM SOLUTION	80
5.3.1	Peak Algorithm Overview.....	80
5.3.2	Peak Algorithm Design.....	83
5.3.3	Algorithm Testing Method.....	88
5.3.4	Signal Noise Analysis	90
5.3.5	Algorithm Simulation	93
5.3.6	Algorithm Design Results.....	95
5.3.6.1	Peak Algorithm Results.....	95
5.3.6.2	Signal Analysis Results.....	96
5.3.6.3	Algorithm Simulation Results	97
6.0	STAGE 5: SPEED INCREASE	101
6.1	HIGH SPEED PASS OVER SYSTEM.....	101
6.2	TAG DESIGN CONSIDERATIONS.....	104
6.3	SPEED TESTING.....	106
6.4	SPEED RESULTS	107
7.0	CONCLUSION.....	109
7.1	PHASE II OPTIMIZATIONS.....	110
7.2	PHASE II CONSIDERATIONS	111
7.3	FUTURE CONSIDERATIONS	111
	APPENDIX A.....	112
	APPENDIX B	115
	APPENDIX C.....	117
	APPENDIX D.....	119
	BIBLIOGRAPHY.....	121

LIST OF TABLES

Table 1: Approximate TI System Distance and Speed Measures.....	32
Table 2: Possible EEPROM Writes Versus Speed	46
Table 3: Possible LC Tuning Values For Tag B L Matching Network	58
Table 4: Tag B Tuning Elements and Results	62

LIST OF FIGURES

Figure 1: High Level RFID Diagram.....	2
Figure 2: Inductively Coupled Loop Transposition Distance Determination.....	4
Figure 3: Basic Passive RFID Inductive Antenna Coupling System.....	8
Figure 4: Reader Antenna Electromagnetic Flux Lines and Maximum Tag Excitation.....	9
Figure 5: The induced, Bell Shaped Voltage Curve.	10
Figure 6: Tag and Reader Antenna Electromagnetic Flux Line Interaction.	11
Figure 7: Unmanned Train Application.....	12
Figure 8: High Level System Diagram.....	16
Figure 9: Stage 1 Block Diagram.....	17
Figure 10: Tag A Design and Reader A Option.	22
Figure 11: Tag A and Reader A PCB Design, Respectively.	24
Figure 12: Tag A-Reader A RF Power Test Setup.	26
Figure 13: A PIC Program Written to Test Tag RF Powering.	27
Figure 14: Texas Instruments Passive HF Tag-It Tags.....	28
Figure 15: Tag A Voltage Doubler Tests.....	29
Figure 16: RF Powered Blinking LED Load Test.	30
Figure 17: TI Reader, Inside Antenna, RS232 Serial Connection, and Power Supply.....	32
Figure 18: Sonnet Spiral Antenna Design Check List.....	36
Figure 19: Sonnet Simulation Software Tag Antenna Designs (clockwise A, B, D, C).	37
Figure 20: Sonnet Inductance Plot of Tag A Antenna Simulation.	38
Figure 21: Sonnet Inductance Plot of Tag B Antenna Simulation.....	38
Figure 22: Sonnet Inductance Plot of Tag C Antenna Simulation.....	39
Figure 23: Sonnet Inductance Plot of Tag D Antenna Simulation.	39

Figure 24: LCR Meter Inductance Measure of 1x1 Inch Tag A.....	41
Figure 25: LCR Meter Inductance Measure of 4x2 Inch Tag B.....	41
Figure 26: Model Train 1 mph Setup, With Reader Antenna Under Table.....	42
Figure 27: Tag Circuit With Resistive Load Incorporated.....	44
Figure 28: Tag A Battery Power PCB Design.....	45
Figure 29: Tag B Battery Power PCB Design.....	46
Figure 30: A PIC Program Written to Capture the Voltage Curve.....	47
Figure 31: Tag A Voltage Curve, Captured at 7 Inches Away From Reader Antenna.....	49
Figure 32: Tag B Voltage Curve, Captured at 13 Inches Away From Reader Antenna.....	50
Figure 33: Oscilloscope Capture of the Interference Pattern.....	51
Figure 34: Tag B, Amp Powered, Voltage Curve, Captured at a 10 Inch Distance.....	54
Figure 35: Basic L Matching Network Between Antenna and Circuitry.....	56
Figure 36: Tag B v1 Circuit Design For RF Powered Tuning.....	59
Figure 37: Tag B v1 RF Powered, Tuning PCB Design.....	60
Figure 38: RF Powered Tuning Test Setup.....	61
Figure 39: Intermediate Circuit Design Highlighting Regulation.....	68
Figure 40: Tag B v3 Circuit Prototype Design For RF Transmission.....	70
Figure 41: Tag B v3 PCB Design with Transmitter Elements.....	71
Figure 42: Tag B v3 PCB Design, Regulator Detailed.....	71
Figure 43: Tag B v3 PCB Design, Transmitter Detailed.....	72
Figure 44: Circuitry Side Photo of Tag B v3 Design.....	72
Figure 45: Spiral Antenna Side Photo of Tag B v3 Design.....	73
Figure 46: LINX Transmitter Test PCB.....	74
Figure 47: LINX Transmitter Test Setup.....	74
Figure 48: RF Powered, Tag B Transmission Setup.....	75
Figure 49: A PIC Program Written to Transmit a Character.....	76
Figure 50: Oscilloscope Capture of Failing RF Transmission.....	77
Figure 51: Oscilloscope Capture of Successful RF Transmission.....	78
Figure 52: Oscilloscope Capture of a Rapid Succession of RF Transmission.....	79
Figure 53: Peak Algorithm Pseudo Code.....	81
Figure 54: Tag Movement Through Reader Field and the Voltage Curve.....	82

Figure 55: Noise Example with Inherent Delay.	83
Figure 56: Full Voltage Curve Oscilloscope Capture at 1 mph.....	84
Figure 57: Peak Algorithm Program Flow Chart.....	85
Figure 58: The PIC Program Written to Transmit the Voltage Peak.....	87
Figure 59: 1 mph Tag B Peak Determination Test Setup.	88
Figure 60: 1 mph Tag B Peak Transmission Test Setup.....	89
Figure 61: Porting a Voltage Curve from Scope to Excel to MATLAB.	90
Figure 62: MATLAB 1 mph Voltage Curve FFT Analysis.....	91
Figure 63: FFT Analyzer Images of the Voltage Curve.	92
Figure 64: MATLAB 1 mph Voltage Curve Butterworth Order 2 Filter.	93
Figure 65: MATLAB Script Segment For Algorithm Simulation.....	94
Figure 66: Oscilloscope Capture of a Peak Transmission.	95
Figure 67: MATLAB 1 mph Voltage Curve Filter Delay Comparison.....	97
Figure 68: Noisy Voltage Curve Peak Algorithm Simulation, NVar 35.	99
Figure 69: MATLAB Noisy Voltage Curve Peak Algorithm Simulation, NVar 45.	99
Figure 70: MATLAB Noisy Voltage Curve Peak Algorithm Simulation, NVar 95.	100
Figure 71: MATLAB 1 mph Voltage Curve, Filtered Data, Peak Algorithm Simulation.....	100
Figure 72: The HSPO System Design.	102
Figure 73: The Tag Base Assembly with PCB Structure.	103
Figure 74: High Speed Test Setup.	106
Figure 75: Oscilloscope Capture of Tripped IR Sensors.	107
Figure 76: RF Transmission Captured by Tektronix Spectrum Analyzer.	108

PREFACE

I would like to extend my thanks to my advisors, Dr. Mickle and Dr. Cain, who have afforded me this great opportunity to become a master of RFID technology, and to experience the immense satisfaction of completing such a challenging project. I would also like to thank Leo Mats and Kevin Wahila, my sounding board, who continually helped me to increase my own resonance. Finally, I'd like to express my thanks to Joe Schaad, of US&S, for his thoughtful cooperation in developing this device.

1.0 INTRODUCTION

Radio Frequency Identification (RFID) technology has been utilized since at least the early 1940's, when it was used to identify "friendly" planes during World War II. Development of the technology has been slow and steady, until recently, and has seen the advent of active, passive, and semi passive systems. As technology advanced and the size of the transistor shrank, the cost of using RFID became more reasonable. Organizations that track and manage inventory began looking at RFID as an improved bar code concept, and a real time tracking solution. The potential benefits of RFID include: non line of sight serial data, reduced human intervention, higher "inventory" throughput, real time information flow, and increased "inventory" security [1]. The current RFID revolution began when the three largest supply chain organizations set mandates to incorporate RFID into their distribution centers, and forced their top 100 suppliers to comply. Walmart, the Department of Defense, and Target have incited a huge wave of new research, and the creation of a widely expanded RFID industry. An RFID system has three main components: a tag, a reader, and the "consumer". Figure 1 is a basic diagram and shows its high level interaction. A reader communicates with a tag using radio frequency and queries its information. The tag can store any information, but typically stores a unique number that identifies it from all other tags. The tag sends its information to the reader and then the reader does some processing, such as updating the tracking status. It will then communicate with the outside world, which is typically a wired link to a database, and subsequently relay its newly acquired information. Some tag side options available are active, semi-active, and passive tags. Active tags use a battery for power and transmission, semi-active tags use a battery also, but only for transmissions or memory backup, and passive tags use energy harvested from the reader RF wave to power itself and transmit its ID.

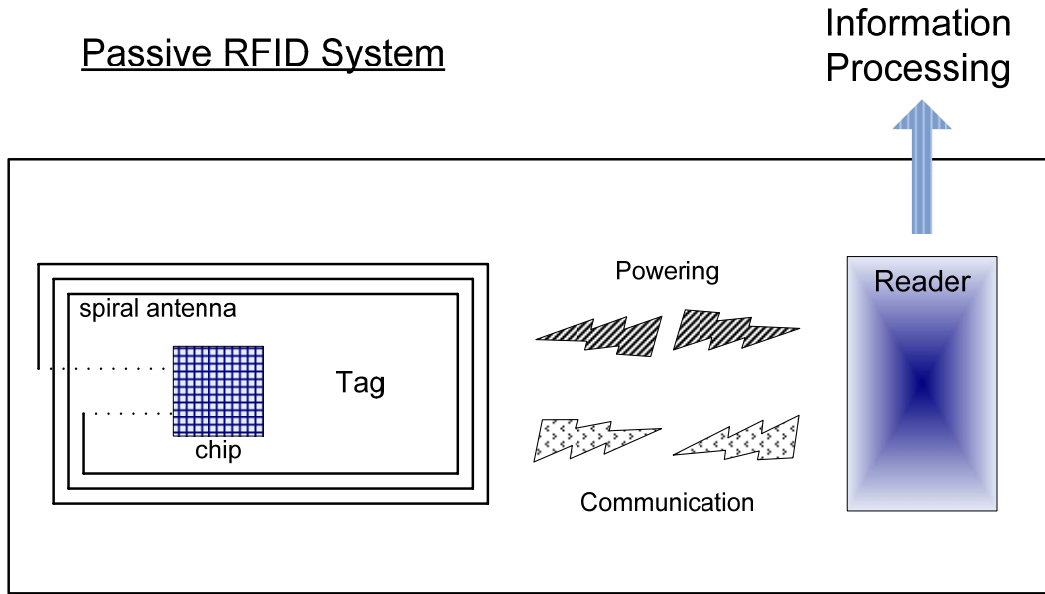


Figure 1: High Level RFID Diagram.

With RFID in the headlines recently, and it becoming a truly viable technology, many different industries are looking at business solutions involving RF. One industry that is seeking an RFID solution is the transit industry. Unmanned transit systems, for instance, present a unique problem to system control, and could benefit greatly from “human free” tracking. In this case, being able to determine the position of the “item” would allow a computerized controlling system to precisely manage the flow. An “RFID in a box” solution does not exist, but the wide variety of available technology and devices typically allow a solution to be developed. This section will review the background of the automated transit industry, one company’s solution, the problems with it, some evolving RFID solutions, and will present the problem statement of this thesis, with a discussion of the theory of inductive coupling.

1.1 BACKGROUND

The idea behind automation in the transit industry is the great potential for increased safety and reduced operating costs. Computer based system control can monitor track conditions, monitor track utilization, and monitor status conditions, all of which can have a positive affect on safety and cost. At the vehicle level, on a train or tram for instance, it can lead to autonomous operation and unmanned trains. Among other problems, however, unmanned transit systems require the additional ability to determine their position. To be able to start, regulate speed, and stop properly, the unmanned train must continually track its location. Currently, several different systems are employed together to handle the full range of issues. Some of these issues are: the wide range of possible speeds, the varying precision required, and the various environmental conditions possible. To focus the problem, emphasis will be on stopping a train as it approaches a station platform.

As a train approaches a station platform, it must reduce its speed from around 50 mph to 0 mph. It must also precisely align its doors with the station platform and platform doors, if they exist. A current method of handling this series of events is a combination of two levels of communication: one to relay the physical track segment number, and another to identify a specific distance from the platform [2]. The second “communication” occurs inductively, by identifying null points between loop transpositions (Figure 2). A null point represents a fixed, known distance from that point to the station platform. This distance is used in conjunction with the first communication, which had transmitted speed limiting information. Together a braking profile is calculated and initiated. The stopping accuracy is approximately ± 11.8 inches.

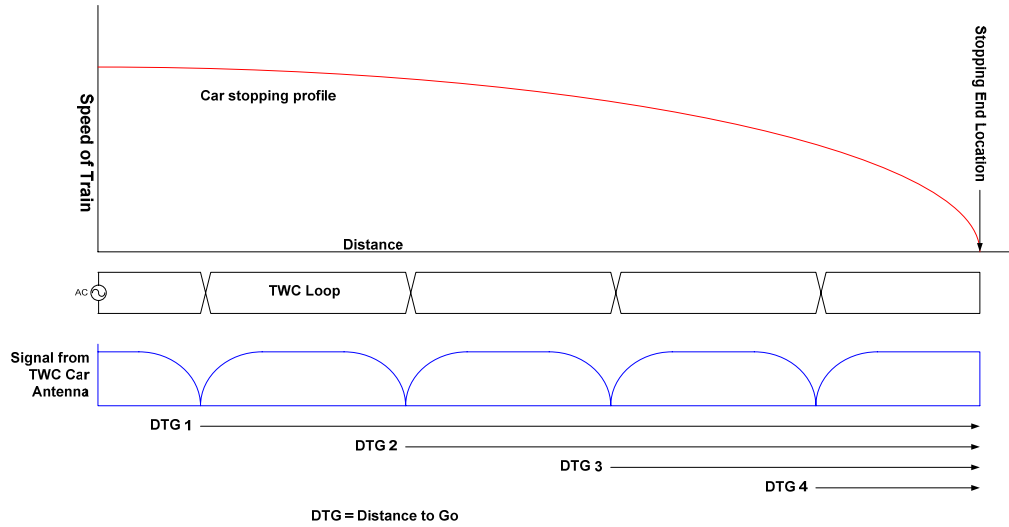


**Figure 2: Inductively Coupled Loop Transposition Distance Determination
(Reproduced by Permission of Union Switch & Signal)**

The problems and limitations of this system are due to the use of multiple communications, noise problems in the RF communication, the system's tuning requirements, and a lack of obtainable precision. Using multiple communications to determine position increases the risk of error and increases the complexity of the system, which also increases error probability. Reliability is as important as precision in this type of system. Environmental noise, due to the train and the surrounding materials, adversely affects communication by radiating into the transposition loops and significantly reducing the quality of the signal. The system uses a two frequency, FSK modulated transmission, with a 10 kHz bandwidth. In this system the loops must be tuned exactly, but it is extremely difficult to balance frequency versus bandwidth in these inductive loops. Finally, the accuracy of this method is simply not sufficient for ease of station alignment. The answer to these problems is being sought in an RFID type technology solution.

1.2 CURRENT RFID SOLUTIONS

Some typical RF localization solutions include triangulation, zone based methodology, and response time calculation. Each of these methods falls short for a reliable, accurate, precise position determination. Triangulation, for instance, is only moderately adequate for outdoor position determination, with a tolerance of approximately 1 meter [3]. It suffers from significant multipath signal propagation interference in indoor applications, however, and is therefore not very useful as a complete solution. It also requires three readers to perform the triangulation increasing the overall cost. Zone based localization is simply a method that identifies when a tag has entered the reader's read range. Knowing this, the system can track movement on a high level, but not precisely. Response time systems use the time it takes a tag to respond to a reader's query to determine how far away it is. Using this information, the reader will attempt to calculate the tag's position relative to its own. Because timing is the key factor, a high clocking rate is required for accuracy, which generally means using more complex circuitry and a battery. This solution also suffers from multipath problems, and is not an acceptable solution.

More specific RFID solutions have begun to address these problems and some to even focus on unmanned transit systems. Two companies, Amtech and Siemens, are developing RFID solutions to specifically address battery life, precise position determination, and to be able to perform at high speeds. Amtech's solution involves using higher frequencies, 915 MHz and 2.45 GHz, and a semi-active tag [2][4]. Using these frequencies allows for very fast communication and higher achievable speeds, but still requires a battery and has a shelf life limited to about 10 years. The system is said to perform the total communication in "milliseconds", at speeds of up to 100 mph. For reference, traveling at 100 mph, a tag will cross a 16 inch area in approximately 9 ms. As for precision, Amtech has narrowed the gap to ± 30 cm, approximately ± 12 inches. While this is a good improvement, it is hardly precise.

Siemens' solution is passive, using a 128 kHz frequency to power the tag [5]. This solves the "shelf life" problem, and these tags will undoubtedly last the lifetime of the transit system. In the reference there is no mention of obtainable speed, however, and the longer (slower) kilohertz wavelength may be a limiting factor. If this is the case, then two separate systems

would be needed to handle the braking, and complexity is increased. Further, position is achieved by having the tag transmit as soon as it has sufficient power; That is, as soon as the tag has harvested enough energy from the reader frequency. The tolerance is ± 15 cm, or about ± 6 inches. This is better, but is still not precise. There is no algorithm for determining the position; it is simply an extremely narrowed version of the zone based method. Lastly, the read distance between tag and reader is about 7 inches maximum and 6 inches nominal. This makes train to track clearance somewhat of an issue, and setup a little more complex. A typical train wheel is between 10 and 18 inches away from the track and railroad ties, and can wear as much as 2 inches between replacements [2].

A complete solution does not currently exist. Again, for this type of application, the system should be flexible enough to accommodate a wide range of speeds, flexible enough to handle the wear of the transit system and the distance between the train and tracks, it should have a life time that matches or exceeds the transit system, and, of course, should precisely determine the position of the train relative to a fixed marker and the station platform.

1.3 PROBLEM STATEMENT

While the ability of a reader-tag system to determine position, in a linear plane, applies to a broad scope of applications, this thesis explains the problem, and solution, as it applies to unmanned transit systems. The recent trend to adopt RFID, in product management roles, has made it possible for many industries that use computer-aided system automation to explore RFID technology application options. Union Switch and Signal (US&S) is such a company, and has teamed with the University of Pittsburgh to provided funding for RFID research. “US&S is a leading developer of Automatic Train Control (ATC) systems for all types of heavy and light rail transit properties” [6]. A precise, reliable, and cost effective method to control trains as they approach a station platform would increase the system safety and reduce operating overhead, sustaining growth in the unmanned transit sector. In this research, RF is examined for environmental suitability, antenna designs are explored for sufficient operating distance and passive powering capability, tag devices are designed for microcontroller integration, and algorithms are developed to determine a tag’s position relative to a reader. The objective is to be able to passively power a tag as it moves through a reader antenna field, determine when the tag is directly in the center of the reader, and transmit a position ID at that instant. The scope of the research involves developing a 5 level proof of concept model: (1) reach a passive powering and communication range of at least 10 inches, (2) confirm that, as a tag moves through the reader antenna field, a bell shaped voltage curve exists, (3) develop an algorithm to determine the peak voltage, (4) verify that the voltage translates into precise position determination, and (5) test the device at various speeds.

1.4 PASSIVE COUPLING THEORY

This body of work is based on the theory that, as an energy harvesting tag passes through a reader excited electromagnetic field, the induced voltage follows a bell shaped voltage curve. If the theory is correct and the peak is at the center of the reader antenna, then the position of the tag relative to the reader can be precisely determined. This section describes the basic physics of inductively coupled antennas, and explains why the bell shaped voltage curve should exist.

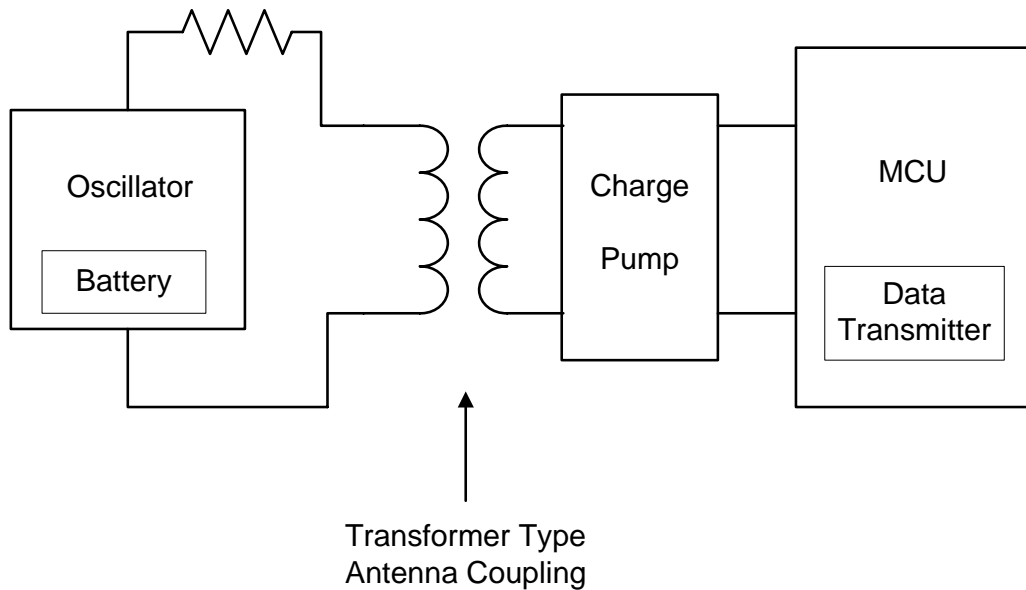


Figure 3: Basic Passive RFID Inductive Antenna Coupling System.

Figure 3 shows a high level view of a passive RFID system that is inductively coupled. The tag and reader essentially create a transformer [7][8]. The reader is given all the power it needs and, oscillating a specified frequency, it generates current through its antenna. The current flowing through the antenna produces an electromagnetic field, which is referred to as the near field in RFID terminology. As a tag moves through this field a voltage will be induced across the tag antenna coil that will in turn cause current to flow through the circuit [7]. A charge pump, or voltage doubler, is typically included to increase the voltage to a level that is sufficient

for elements, like the microcontroller, to operate. This voltage is used to power the device and communicate the tag's ID back to the reader. In this application, it will also be used to determine the peak voltage achieved, and thus identify the theoretical center of the reader antenna.

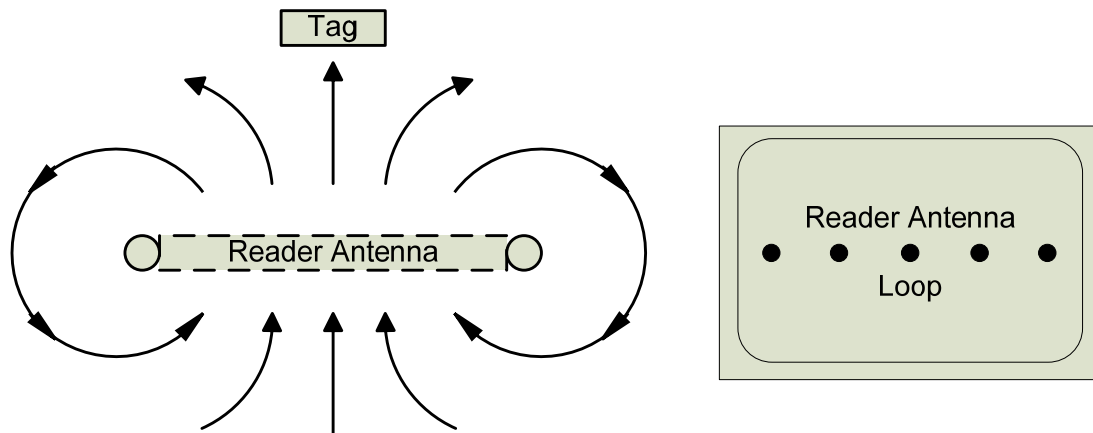


Figure 4: Reader Antenna Electromagnetic Flux Lines and Maximum Tag Excitation.

The electromagnetic field created by the reader forms flux lines that circle the antenna, as shown in Figure 4 [9]. The lines are determined by the amount of current flowing through the reader antenna and the shape and size of the antenna [7]. Because this electromagnetic flux is responsible for inducing the voltage in the tag, it can be shown that the orientation of the tag, or more specifically the tag antenna, is critical. For maximum excitation, the tag should be parallel and centered to the reader antenna, which makes the tag perpendicular to the flux lines [7]. As a tag moves through the field, the bending of the flux lines changes the tag's orientation to them; it is no longer ideal (perpendicular), and the induced voltage decreases (Figure 5) [9]. In terms of the antennas, it can simply be thought of as how much the two antennas overlap (Figure 6). When just one edge of each antenna is overlapping, the induced voltage is minimal. "Edge" is one length of the antenna. That is, if the antenna was cut in half so that one could look into the antenna conductors, then two sides of the antenna would be observable as in Figure 6. When two edges overlap, the induced voltage begins to increase steadily. This occurs until they are centered and directly overlapping, which is the point of the greatest coupling of flux lines and the highest induced voltage. And, as the tag moves the rest of the way through the field and past the other edge of the reader antenna, essentially the same occurs except for addition of some residual

flux linkages. Therefore, if the tag moves linearly and centered across the reader antenna, at the appropriate distance, the tag should realize a fairly typical bell shaped voltage curve. Figure 5 and 6 together demonstrate this relationship.

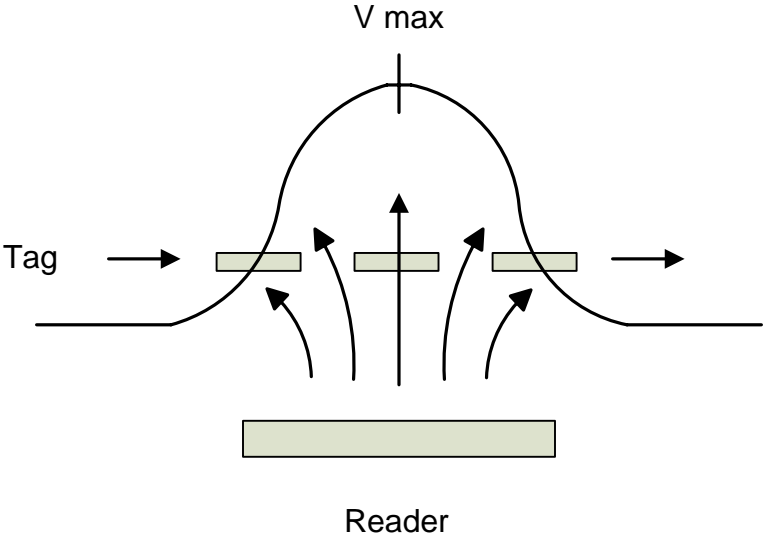


Figure 5: The induced, Bell Shaped Voltage Curve.

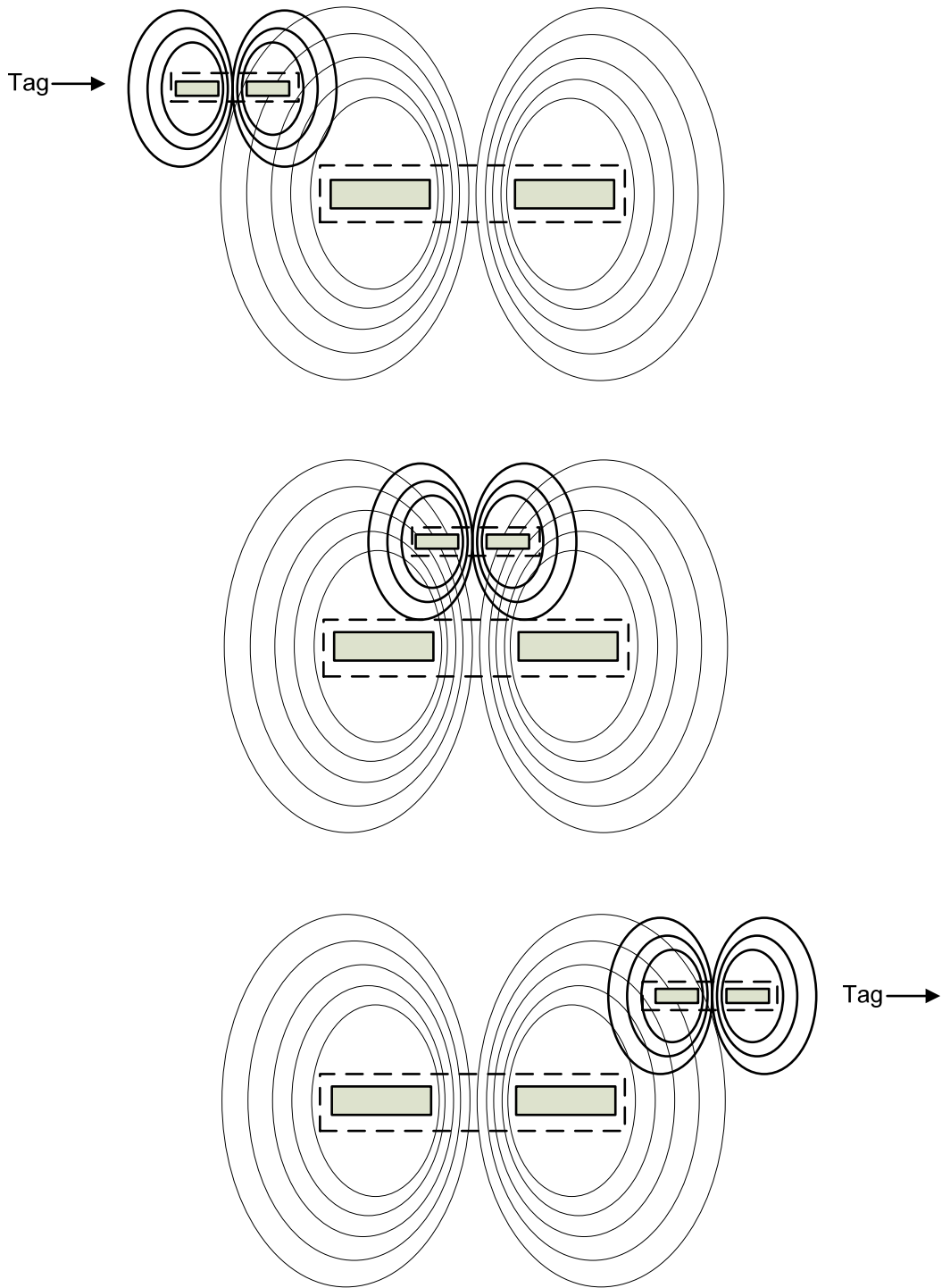


Figure 6: Tag and Reader Antenna Electromagnetic Flux Line Interaction.

1.5 REQUIREMENTS AND SPECIFICATIONS

This section defines the requirements for a product that addresses US&S's current position determination solution's limitations: noise interference, tuning difficulties, multiple communications required, and precision. It also defines the device in terms of functional and non-functional behavior.

1.5.1 Overview

The typical application is shown in Figure 7. As a train approaches the station platform, a series of track-embedded tags communicate their individual position to the reader, and the on-board controlling unit regulates the speed. At the station, the train will be precisely stopped at a predetermined point. This is critical in accomplishing tasks such as aligning the train doors with the station platform doors. The remainder of this section will describe the specific goal of the system.

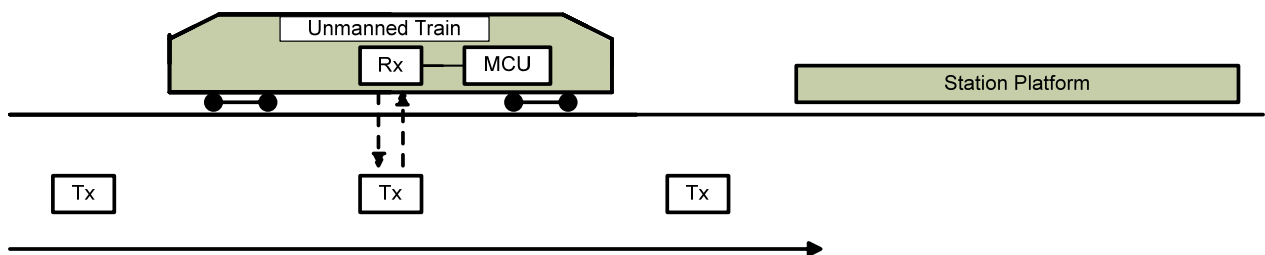


Figure 7: Unmanned Train Application

1.5.2 System Functionality

An ideal system is one that does not need a battery, and has a life time longer than the transit system. It can operate at high speeds, and works within the dimensions of the train. The

system is unaffected by noise and close proximity materials, especially the metal of the train. It will operate in a variety of environmental conditions. And, it reliably determines the precise position of the train.

To satisfy this set of general requirements, we must examine the operation of the train, define the environment, and consider device properties. Powering the system is a critical factor. To eliminate the battery and extend the life time of the tag, a passive RFID system is required. Therefore, this system will be inductively coupled, where the tag powers itself using energy harvesting techniques. The reader will be powered by the train, and be capable of producing at least 4 watts of power, determined and limited by FCC regulations.

A typical unmanned train operates between 0 and 80 mph, so the system must be able to handle this range of speeds. The tag must be mountable to a standard railroad tie, so its maximum length is 9 inches due to the width of the railroad ties. The train clearance is between 10 and 18 inches from the railroad ties, and so the system must be flexible enough to cover this read range. The reader antenna must be mountable to the underside of the train and be relatively unobtrusive. Size is not a big issue, though a minimalist approach will be used. The weights of the tag and of the reader are not critical aspects either, but these will also be kept to a minimum.

The passive tag communication must be able to deal with the reflectivity of the surrounding metal, which means that a frequency below the microwave range will be utilized. The circuit must be minimally affected by noisy conditions in the environment and within the circuit. Also, the system must operate worldwide, which means that the chosen frequency will be available everywhere.

It must also operate unaffected by water, snow, ice, and dirt. It must operate in temperatures ranging from -40°C to 85°C , vibration conditions of 5-20 Hz – 0.2” p-p and 20-200 Hz – 4.2g peak, and tolerate shock up to 10g.

It must be reliable and have a horizontal accuracy of ± 2 inches at slower speeds.

1.5.3 Phase I: Proof of Concept

The research and development of this system is separated into two phases: proving the feasibility of the product, and, provided the results of Phase I are positive, designing a prototype that meets the full specification. This is an effective strategy for designing this new product,

because it is based on theoretical concepts that should be validated prior to extensive work on the many system components.

The goal of Phase I is, thus, to develop a rapid prototype that proves the product to be commercially viable. While the system is comprised of a tag and reader, with its antenna, the focus is on tag device design, because it is the functionality of the tag that determines success. Areas of research include powering/communication frequencies, antenna design, circuit design, and development of an algorithm that finds the peak voltage.

Success is defined to be a PCB tag, discreet component solution that identifies the peak, and transmits an 8-bit value to a receiving device. Again, the reader is not the focus of the research, so off the shelf components are acceptable. The read range has to be at least 10 inches, however, and the system has to be successfully tested at different speeds. It is deemed satisfactory for initial testing to be between 1 and 10 mph. This last requirement means a separate system must be developed to be able to test the tag and reader interaction at various speeds, and be able to calculate that speed. The sections of this thesis labeled Stage 1 through Stage 5 detail the development of this prototype.

1.5.4 Phase II: Beta Prototype

Phase II will be dependent on the evaluation of the first prototype as a success by the University of Pittsburgh and US&S. While proof of concept may be achieved, the effort to meet the full specification must be considered. Again the goal is communication at speeds up to 80 mph, read distances of up to 18 inches, and reliability in real world environmental conditions.

The focus in this phase will be on optimizing the circuit and the tag-reader exchange. Possible areas of optimization will be tag antenna design, tag transmitter design, the reader design, and generated output power levels, which translate into specific voltage curve representations. The quality of the signal will be an area of research as well, because it will depend on the environmental conditions, the metal of the train, and perhaps the design of the tag circuitry.

2.0 STAGE 1: GETTING STARTED

In the development of this system, the first step is to create a design methodology, gain a complete understanding of the problem, and analyze and choose components for use in this application. Each stage in tag development contains a discussion of the design and related issues, a description of the testing methodology, and then an examination of the results obtained.

2.1 THE SYSTEM

The system described in the introduction consists of a reader and a tag. While the tag is the focus of this research, the reader is a vital part of the system and cannot be overlooked. Figure 8 shows a high level block diagram of the system. The reader, minimally, has an oscillating RF energy source and a receiver to capture the tag response. The tag is comprised of an antenna, tuning elements, a voltage doubler, a controller, and some method of transmission. Each of these areas is integrally connected to one another and makes the design process fairly challenging. For instance, if a top down approach is performed and analysis started with achievable distance, it would quickly be hindered by the fact that the actual circuit load is not yet known. Without the values of the circuit capacitance and resistance, the tuning elements can not be chosen for power matching with the antenna. If a bottom up approach is tried instead, it would be quickly hindered by the lack of knowledge about the overall system, e.g., the frequency that the reader is using and the communication scheme necessary. For this reason, a design-test-redesign iterative approach is required that combines the two methods. A high level description must be defined, but then the first problem identified must be resolved. Upon completion of the problem and obtaining the knowledge, the system must be reevaluated and the next problem

identified and solved. In this way the unknowns are eliminated one by one, and used to mold the device into its final form.

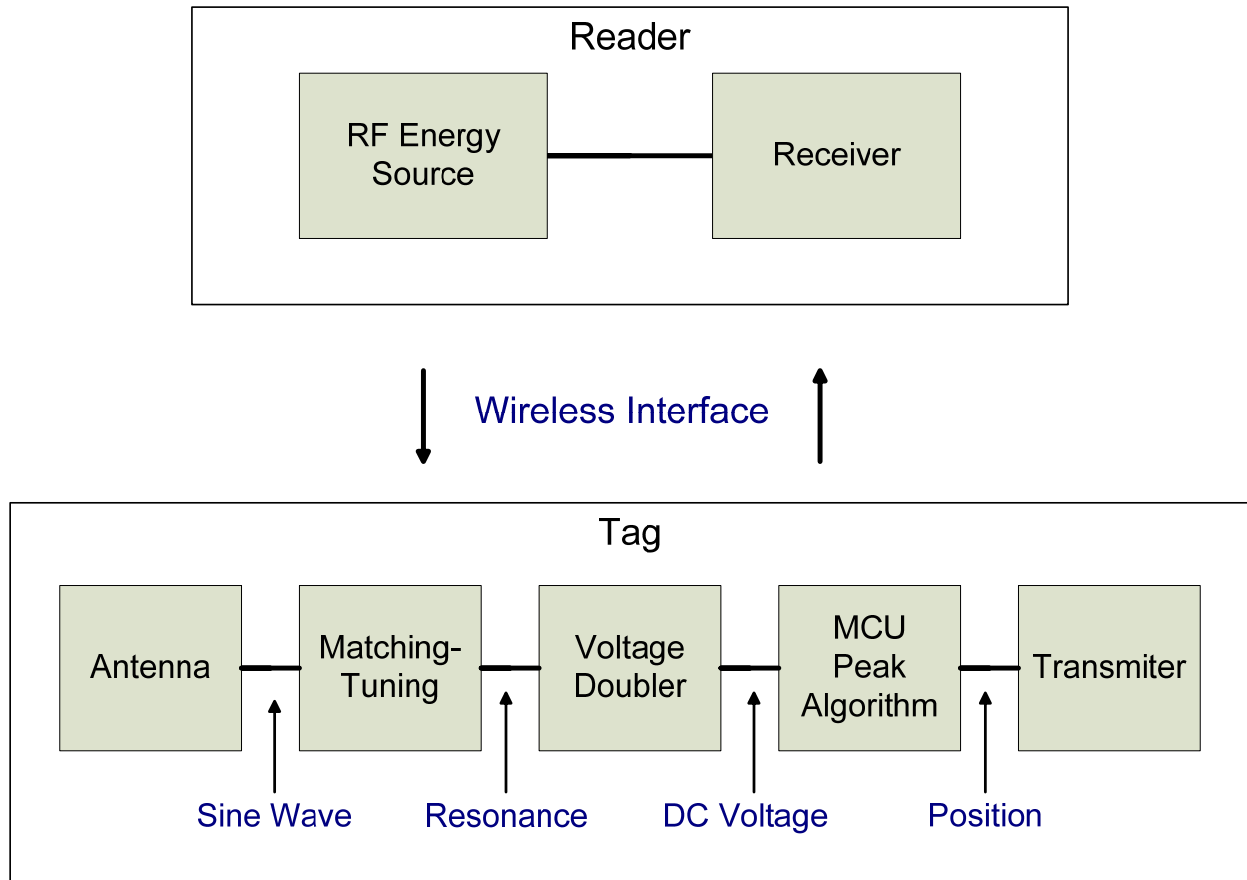


Figure 8: High Level System Diagram

The high level problems of the system are: powering, which is a function of the reader, movement of the tag past the reader, and choosing tag components, which is dependent upon the application and its environment. While all issues will be addressed, decisions will be based on the desire to create a working prototype.

Powering is essential, but because the final reader design is part of Phase II, an off-the-shelf product is sought. The product desired will allow continuous wave (CW) radiation, have adjustable power output, and use a standard communication protocol. The decision to purchase a reader, however, will be based on initial choices regarding the tag.

Single dimension movement is also required. The reader must move linearly, stably, and consistently across the tag. It must also be scalable, and allow for a variety of speeds to be reached. This problem is also quite involved, and while a system will be developed, high speed tag testing is a Phase II issue.

Tag design is the focus here, and several issues must be addressed. The frequency that the system will use is the initial concern. This affects both the tag and reader, and must be chosen based on the application. As is shown in Figure 8 above, there are several areas that need to be addressed, but for initial development the areas are the antenna, the voltage doubler, and the circuit or load (Figure 9).

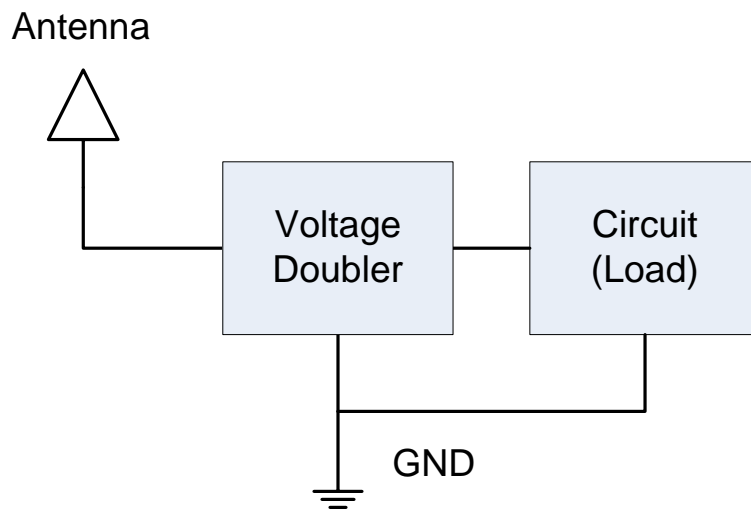


Figure 9: Stage 1 Block Diagram.

With this subset of elements, the tag will be able to harvest energy, increase the voltage above required operating levels, and perform some function. Functionality is minimal at this stage, requiring only a means to start and verify operation. The two important aspects here are circuit load simulation and visual confirmation of operation. This thesis provides a sequential series of problems and solutions towards the final prototype, but it is more so a sequential series of breakthroughs, because many of the design aspects are considered in parallel.

2.2 PROBLEM ANALYSIS

2.2.1 Tag Components

Choosing the right frequency is critical. Available RF bands include LF, HF, VHF, UHF, and Microwave, and all have been used in various RFID products. While a comprehensive discussion of frequencies is beyond the scope of this paper, one reference [9] states that frequency choice is one of the most important criteria and provides a good breakdown of the options. Factors pertinent in this application are near field utilization, powering ability, achievable distance, communication rate, good operation around metals and liquids, and a frequency that is globally available. This results in the choice of 13.56 MHz [10][9]. It is a US ISM band frequency that is available around the world, it is fast enough for high speed communication, and is tolerant of metals and liquids. Where as higher frequencies, with shorter wavelengths, are adversely affected by the reflectivity of metal and the absorption properties of liquids. The former is especially important because the reader will essentially be mounted on a big block of metal, the train, and it is important to create a system that does not require complex tuning.

With the frequency chosen, system antenna issues can be addressed. Reader side issues are discussed in section 2.3.2. Tag side design is open ended, however, in the sense that the antenna-circuit relationship is still an unknown. In order for an antenna to resonate and induce current flow through the circuit, a matching condition must exist between the two parts. This is equivalent to the maximum power transfer theorem. For antenna/load matching, antenna theory states that the complex impedance of the antenna must be the conjugate of the complex impedance of the circuit. With the circuit design in its initial stage, however, this is a major problem. To break the problem into more manageable pieces, it is divided into antenna design and simulation, circuit component evaluation, and finding an existing or similar RFID product to reference. Antenna design is left to a subsequent stage, and the latter two are investigated.

A similar RFID project can be found in the University of Pittsburgh deep brain stimulation (DBS) research. This project is defined in [11], and uses the 13.56 MHz frequency

to power up a PIC microcontroller. A proof of concept system is designed with both a 13.56 MHz oscillating reader and the matching tag that worked to harvest the energy. The antenna design and voltage doubling unit are selected to be the base components, because together they provided enough power to periodically operate a microcontroller in that project. This meant that the antenna used is at least partially matched to a relatively similar circuit construction. The antenna is a square, spiral, metal trace type design that is commonly used in PCB circuits (Figure 11). One major advantage is that tag operation testing can immediately begin, because the reader can be duplicated and used for RF powering, which is a good temporary solution.

Tag component research includes the microcontroller and the voltage doubler components: diodes and capacitors. A Microchip Technologies CMOS microcontroller has a simple architecture, which makes it a low power consumer and inexpensive. Component power consumption is another critical factor in a batteryless system, so the Microchip “nanoWatt” technology makes this an ideal choice. An 8-bit, 4 MHz chip (12F683) is selected. The 12F683 has Flash reprogrammable memory for rapid prototyping, and also has a non volatile EEPROM data memory for data collection. It is chosen as the MCU, because it also fulfills the other requirements that would be needed in later stages: low voltage turn on level, fast instruction cycle, and an integral analog to digital converter (ADC).

The DBS project used BAT 54 type diodes in the voltage doubler, along with 0.1 uF ceramic capacitors (reference Figure 10). The 0.1 uF ceramic capacitors are kept, but the diodes are changed to the Agilent HSMS 282C. Previous research on diodes has shown that these diodes perform well in RF applications. Agilent’s datasheet provides excellent information of how the parasitic capacitance and resistance impact the diode switching [12].

2.2.2 System Motion

Movement concerns are addressed by focusing on two pathways: creating a simple solution that can travel at 1 mph and facilitate testing, and also developing a system that could perform consistent higher speed tests reliably and without interfering with system RF performance. The first decision is to purchase an HO scale train set. This train set allows the tag to “piggy back” on the plastic cars, and uniformly move across the reader antenna. The advantage here is that the tag is not the fixed element. To facilitate design and testing, the reader

which requires AC power will be stationary, and the tag will move through its field. This is theoretically the same motion. At this slower speed a detailed analysis of the voltage is possible.

The second decision is to determine a way for the tags to be moved past the reader at speeds ranging from 1 to 80 mph. This system would be based on the dimensions of the prototype, the equipment necessary, and, of course, proper operation. The movement must reasonably emulate the unmanned train's single dimensional motion. Design and development will be discussed later in Stage 5, when speed problems are explored.

2.2.3 System Power

RF powering to be is provided by a Texas Instruments (TI) unit. Operating at the necessary 13.56 MHz frequency, it is designed to be a long range reader with read range distances of up to 32 inches. FCC regulations limit the output power of any radiating device. Currently, the FCC allows a device to radiate 4 watts EIRP (effective isotropic radiated power), but allows higher powers using a scaled down duty cycle. The TI reader is highly versatile using a software programmable method to output 0.5 to 10 watts of power in 0.5 watt increments. It handles four standard protocols for tag communication and performs a continuous signal scan. It will also accept any standard 50 ohm tuned antenna. The antenna chosen to complement this long range reader is a 13.56 MHz "Inside Contactless" antenna. Its dimensions are 16 inches by 12 inches, and it is a loop antenna that has a read range of approximately 25 inches. This system is more than sufficient to do testing for the full specification.

2.3 SYSTEM DESIGN

Having selected the components for the initial design, the tag layout is the next step. This discrete component solution is chosen to aid in the prototyping, and custom design work is reserved for integration and creating a working model. A small redesign of the DBS reader is performed to use as a temporary reader, and the first tag is produced. Figure 10 shows the design.

2.3.1 Tag Solution

The first tag is identified as Tag A, and the versions subsequently tested are labeled starting with version 1, v1. The DBS project placed the components inside the spiral antenna, and they did not seem to interfere significantly with the electromagnetic field flux lines, so the same approach is used. The spiral antenna is a 1 inch by 1 inch square with 7 mil thick metal trace lines and 25 mil wide spacing between trace lines. These are important characteristics because they create the inductance of the antenna which is directly related to the flow of current through the circuit [7]. Functionality is also based on the frequency and is discussed more in section three.

The antenna and the load circuitry form a loop design, which means that it is a closed circuit and ground is referenced to the negative cycle of a sine wave. For simplicity, one end of the antenna will be called the ground terminal (GND), and the other end will be called the positive terminal (V+). Because of the loop design a ground plane is not necessary, so circuitry can be placed on both sides of the PCB. As mentioned earlier, the inductance of the antenna and the capacitance of the circuit are critical to creating a resonant circuit. Trace lines are part of the impedance of the circuit, and while tag size is not greatly limited, the circuitry is kept compact to eliminate unknown influences. The voltage doubler is therefore immediately connected to the V+ side of the antenna.

The voltage doubler (See Figure 10) is circuitry that rectifies the 13.56 MHz frequency sine wave and increases charge and voltage. It is the switching action of the diodes that allows the voltage to build, and the capacitors that are used as storage devices. Refer to Appendix D for an explanation of single stage voltage doubler operation. Agilent makes a series diode package that contains two diodes in a three pin configuration that conforms to the concept of reducing trace and other parasitic effects. Combined with the capacitors, the 3 stage voltage doubler, used in the DBS project, is built in very compact profile. “Stage”, n, refers to the increase of voltage, where each stage essentially doubles the input voltage. If the input voltage is 1 volt, this 3 stage voltage doubler outputs approximately 6 volts, so the name *voltage doubler* is a slight misnomer. Also, this is an ideal value, and in reality, parasitic components limit this value to about 80 % of ideal V_{out} . While the number of stages should be kept low, to reduce complexity, the ultimate design depends on the output voltage required.

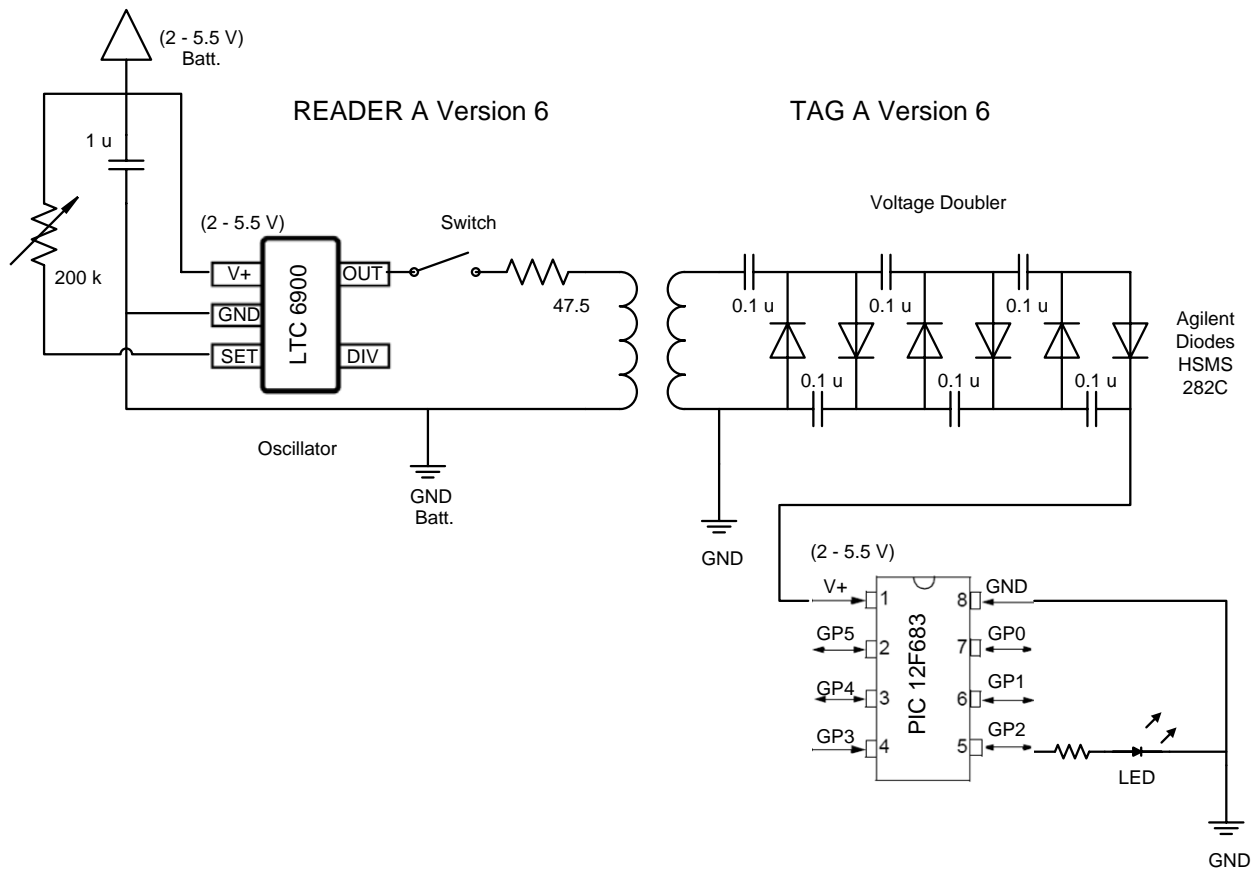


Figure 10: Tag A Design and Reader A Option.

Figure 10 shows the initial tag design and the temporarily reader that is used with it. The reader is described below. The last component to incorporate into the tag is the MCU, and it is placed on the side opposite the antenna trace. While this decision probably has little affect on the overall tag performance, the intent is to minimize circuitry influence on antenna performance. To create a load and be able to visually confirm operation, an LED is added to the output pin of the PIC. The supposition is that if the tag can power itself and light the LED, then it can handle the data transmission to be performed in subsequent designs. The LED typically requires 1.7 volts and 20 milliamps to operate, which equals 34 milliwatts of power, a relatively heavy load for a passively powered device. For prototyping, an 8 pin IC socket is used. This component is soldered to the PCB, and the PIC is inserted into it for tests, providing a way to remove it from the tag and to reprogram the chip.

The control of the PIC is very simple. Initialize the PIC, and send an output high signal to the GPIO2 pin every 0.5 seconds. The delay is necessary at this stage because there is no load capacitor, which is necessary to sustain continuous operation.

2.3.2 Temporary Reader Solution

Reader design is taken directly from the DBS project, except for the addition of a dip switch, which allows the output to be turned off. The switch is incorporated so that the field can be created instantaneously, without waiting for circuit components to turn on. In this way it is possible to test the performance of the voltage doubler and get an idea of the delay. The rest of the reader is comprised of a Linear Technologies, LTC 6900 oscillator, capable of 13.56 MHz, an antenna identical to that of the tag, and a capacitor and variable resistor, which allows the oscillator to be tuned. It also has a port for power to be attached, which accepts between 3 and 5 volts DC. This reader is referred to as Reader A.

The PCBs are manufactured through ExpressPCB, and so the layouts are created using their proprietary PCB design software. Figure 12 shows the design. The green color indicates the GND layer items, red indicates the V+ layer items, and yellow indicates a component part.

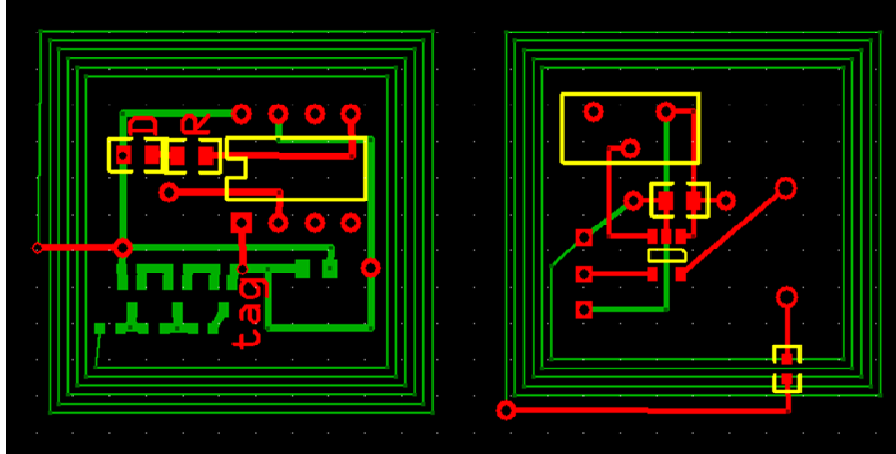


Figure 11: Tag A and Reader A PCB Design, Respectively.

The component pads are sized for the smaller 603 variety surface mount elements maintaining the compact design. The via holes are sized to allow 22 AWG wire to be soldered on for testing purposes. The interior metal trace lines are chosen to be 25 mil thick, which is a mid range size. It should not have a negative impact on the resistance of the circuit, which is to say the current flow.

2.4 TESTING AND INTEGRATION

After soldering the components to the PCBs, the testing procedure begins. The temporary DBS reader, Reader A, is tuned to 13.56 MHz and verified. The tag is then tested in two design steps: voltage doubler only, and then with the PIC controller integrated. Finally, the train setup is tested for its “full-on” speed, and TI reader system operation is verified for usage in subsequent stages.

2.4.1 Tag Testing

Prior to testing the tag, Reader A required 13.56 MHz tuning and verification. A wide band antenna is connected to an HP signal analyzer to capture the output of the reader. The variable resistor (Figure 10) is then adjusted until the spectrum analyzer peak is on the 13.56 MHz marker. The value of the resistance is measured to be 14.5 k Ohm, using a digital multi-meter. The powering value is also verified in this manner. A DC power supply is attached to the 22 AWG wires, which are soldered to the power port on the reader, and adjusted from 3 volts to 5 volts. The signal analyzer peak increased when 5 volts is used, indicating that a stronger electromagnetic field did exist.

In order to get a sense of potential performance, the voltage doubler is tested without a load. An oscilloscope is attached to the voltage doubler output, and the reader switched on. Figure 12 shows the setup of this test. In this way, the voltage doubler operation is checked for maximum voltage levels, charging delay times, as well as verification of Agilent diode improvement over the BAT 54 version. The result is found in Section 2.5.

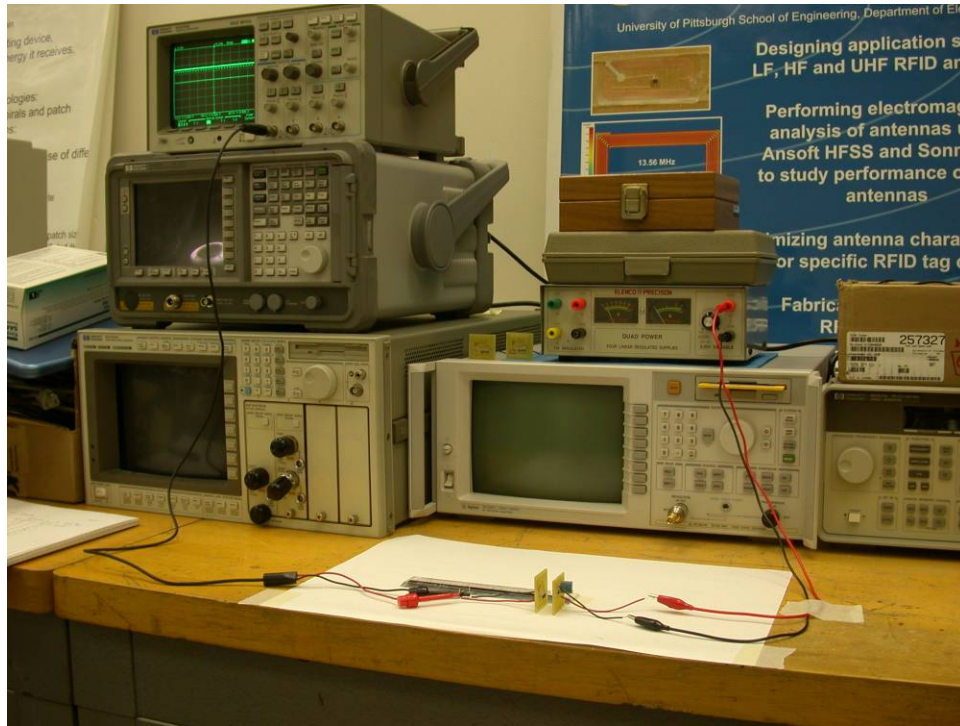


Figure 12: Tag A-Reader A RF Power Test Setup.

Next, the PIC is incorporated into the tag and RF powered load tests are performed. The successful blinking of the LED is a major success, and provides the first indication of the operating distance that is possible, as well as helping to provide direction concerning the antenna design.

The test program created is shown in Figure 13. A C compiler from Custom Computer Services (CCS) is used to compile the programs written in C code and to utilize some of their predefined functions, such as “output_high(Pin_x)”[13]. The compiled HEX files is then imported into MPLAB and downloaded to the controller. MPLAB is Microchip Technologies’ integrated development environment (IDE) design software, which communicates with its PICSTART Plus development programmer to write and read PIC memory. The firmware for this device is upgradeable to handle a variety of chipsets and is suitable for programming to the 12F683.

```

// Blinking LED Test

#include <12F683.h>
#define adc=8
#fuses NOWDT,INTRC, NOCPD, NOPROTECT,
        MCLR, NOPUT, NOBROWNOUT, IESO, FCMEN
#use delay (clock=4000000)

void main()
{

    setup_adc_ports(NO_ANALOGS|VSS_VDD);
    setup_adc(ADC_OFF);
    setup_timer_0(RTCC_INTERNAL|RTCC_DIV_1);
    setup_timer_1(T1_DISABLED);
    setup_timer_2(T2_DISABLED,0,1);
    setup_comparator(NC_NC_NC_NC);
    setup_vref(FALSE);

    while(1)
    {
        output_high(PIN_A2);

        delay_ms( 500 );

        output_low(PIN_A2);

        delay_ms( 500 );
    }
}

```

Figure 13: A PIC Program Written to Test Tag RF Powering.

2.4.2 Motion Testing

A Bachman HO scale train set, the “Challenger”, is purchased and set up. The power control for the train set is defined in percentages, with 100% being “full-on”. The target speed desired is 1 mph, which is a convenient testing speed, so a number of tests are performed to determine which percentage setting this is. The goal is to be able to test the circuit repeatedly at a uniform speed. The tests begin at 100% power and reduce until the 1 mph mark is reached. A stop watch is used to time the train over a 12 inch distance and then calculate the speed. The high speed system will be discussed in Section 6, which is Stage 5 - speed increase.

2.4.3 Power Testing

Having purchased and set up the TI long range reader system with the Inside Contactless 13.56 MHz antenna, the TI supplied reader software is installed. The software is OBID i-scan from FEIG Electronic. After several configuration issues are worked out, the system is tested for a read operation. TI tags, the Tag-It version, are purchased as well and are used to perform the system check. The areas of interest, aside from simply working, are the distances that could be achieved, and the data obtained for an examination of the field.

Three different sized tags are obtained: a rectangular tag, approximately 3 inches by 1.5 inches, a square tag, about 1.5 inches by 1.5 inches, and a mini tag, about 1 inch by 1.5 inches. These tags are shown in Figure 14. Each is tested for read range. The TI software is used to set the output to 4 watts and perform a continuous read scan, which is the fastest read method. For this test the tags are positioned parallel to and in the center of the reader antenna. The results from this set of tests give a good estimation of meeting the 18 inch specification goal.

The three tags are also used to determine how far off center the tag can be read. This is important because it provides a glimpse into the earliest moment a tag can transmit when entering the electromagnetic field. Crude speed tests are also tried, such as simply waving the tag through the field and estimating the speed.



Figure 14: Texas Instruments Passive HF Tag-It Tags.

2.5 RESULTS

This section reviews the results of the Getting Started Section tests, and discusses what they mean in defining the next stage.

2.5.1 Tag A Testing Results

The voltage doubler tests proved to be informative giving a good indication of voltage ramp up and delay. Figure 15 shows the setup and a series of voltage doubler tests.

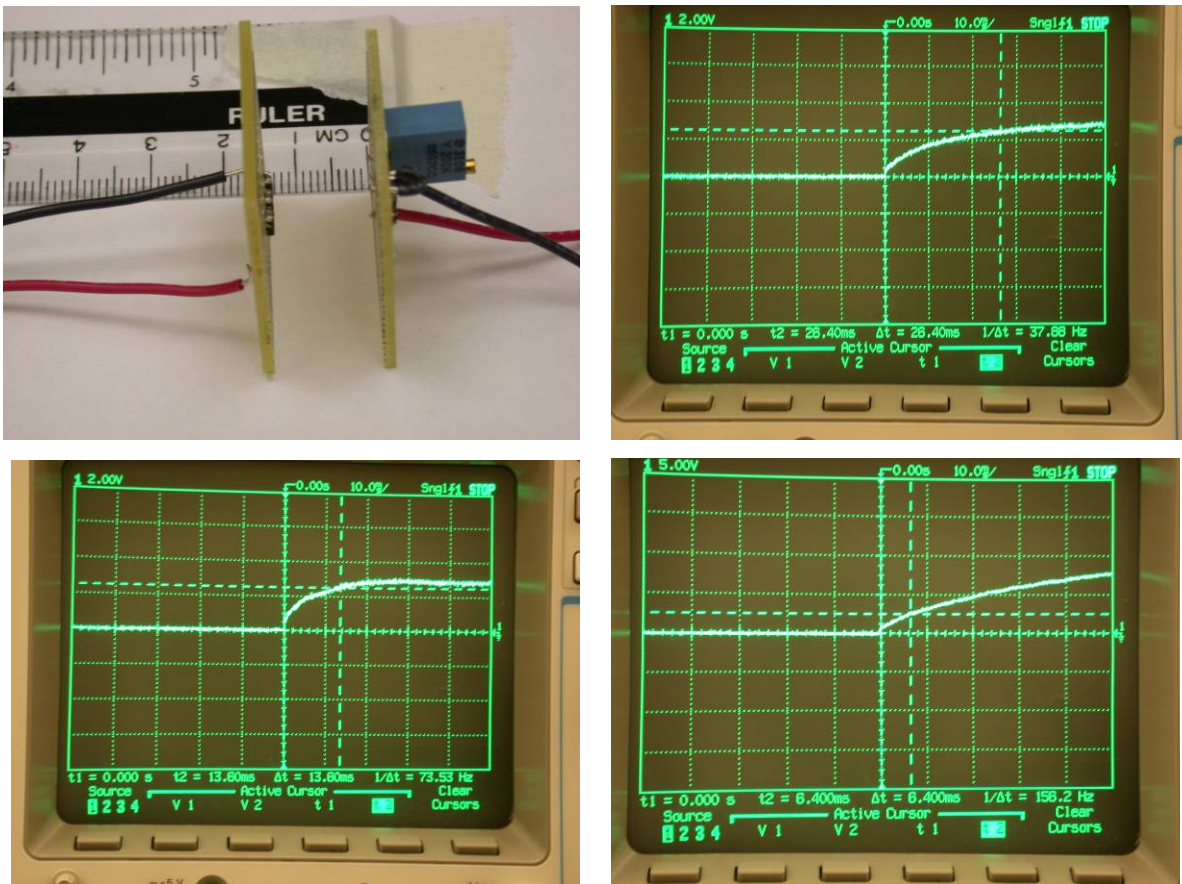


Figure 15: Tag A Voltage Doubler Tests.

The top right image shows the ramp up of the voltage doubler with the original BAT 54 diodes. The oscilloscope capture shows that it took 26.4 ms to reach 2.5 volts at a distance of 1.3 cm. Reader A is operated using 5 volts DC. The tag capacitors are changed to half their value, 0.056 uF, to observe the ramp up delay difference and tested again. The bottom left image of Figure 15 shows the oscilloscope capture resulting in a ramp up time of 13.6 ms. And, the bottom right image shows the results having changed the diodes to the new HSMS 282C version and the capacitors back to their 0.1 uF value. The time recorded is 6.4 ms. This result set supports previous research and the decision to use the Agilent diodes in this application. It also showed another interesting result. The scale of that image is increased to 5 volts per division in the Agilent diode test, as opposed to 2 volts, because the voltage achieved is much higher than that of the BAT 54 diodes. The HSMS 282C diode circuit reaches approximately 7.5 volts compared to the BAT 54's 3 volts. The conclusion is that the 282C diode creates a better resonating circuit, which produces more efficient energy harvesting and higher unloaded voltage input.

With the tag populated with the above components, including the chosen PIC MCU and the LED, the first RF powering tests are performed. Reader A is used to generate the 13.56 MHz oscillating electromagnetic field and the tag is placed parallel and center to it. The result is successful LED blinking. There is bright blinking at 0.8 cm (Figure 16), and dim blinking at 1 cm. The basic passive tag operation is verified and proven to power a significant load. As mentioned, this surface mount LED requires about 34 milliwatts of power to operate [14]. This amount of power is a large load for a batteryless circuit.

The same test is performed using the TI reader and Inside Contactless antenna, but the results are inconsistent and no conclusion could be drawn.

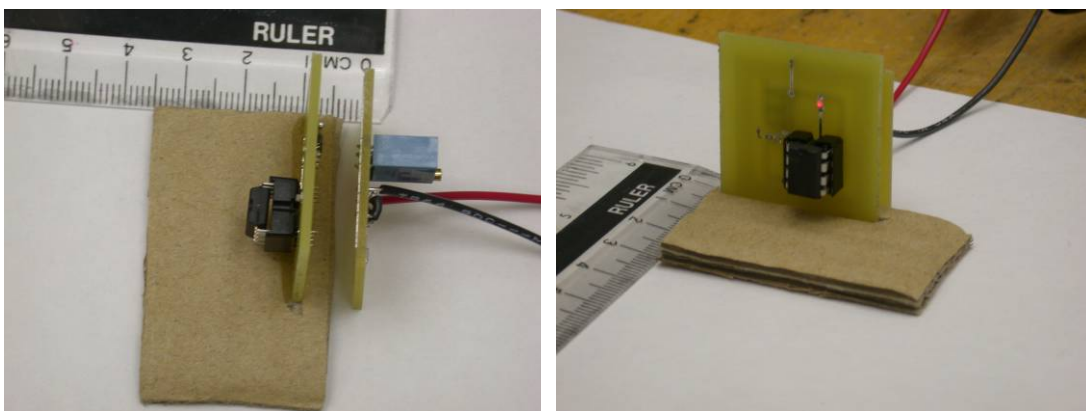


Figure 16: RF Powered Blinking LED Load Test.

2.5.2 Train Motion Testing Results

Simple stop watch tests are sufficient to answer the question of train speed. The first test is run at full-on speed - 100% power. The time recorded to traverse 12 inch is 0.6 seconds. Calculating it into mph then,

$$(1/0.6\text{sec})*(60\text{sec}/1\text{min})*(60\text{min}/1\text{hr})*(1\text{mile}/5280\text{ft})$$

produces a result of 1.14 mph. The second test is run at 75% power. The velocity result is 0.97 mph. Considering the inaccuracy of the test procedure, it is concluded that full-on speed is representative of 1 mph. This result provides a good test bed for any future tag movement tests. The motion would always be estimated at 1 mph and compared to expected results of subsequent tests.

2.5.3 TI Power Testing Results

The TI reader system setup is shown in Figure 17, with the amplifier on the left, the TI reader in the middle, and the Inside Contactless antenna on the right. The cable off of the front of the reader is the serial cable used to connect the reader to a PC. A set of masking tape lines identifies the distance directly in front of the antenna and the distances to the sides of the antenna.

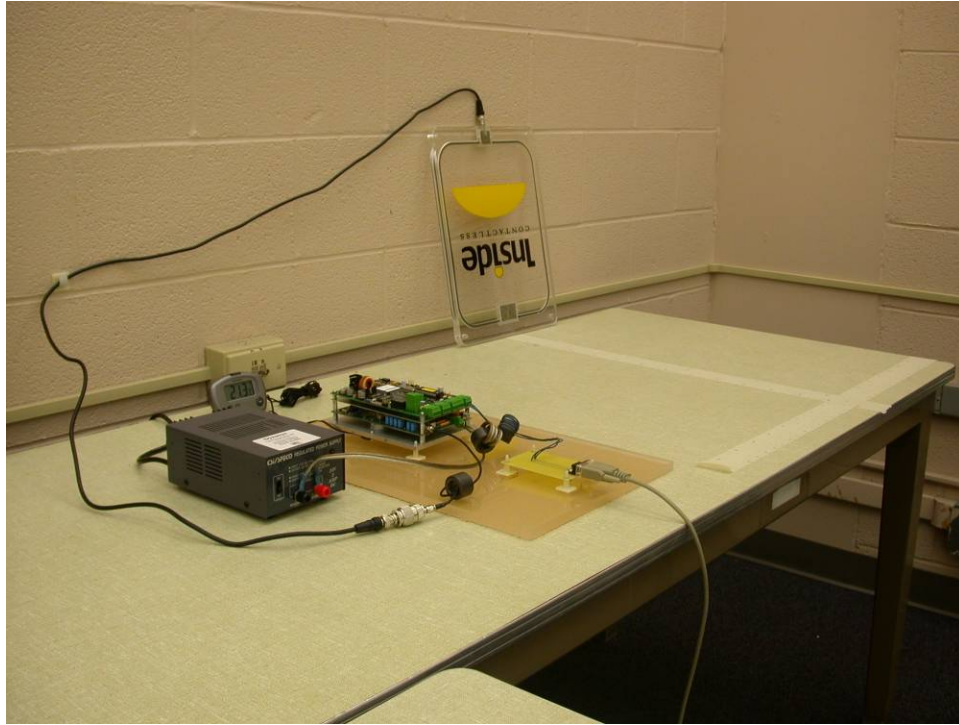


Figure 17: TI Reader, Inside Antenna, RS232 Serial Connection, and Power Supply

Table 1 lists the results for this set of distance tests, as well as the other two test procedures: off center tests, and basic motion tests. Range specifies the maximum distance achieved. It is clear that the larger rectangular TI tag outperformed the others reaching 75 cm - approximately 29.5 inches.

Table 1: Approximate TI System Distance and Speed Measures

	Range (cm)	Left (cm)	Right (cm)	Speed (mph)
Rectangle	75	21	19	5-10
Square	53	11	13	5-10
“Mini” Rect.	38	10	11	10-15

The off center tests are referred to as the side read distance, i.e. how far the tags can be read from the center of the reader antenna. For the side read distance, the larger rectangular tag is again better reaching about 20 cm - 7.5 inches. The speed tests are too crude to draw any substantial conclusion except that this particular reader system is limited in its ability to read a

rapidly moving tag. The mini tag results are slightly better for speed, because it had to be placed closer to the reader antenna for it to work, which meant greater field strength. Overall, however, it is a positive sign that the TI reader system would work for this project's testing needs, because even the mini tag reached a distance of about 15 inches.

2.5.4 Conclusion

The combined results of this set of experiments indicate that the project appears to be feasible. A voltage doubler is designed to charge up for quick operation, and the tag is capable of harvesting RF energy and powering a relatively substantial load. A means to accomplish motion testing is available and a long range reader system is established. The next problem is that of verifying the existence of the theoretical voltage curve. The sub problem is that very little read distance is obtainable at this point. Through these experiments, and related antenna research, it is apparent that a larger antenna is necessary. And so, the next stage is defined.

3.0 STAGE 2: VOLTAGE CURVE VERIFICATION

Development of the resulting system depends on the identification of the bell shaped voltage curve. If the theoretical voltage curve does not translate into a practical voltage curve, the project is not viable as originally specified. In order to manage this stage, a more realistic test bed is necessary. However, this means that the target distance must be achieved. The two tasks are: create a new antenna that will likely reach a distance of at least 10 inches, and develop a method to observe the voltage curve.

3.1 TAG ANTENNA DESIGN

3.1.1 Antenna Design Method

A method for analyzing the current antenna and designing a better antenna is found in a software package called Sonnet. Using this tool, Tag A is redesigned and simulated. From related research, it is apparent that the size of the antenna is a basic factor in read distance; the more of the electromagnetic field that it contacts the more induced current that is realized. As is discovered, however, the inductance of the tag is also important. Without requiring a full understanding of antenna theory, three different sized antennas are designed and simulated: a 4 inch by 2 inch rectangular design, and two square designs, a 5 inch by 5 inch and a 9 inch by 9 inch spiral. The 4x2 inch design is a convenient testing size and is modeled after the rectangular TI tag that worked well. The 9x9 inch design is the largest size allowed in the specification, and the 5x5 inch design simply fell between these two.

The Sonnet software package has tutorials that make learning the tool easier. Some knowledge of antenna design is required, but this tool greatly simplifies the job. A user friendly

design step check list is viewable on screen to ensure all the necessary parameters are entered (Figure 18). These include the bounding box, which the antenna is simulated inside, the dielectric layers of the antenna, which account for the physical PCB, and the metal types used for conductors. EM is the Sonnet electromagnetic analysis engine, and it performs a modified method of moments, three-dimensional current analysis, which is based on Maxwell's equations. It creates a "mesh" over the modeled surface and calculates boundary values. Important factors are cell size, box dimensions, and air layers. Simulation is run as though the object is inside a "true metal" box, and thus, the distance of the antenna to the box sides becomes critical. It is determined that the box should be 2x the size of the antenna for proper simulation results. The manner in which this is handled for the top and bottom of the design is to make the air layers larger. Lastly, to make simulation as efficient as possible, thereby reducing simulation time, the cell parameters should match or be a factor of the size of the metal trace. If the spiral trace is 10 mil thick, for instance, then the cell size should be made 10, or 5, or 2. The spacing between trace lines must also be considered as well. The smaller the size the more accurate the simulation, but the longer it takes to compute. Because a general result is sufficient for the purposes of comparing antennas, the largest possible cell size is used.



Figure 18: Sonnet Spiral Antenna Design Check List.

3.1.2 Antenna Simulations

Tag A is recreated and simulated first in order to have a base to compare the new antennas. Then, the other three antennas are designed in Sonnet. Figure 19 shows the 3-D designs, and Figures 20, 21, 22 and 23 show the simulated inductances. Each is designed in the same way, and with like parameters, only changing their dimensions. The 4x2 inch antenna is labeled Tag B; the 9x9 inch antenna is labeled Tag C, and the 5x5 inch antenna is labeled Tag D.

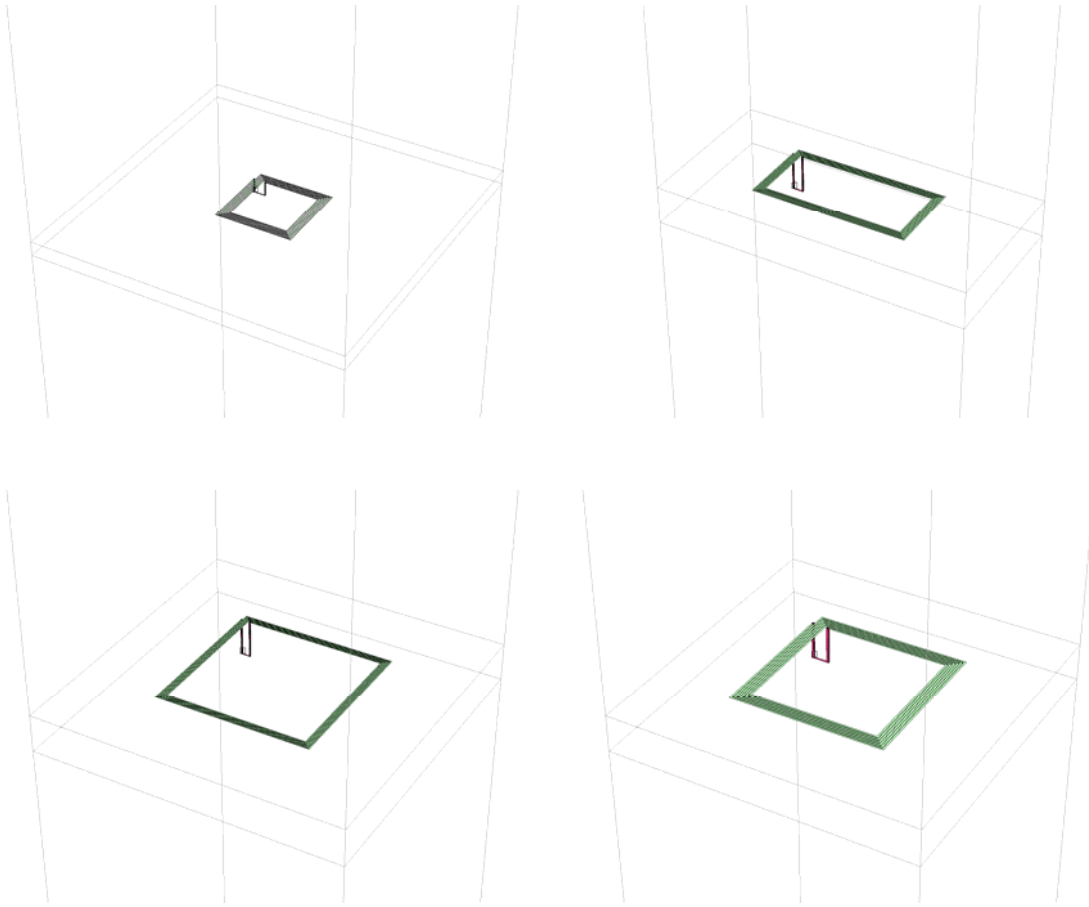


Figure 19: Sonnet Simulation Software Tag Antenna Designs (clockwise A, B, D, C).

The parameters that define the spiral antenna are the lengths of the first two sides, the thickness of the trace, the spacing between trace lines, and the number of turns. To keep the variables to a minimum, the number of turns is fixed at 6, the value of the original 1x1 inch PCB antenna. Tag A, as stated, has a trace thickness of 7 mils and a spacing of 25 mils. A “mil” is defined as 1 thousandth of an inch. The first two sides are of course, 1 inch by 1 inch. Tag B’s trace thickness is simulated at 30 mils, with a spacing of 10 mils. The first two side lengths are 4 inches and 2 inches, forming the rectangle. It is thought that as the size of the antenna increases that the trace must also increase to reduce resistance and facilitate current flow. Tag C is designed with a trace thickness of 60 mils and a spacing of 20 mils. The side lengths are both 9 inches. Tag D thickness is also 60 mils, with 20 mils spacing.

After analysis is performed, plots are produced. Because inductance is an integral part of spiral antennas, Sonnet has a predefined method to plot it. The default plot in viewing the

response is magnitude versus frequency, but an equation can be chosen to use on the data that converts it into inductance versus frequency. The equation used is:

$$1.0E9 * \text{imag}(1 / \text{arg1}) / (\text{TWO_PI} * \text{FREQ}),$$

where arg1 is the simulated data. The plots are shown in Figures 20 through 23.

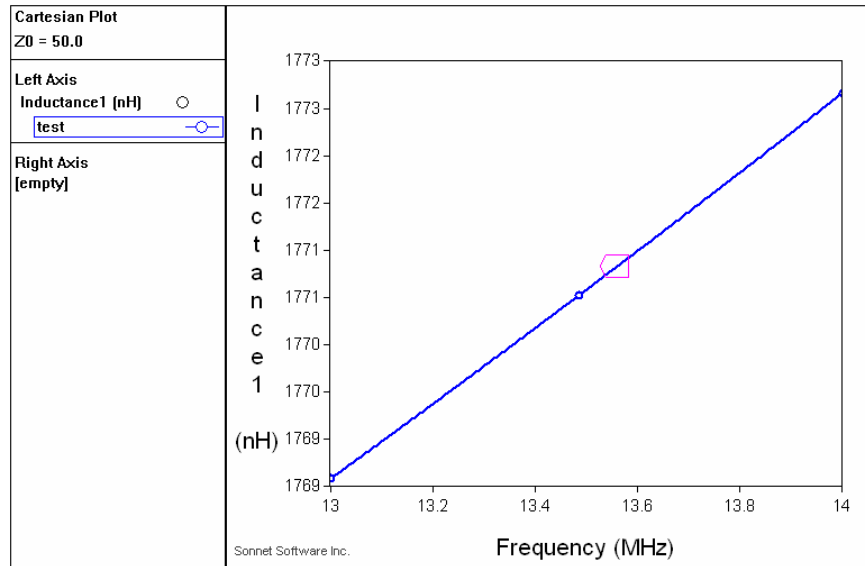


Figure 20: Sonnet Inductance Plot of Tag A Antenna Simulation.

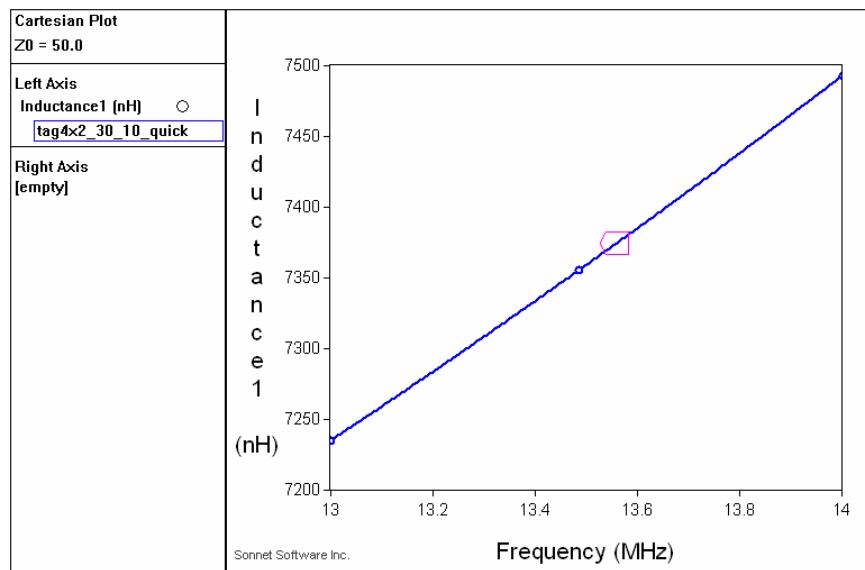


Figure 21: Sonnet Inductance Plot of Tag B Antenna Simulation.

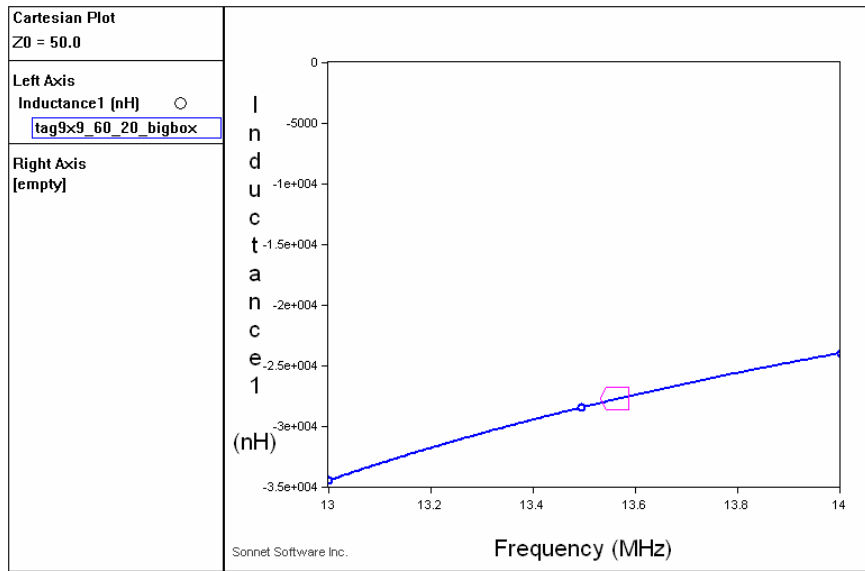


Figure 22: Sonnet Inductance Plot of Tag C Antenna Simulation.

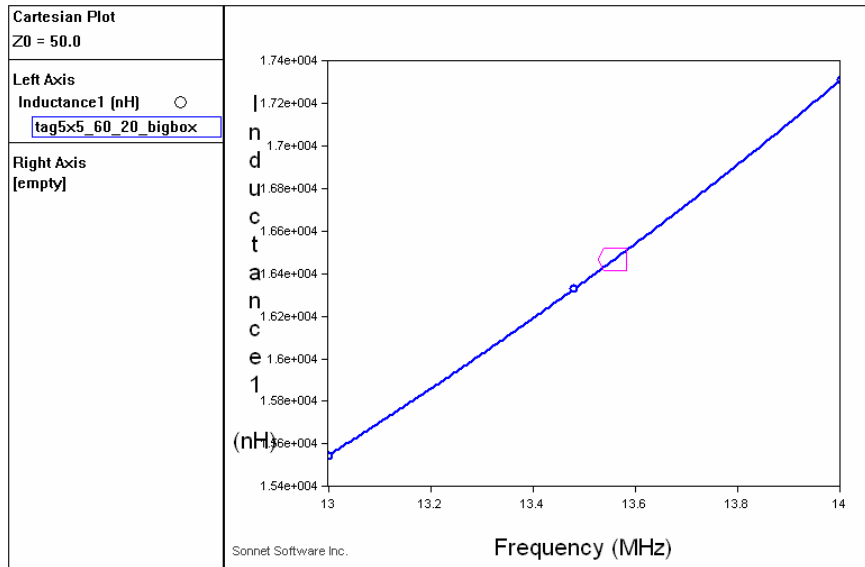


Figure 23: Sonnet Inductance Plot of Tag D Antenna Simulation.

3.1.3 Antenna Simulation Inductance Results

The inductances are plotted over a very short frequency range to further reduce simulation time. The values for Tags A, B, C, and D at 13.56 MHz are 1.9 uH, 7.4 uH, -27.7 uH, and 16.5 uH respectively. Tag B is chosen to lay out on a PCB next for four reasons: its inductance is higher than Tag A, it's size facilitates testing, it is thought to be sufficient for reaching the 10 inch read distance and, it is considered a good intermediate step, toward full specification, providing useful information if a larger antenna is still required. It is interesting, however, to observe the drastic change in inductance between Tags C and D. The parameters are the same except for the size, and yet the Tag C antenna is capacitive not inductive. A much greater depth of research is required to design an ideal antenna for this application, and is left as a critical task to Phase II.

3.1.4 Verification of Simulation Results

Tag B is subsequently laid out in ExpressPCB and manufactured. An LCR meter is used to measure the inductances of Tag's A and B antennas. Figures 24 and 25 show the tags being measured and their respective values. The values are quite close to that of the simulation and support its accuracy. Simulated Tag A antenna inductance is 1.7 uH, while the LCR meter measures it to be 1.9 uH. Simulated inductance for Tag B antenna is 7.4 uH, and the LCR meter measures it as 7.9 uH. While the resistance is shown in the figures, it is not a value that could be verified by another means and is subject to argument. In Sonnet for instance, to calculate accurate resistance of the antenna, a complex set of parameters including PCB properties and metal properties must be known, and this information is not readily available through the manufacturer. Also, because the antenna is not the standard 50 ohm resistance, it cannot be analyzed on most machines. Comparison wise however, it is good that the new tag antenna did not increase its resistance value much higher than Tag A is shown to be, and is still below 50 ohms. Antenna resistance is desired to be as low as possible, in order to reduce losses.

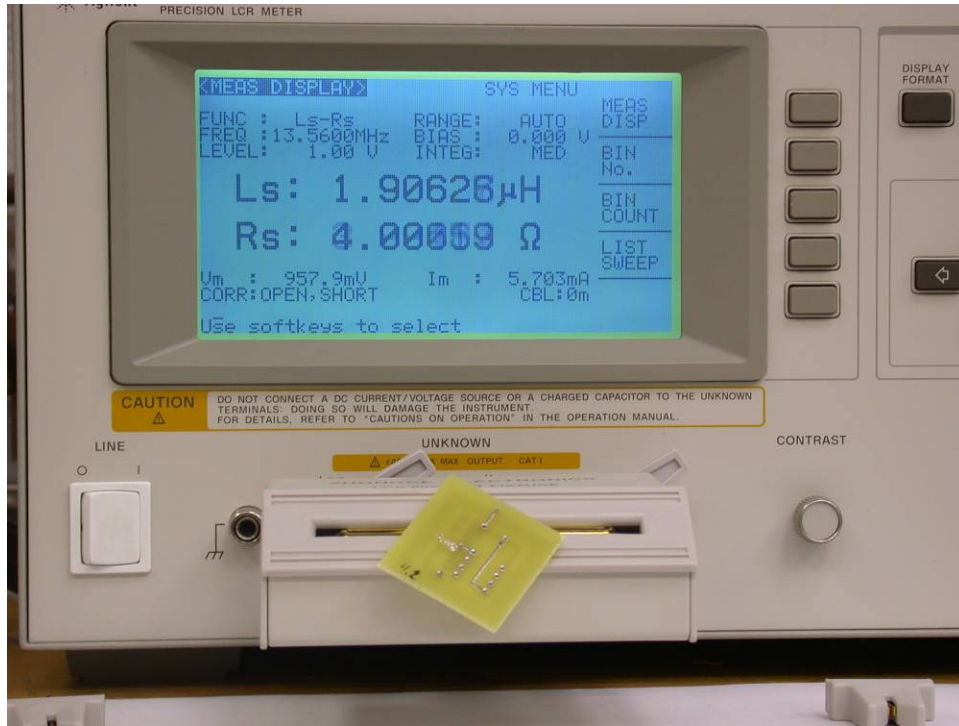


Figure 24: LCR Meter Inductance Measure of 1x1 Inch Tag A.

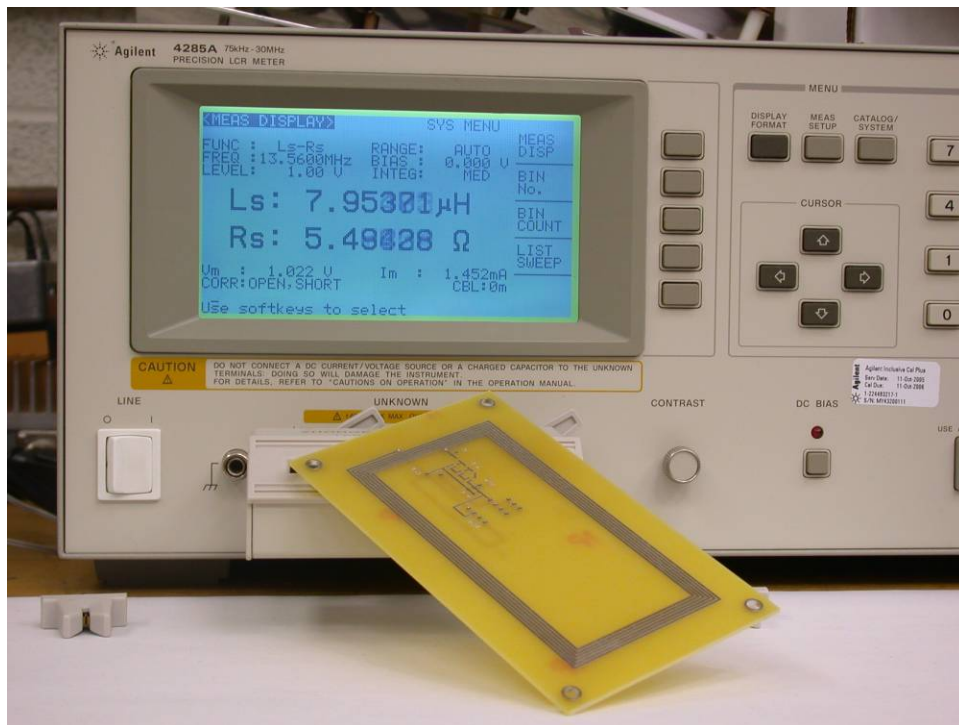


Figure 25: LCR Meter Inductance Measure of 4x2 Inch Tag B.

3.2 VOLTAGE CURVE METHOD

With the chosen two antenna designs available, a method for verifying the voltage curve is developed and tested. The purpose of this stage is to ensure the feasibility of the entire project. Without the bell shaped voltage curve, the research cannot proceed as previously defined. It is a challenging problem to visually represent this intangible aspect of the passive tag system.

3.2.1 Method Devised

The various parts to this problem are: how to record the voltage samples, at what rate, and once obtained, how to graphically represent them to verify the bell shaped curves existence. Starting with the easiest problem to solve, the 1 mph train system is good testing mechanism. The train is setup on a table with a plastic car trailing the engine able to hold the tag parallel to the table. The reader antenna is then positioned parallel under the table, directly in line with the tracks in one dimension and centered on the tracks in the other. Figure 26 shows the setup. In this way the tag could be moved through the reader antenna field at a consistent and reasonable rate for testing. The reader antenna can be raised and lowered easily to test a variety of antenna to antenna distances.

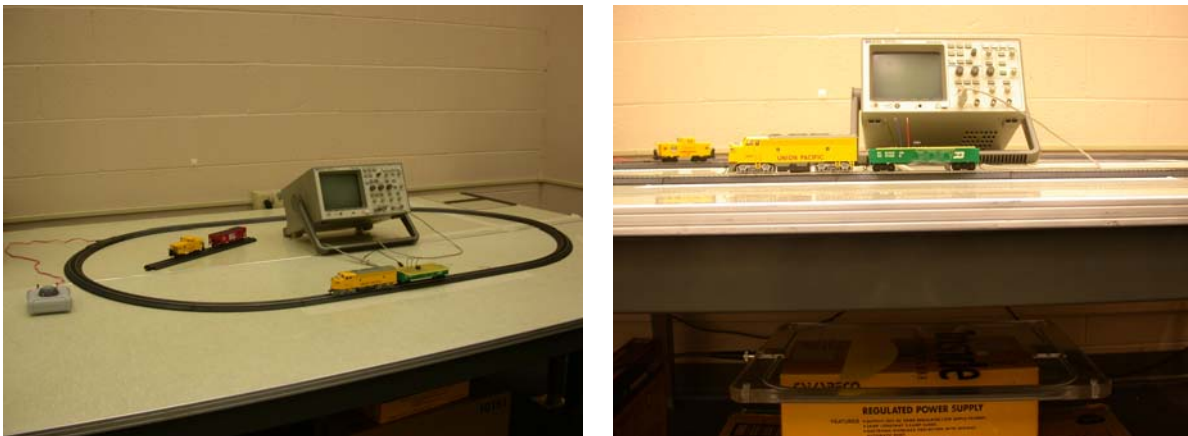


Figure 26: Model Train 1 mph Setup, With Reader Antenna Under Table.

To solve the problem of capturing the voltage levels induced by the electromagnetic field, the functionality of the PIC is considered. The microcontroller chosen has EEPROM data

memory, which is nonvolatile and is able to save the voltage values. The MPLAB IDE is useful, allowing the contents of memory to be read into the software and allowing the EEPROM to be viewed following at test. An export function exists as well to be able to export the HEX data to a file. With this file, the data is easily imported into Excel, converted to decimal, and can be graphed as a voltage curve.

The difficulty with this procedure is that a single EEPROM write takes too much power for a passive device under the specified operating conditions. A method of transmitting the values by RF is not reasonable at this stage of evaluation. Because the problem is one of power, a modified testing solution is developed. The tag design is changed slightly to power the PIC using a battery, and the voltage doubler output is only used as an input into the ADC of the PIC. The EEPROM writes are not a problem then, and the voltage being harvested is not affected. A representational curve of the harvested energy is thus captured.

With this procedure defined, a program is then written to perform EEPROM writes during a specified period. Because it is performing voltage comparisons, it is logical that a voltage level be used to initiate the algorithm. Once a certain threshold is reached, the PIC can perform a series of ADC read - EEPROM write operations saving the voltage samples obtained as the tag moves through the reader field. The number of operations depends on the speed of the train, and the time it takes to do a read-write.

3.2.2 Tag Design

A 3 volt battery is used to power the PIC instead of the voltage doubler harvested energy. All other aspects are the same except that the voltage doubler output is now routed to the PIC ADC input pin. The issues to this design are: the load on the voltage doubler, the voltage level of the doubler output, and the EEPROM write time versus the movement of the tag through the reader. Several iterations are considered in working out a good testing procedure.

The first issue is that the ADC pin on the PIC is a high impedance pin, so the voltage doubler did not have a significant load. The LED load is not used because the PIC's Vdd is not supplied by the voltage doubler in this test. Because of this, the input voltage to the ADC is not representative of the conditions for the end circuit's true voltage curve. A resistive load element is incorporated to represent a more realistic circuit load and get a more accurate result (Figure

27). A load capacitor can also be added to provide the ability to sustain a small, but constant current draw. It is a more accurate model of the circuit that is to eventually be created.

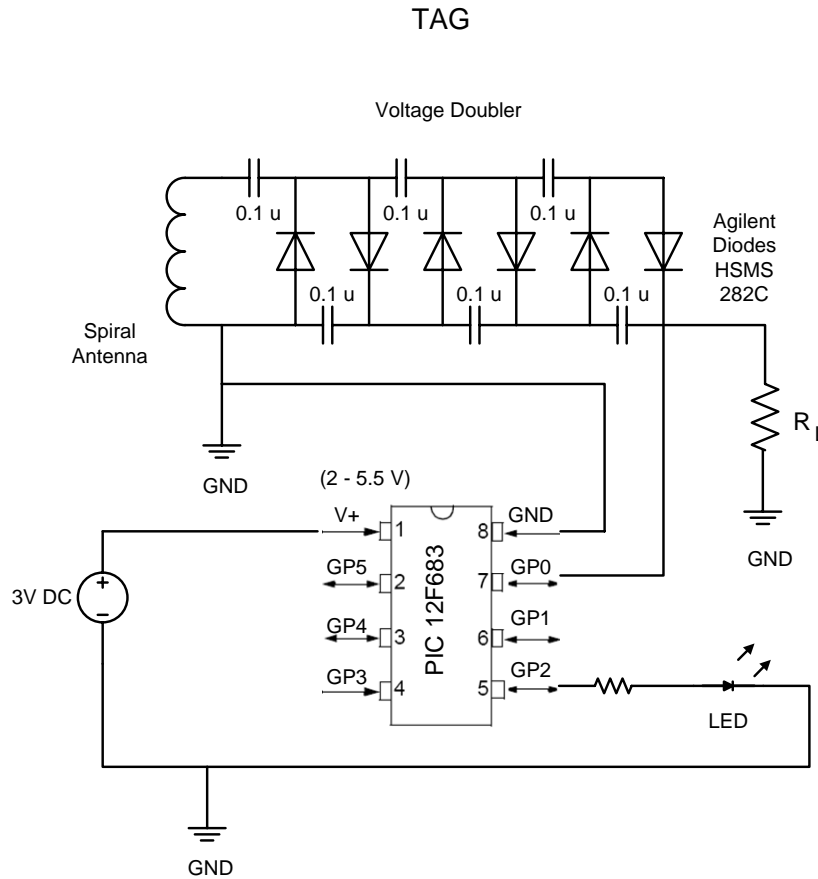


Figure 27: Tag Circuit With Resistive Load Incorporated.

The operation is still not accurately portrayed, however, and it is determined that the internal PIC ADC voltage reference is being exceeded. A solution to this problem is to incorporate a voltage divider between the voltage doubler output and the PIC ADC input pin, but it is not implemented in this initial iteration. It is addressed in section 5, with a discussion about creating the peak detection algorithm. An easier, temporary solution existed to expedite voltage curve verification; the tag distance would be adjusted away from the reader antenna until the voltage passes the turn on level, 2 V, but is still below 3 volts, which is the value of the ADC voltage reference (V_{ref}). V_{ref} is the same value as V_{dd} in this project, default, because an external V_{ref} would mean adding more components and complexity. Because a 3 volt battery is

being used, this is the maximum voltage that could be compared. Using this method, tag antenna performance could be observed too.

The PCB's for Tag A and B are shown in Figures 28 and 29 respectively. The Tag B design incorporates a variety of features, or options, in the same PCB. For instance, inspecting Figure 29, one notices that the square power pin is connected to the voltage doubler and to a power input port. If the tag is to be used for RF power tests, it is simply not connected to the battery. If it is to be used in battery power tests, as it is here, then the trace between the voltage doubler and the PIC Vdd pin is cut.

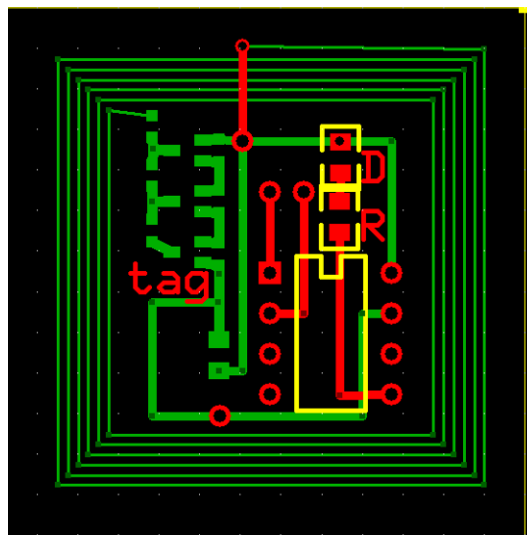


Figure 28: Tag A Battery Power PCB Design.

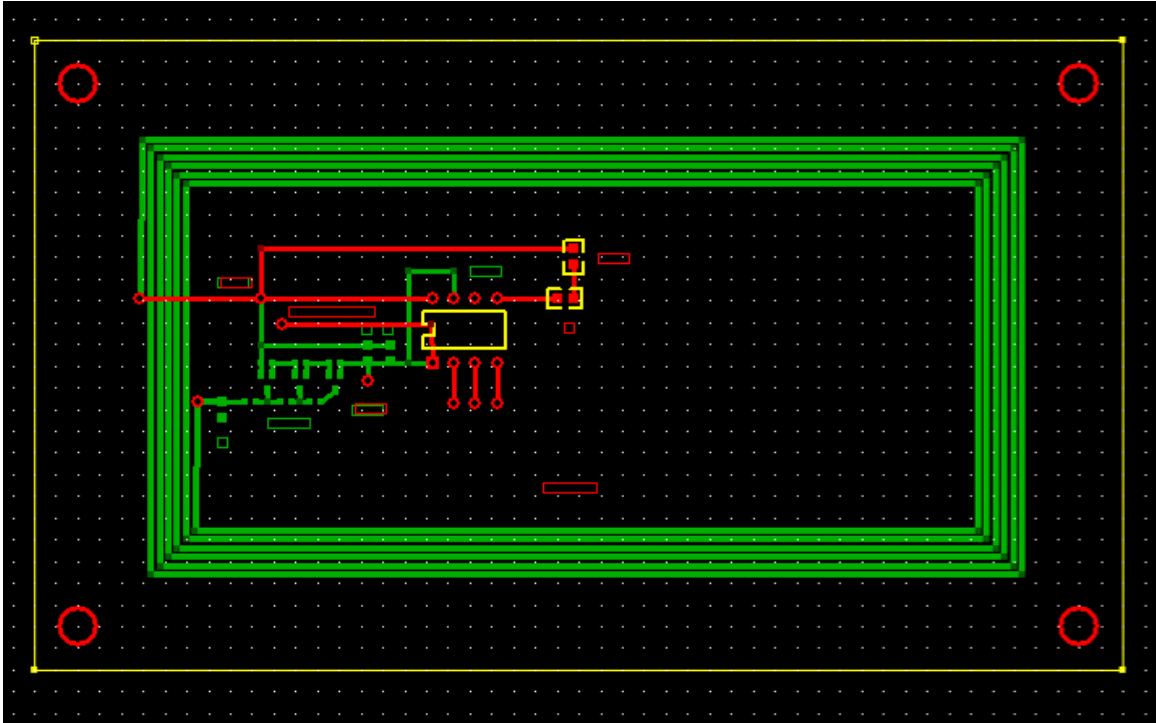


Figure 29: Tag B Battery Power PCB Design.

In order to determine the proper operation of the algorithm, the EEPROM write time needs to be related to the tag speed. EEPROM writes take a maximum of 6 ms [15] and the instruction cycle works out to be 1 us. Approximately 100 instructions are used in the ADC comparison process, so the total time is estimated to be 6.1 ms. The 1 mph train speed facilitates the calculation. The 6.1 ms execution time is a very long in terms of moving across a 16 inch antenna at any significant speed. Table 2 shows the number of EEPROM writes possible traveling at various speeds. The formula is:

$$(16\text{in} / [(1\text{mi/hr})(1\text{hr}/3600\text{sec})(5280\text{ft/mi})(12\text{in/ft})]) / 6.1\text{ ms}$$

Table 2: Possible EEPROM Writes Versus Speed

Speed	EEPROM	Time Available	Writes
1 mph	6.1 ms	909.1 ms	149.03
10 mph	6.1 ms	90.9 ms	14.9
25 mph	6.1 ms	36.4 ms	5.96
50 mph	6.1 ms	18.2 ms	2.98
80 mph	6.1 ms	11.4 ms	1.86

It is clear that this method for identifying the voltage curve is only sufficient for speeds less than 10 mph. It will provide results to support or negate the theoretic claims made, however, and is worthwhile. The 16 inch value at the beginning of the above calculation is the distance to be traversed, i.e. the antenna length.

With this information, it is possible to develop the algorithm needed. Start recording at approximately 1 volt, perform 250 voltage reads and EEPROM writes, and then cycle through a while loop visually indicating that it has completed. Figure 30 displays the body of the code developed. The calculation for the decimal equivalent voltage turn on level is

$$(1 \text{ V threshold}) / (3 \text{ V reference} / 256 \text{ bit resolution}),$$

where the threshold is chosen by experimentation. The voltage reference is determined by the battery used, and the ADC resolution is determined by the PIC's 8-bit functionality. The outer denominator is the minimum voltage step that can be discerned.

```
while(1)
{
    voltage = read_adc();

    if( voltage > 85 ) // begin to write eeprom at 1 Volt
    {
        for(i = 0; i < 250; i++)
        {
            write_eeprom( i, voltage ); // addr , value
            voltage = read_adc();
        } // end for loop

        while(1)
        {
            delay_ms(1000);
            LED = 1;
            delay_ms(1000);
            LED = 0;
            //delay_ms(500);
        }
    } // end if
} // end while
```

Figure 30: A PIC Program Written to Capture the Voltage Curve.

3.2.3 Testing Procedure

In this voltage curve verification experiment the testing procedure is simple. The reader field is energized, the tag is connected to the battery and placed “piggy-back” in the train car, the train is turned to full-on position, and after the tag moves through the field, the battery is disconnected. The only variables are the tag to reader antenna distance and the load resistor value. Both are determined in a trial and error manner using cardboard boxes to adjust the height of the reader antenna, and simply soldering new resistors on in place of the old values.

Having successfully executed the program, identified by the blinking LED, the PIC is removed from the tag, and inserted into the IDE programmer and read. The data is exported to a text file, imported into Excel, converted to decimal, and plotted. The testing in this stage terminated when the expected voltage curve is observed in the Excel chart.

3.2.4 Voltage Curve Results

Results from the voltage curve verification tests are very positive identifying a bell shaped curve. After several iterations, it is found that the best resistive load to use is 10 k ohm, and an acceptable load capacitance is 1.0 uF. Figure 31 shows the charted EEPROM data results of the successful Tag A test. It captures the full curve at a tag to reader distance of 7 inches away. Figure 32 shows the charted results of the successful Tag B test. Tag B is able to capture a full peak curve at a distance of 13 inches between tag and reader antenna. This result is nearly double the distance using Tag A. It positively shows that a larger antenna can achieve more distance; it also shows that a greater voltage can be obtained. Tag B reached about 3 volts, while Tag A reached about half that level, 1.6 volts. While these tests are not specifically related to the voltage levels achieved, there is room to speculate about the result. As a simple comparison, these results are useful.

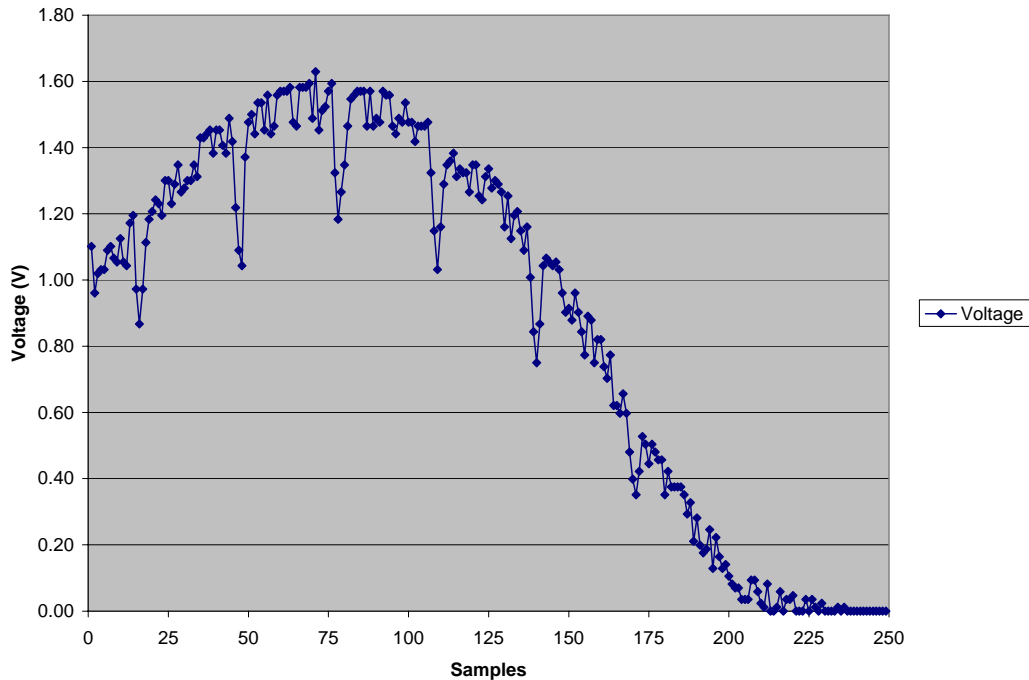


Figure 31: Tag A Voltage Curve, Captured at 7 Inches Away From Reader Antenna.

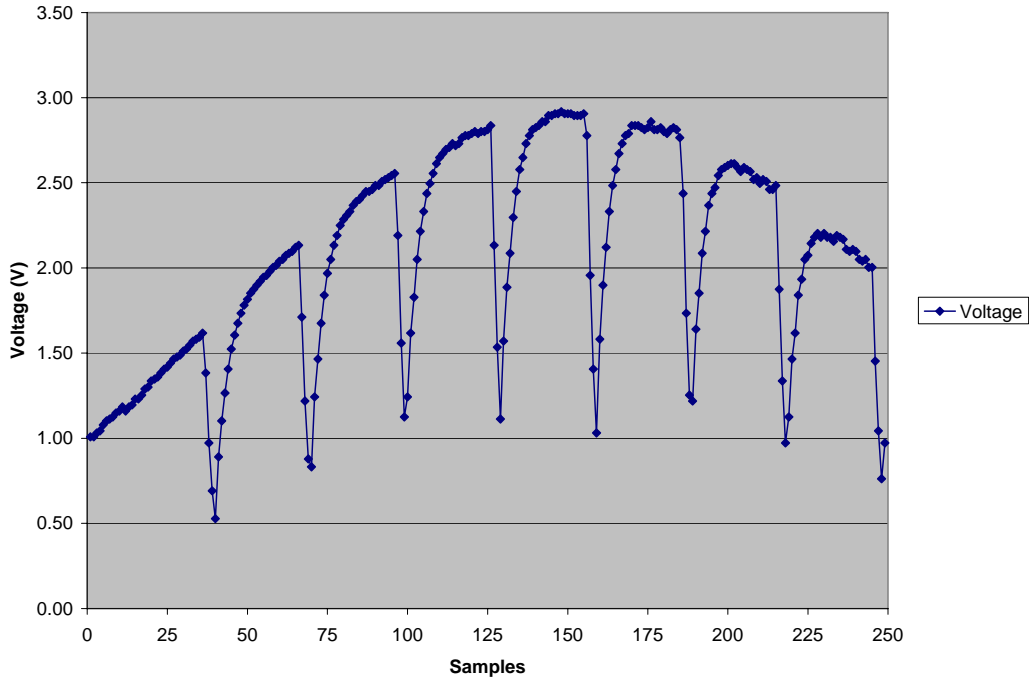


Figure 32: Tag B Voltage Curve, Captured at 13 Inches Away From Reader Antenna.

The main point is that these tests clearly show the bell shaped voltage curve. It exists, and can be used in determining the center position of the reader antenna. The ultimate goal appears to be feasible.

A few issues must be discussed. There is an extremely obvious interference pattern repeated in the graphed data points. The possible causes are: some internal tag switch aspect, ambient noise, possibly from the track, or some functional problem of the reader or reader antenna, which has circuitry incorporated into it for tuning and amplifying. It is determined to be a break in the continuous wave output of the reader (Figure 33), due to duty cycle limitations of the reader, and can not be changed. Section 4 presents a solution to this problem.

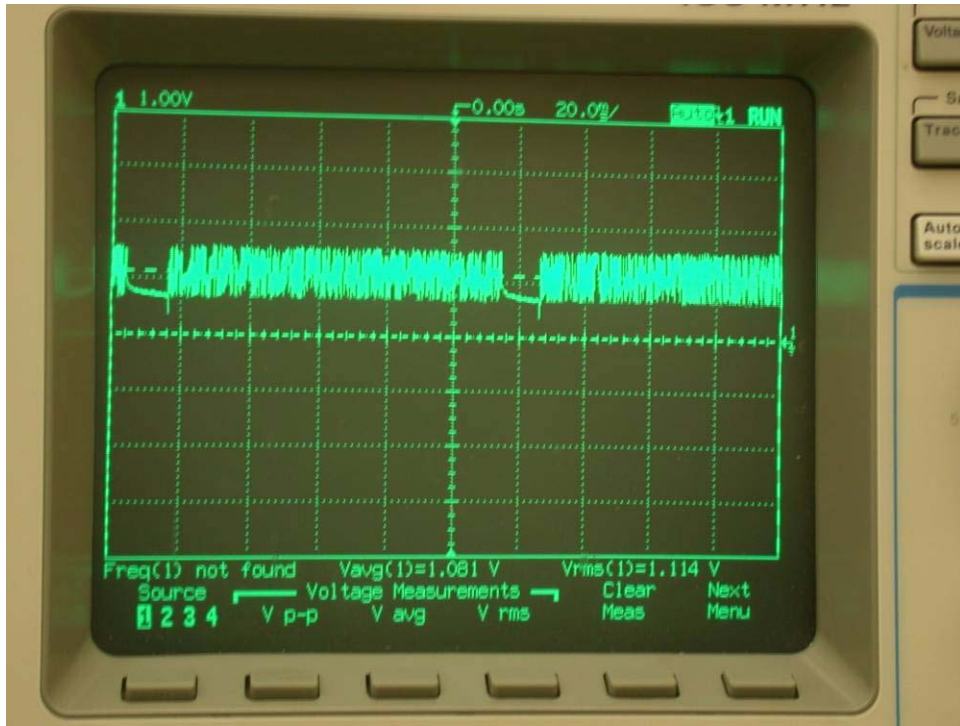


Figure 33: Oscilloscope Capture of the Interference Pattern.

While it is evident that the voltage curve exists, this data is only a general representation of the true curve. This limitation is because of the battery. During testing, it became apparent that internal circuitry, possibly connecting aspects of the ADC and powering, might be tainting the results. Because the results are all affected in the same manner, the bell shape is still confirmed. The data is just not directly usable in future design considerations. A subsequent RF test and verification is required.

The 8-bit resolution can be improved, but using the available 10-bit resolution would double the time it takes to save and retrieve the data, because it requires two bytes instead of one byte. The resolution seems adequate for this purpose, and efficient for passive tag operation. This issue is potentially an area of optimization and can be explored more in Phase II.

Lastly, a number of factors support initial estimates made; the starting threshold level, the number of EEPROM writes possible, the estimated write time, and the estimated speed of the train all affect one another. Assuming the 1 volt turn on level is close to the reader antenna's edge, meaning that the distance traveled is 16 inches, then, 150 6.1 ms writes are possible from edge to edge, or 1 volt to 1 volt. Referring to Figure 31, that is precisely how many writes are accomplished. Therefore, all estimates appear to be confirmed.

4.0 STAGE 3: TAG RANGE INCREASE

Having proven the existence of the voltage curve, the next step required is to determine if the harvested energy can power the circuit at a suitable distance – 10 inches. There are two factors here: the circuit and the distance. Because circuit development depends upon the success of each stage of work, the next task focuses on increasing the distance. This section discusses the method used to increase the distance and the system improvements required.

4.1 NEW READER SOLUTION

As is shown in the previous stage, the TI reader solution is not sufficient due to its duty cycle limitations. Because powering the device is critical to all aspects of this application, the continuous wave (CW) operation of a reader is vital. Instead of searching for a new reader, a different approach is taken in using a signal generator. This solution has two potential problems. First, communication ability is lost, and second, the power output is not sufficient from the signal generators available.

The problem of future tag to reader communication, while important, is simply delayed. Several communication options are possible and available, so obtaining CW is more important to maintain the projects progression, and the focus is turned to the more immediate issue of power output. Stage 5 addresses the problem of communication in detail.

The solution of outputting the desired 4 watts of power is to use an amplifier. In this way, a CW sine wave can be generated, amplified, and ported to the same “reader” antenna. This setup has no duty cycle limitation and will produce the CW signal needed.

4.1.1 Reader Design

To generate the wave, an HP 15 MHz Function / Arbitrary Waveform Generator is used. The 13.56 MHz frequency is achievable, and the machine can be set to sine wave mode, where the amplitude can be selected. Again, the output power is not sufficient for the desired 4 watts, but being able to adjust the amplitude is important.

Amplifiers for this range of HF operation are usually custom designs that take months to receive. A more immediate solution is found in an HD Communications amplifier. It is a fixed 5 watt amplifier, operating in the frequency range of 1 to 500 MHz. It required a heat sink and a cooling fan to operate along with a 24 V, 2 A DC supply. The same RF “friendly” DC supply that was used with the TI reader is a good choice. Because this amplifier is fixed at 5 watts, it is necessary to have the amplitude adjustability on the signal generator.

A power meter is used to determine and set the power output to 4 watts. Because the power meter has a limitation of 100 mW, a 30 dB attenuator is used in series with the amplifier. It turned out that the signal generator, which is adjustable from -20 dBm to +10 dBm, would produce 4 watts while set at 1 dBm. Each piece of equipment has some tolerance, so the value chosen represents 4 watts maximum.

4.1.2 Reader Verification

The battery powered voltage curve test is performed again to verify the performance of the CW system, confirm the elimination of the interference pattern, and reconfirm the bell shaped voltage curve. Tag B is used, and Figure 34 shows the result.

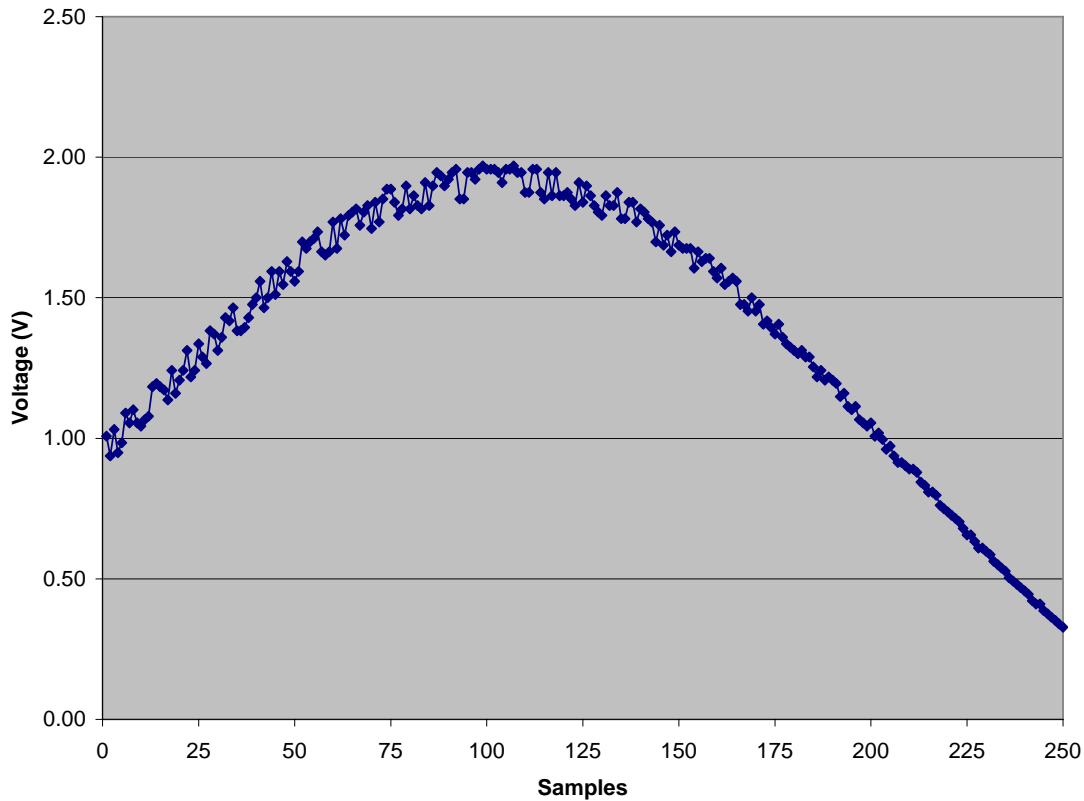


Figure 34: Tag B, Amp Powered, Voltage Curve, Captured at a 10 Inch Distance.

The plot shows the result expected. It identifies the bell shaped voltage curve. It clearly confirms the elimination of the interference pattern and supports the fact that it was indeed caused by the TI reader. A CW signal exists. The voltage is lower than the previous graph, and the distance achieved is less, because different load resistors are being tested. This has no bearing on the outcome of the expected result.

One issue that can be foreseen is that of noise in the signal. This will have to be addressed in creating a peak detection algorithm; options are filtering in hardware, filtering in software, and algorithm noise handling. This problem will be addressed in Stage 5.

4.2 TUNING FOR DISTANCE

Because Tag B proved to be much more efficient than Tag A, it is chosen for the remainder of testing and is redesigned as development progresses. The purpose of this stage of research is to demonstrate that RF energy can be harvested and used to power the circuit. Because the LED had been an adequate load representation previously, the blinking LED concept is reemployed. The goal is to be able to blink the LED at a minimal distance of 10 inches.

4.2.1 Tuning Theory

Tuning is the act of making a circuit, the whole tag, resonate at a specific frequency. For a linear LC circuit tuning values for resonance are determined as follows [9]:

$$\text{Frequency} = 1 / (2\pi * \sqrt{LC}).$$

Because the frequency is a known value, the LC product is easily calculated. For 13.56 MHz, the LC value is 137.759 e^{-18} . Therefore, the inductance of the tag and the capacitance of the tag are developed to have a product that equals this value. The spiral antenna is the primary inductance of the tag, and the circuitry is the primary capacitance. If both components are being developed, then it is rather complex to obtain an immediately optimized solution. The path chosen in this research is to design an antenna first, which is to say, to choose an inductance that is estimated to be adequate for efficient coupling. The difficulty is that the circuit is being created based on the preceding steps, and is not fully known. Thus, the process is iterative; design-test-redesign.

One way of handling this problem is by adding an inductive element and a capacitive element to the circuit (Figure 35) to balance the equation. Based on common knowledge of circuits, for an inductive element to add, it must be in series with the other inductance. Likewise, for a capacitive element to add, it must be in parallel with the other capacitance. This is one of

the common matching, or tuning, techniques – the L Matching Network. It is simple, requiring only two additional elements. This is also referred to as a tank circuit.

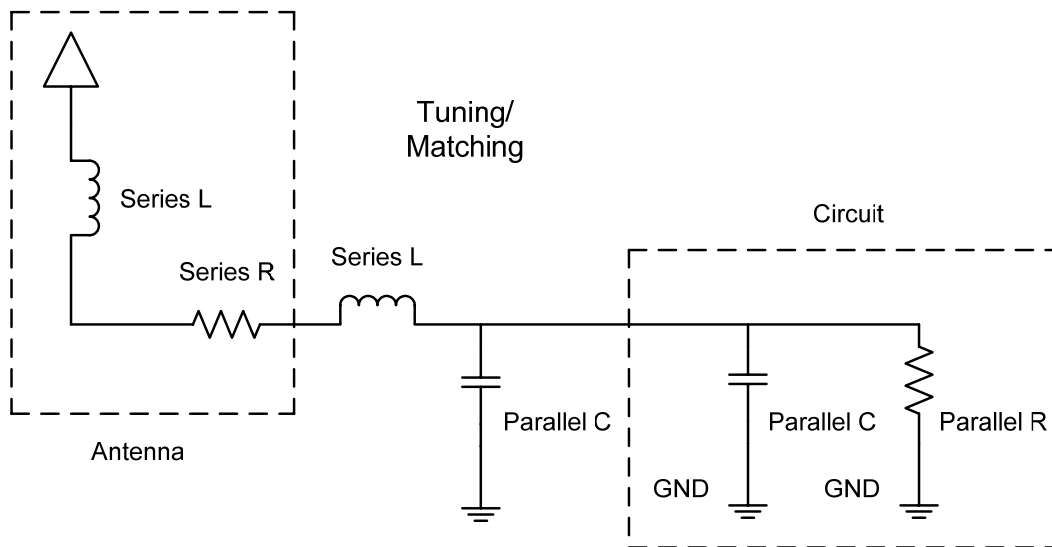


Figure 35: Basic L Matching Network Between Antenna and Circuitry.

Another factor exists, however, in creating a tag that performs well and that factor is the quality factor (Q). Ideally, a high Q value is sought, because the induced voltage is a product of this factor. Longer read ranges are possible with a higher Q. The quality factor is related to bandwidth though, as the following formula shows [7].

$$Q = f_0 / BW$$

The numerator is the carrier frequency, 13.56 MHz, and the denominator is the bandwidth. Because the frequency is set, if the Q value increases, the bandwidth decreases. Bandwidth in RFID relates to the frequency range that the tag will still resonate at for successful operation. If the Q value is too high, the bandwidth is very narrow, and environment influences that affect the tag can easily detune it and prevent operation. Because metal can significantly influence a tag, and because this application must be tolerant of metal, a broader bandwidth is important. As an example, if the metal of the train detunes the tag so that it resonates at 13.00 MHz, the tag should be able to operate with a tolerance of at least ± 560 kHz. Q value must therefore be limited to a value that can accommodate both read range and bandwidth.

4.2.2 Antenna-Circuit Analysis

Standard methods exist for tuning the circuit-antenna system: the S-parameter measurement method, and the voltage measurement method [7]. The S-parameter measurement method requires a network analyzer. The available analyzer has a 50 ohm input impedance. The problem is that the tag being designed is not 50 ohms, and therefore measurements will not be accurate. It is theorized that tag performance can be improved if the resistance of the circuit is allowed to be as low as it can be. That is, it is possible that the resistance could turn out to be less resistive, say 25 ohms, after the circuit and antenna designs are completed, and that this value makes the circuit resonate better. Because powering is a great concern, this is the direction that is taken and so the network analyzer method is not used.

The second method involves using an oscilloscope to monitor the voltage improvement as the tuning elements are adjusted. This method fits the needs of this design stage, though a modified version of this method is used. The oscilloscope, used to determine the voltage, is replaced with the LED. Using the previous blinking LED program and a set of tuning elements, the LED would be observed for luminosity/intensity and operation. Distances could quickly be checked, and trial and error tuning performed.

An appropriate starting point is first established. Using the frequency formula in the above section, the inductance-capacitance product is determined. The inductance of the antenna and the capacitance of the circuit are then measured using the LCR meter, and estimates made for series L and parallel C tuning elements. While the current circuit design does not have the exact final capacitance of the prototype circuit, it is sufficient as a testing start point. The LCR meter measurement determined circuit capacitance to be between 3.6 and 5.8 pF. The variation is due to the blinking LED within the circuit. Measuring the antenna, the series inductance is determined to be 7.6 uH. In an optimized circuit, the spiral antenna can be designed to provide the exact inductance necessary. Optimized antenna design is beyond the scope of this research and is a Phase II consideration. Because the L matching network is used, Table 3 lists a series of potential L and C combinations to use. The first column represents available inductors from Coilcraft. The second column represents the antenna inductance, which is added to the first column to find the total inductance. Total capacitance is then the calculated LC value divided by this total inductance. The measured lower circuit capacitance, column 5, is subtracted from the

column 4 total to determine the matching capacitor value required. This procedure is repeated using the upper circuit capacitance in column 7, which gives the matching capacitor value of the last column.

Table 3: Possible LC Tuning Values For Tag B L Matching Network

Coilcraft (CC)	Antenna (Ant)	Total (L_T) Ind	Total (C_T) Cap	Circuit (Circ1)	Tuning Cap	Circuit Circ2	Tuning Cap
(uH)	(uH)	(CC+Ant)	LC / L_T	(pF)	$C_T - C_{Circ1}$	(pF)	$C_T - C_{Circ2}$
27	7.6	34.6	3.98	3.6	0.38	5.8	-
22	7.6	29.6	4.65	3.6	1.05	5.8	-
15	7.6	22.6	6.09	3.6	2.49	5.8	0.29
10	7.6	17.6	7.82	3.6	4.22	5.8	2.02
8.2	7.6	15.8	8.72	3.6	5.12	5.8	2.92
6.8	7.6	14.4	9.56	3.6	5.96	5.8	3.76
4.7	7.6	12.3	11.19	3.6	7.59	5.8	5.39
3.9	7.6	11.5	11.98	3.6	8.38	5.8	6.18

4.2.3 Tag Design

Coilcraft inductors are chosen to use in tuning the tag because of their RF characteristics, which include ferrite construction and relatively high Q value [16]. Experimentation confirms this by comparing them to general application surface mount inductors. The same multilayer ceramic capacitors that are used in the voltage doubler are used for tuning as well, because they are good for tuned circuits and filtering circuitry [17].

The placement of the tuning elements in the circuit is shown in Figure 36, as “C tune” and “L tune”. This is the “L Matching” configuration discussed, with the inductor in series adding to the antenna inductance and the capacitor in parallel adding to the circuit capacitance. There is no need for the load resistance in this stage, because the LED is the actual load, but the load capacitor is incorporated for correct modeling. The voltage doubler is powering the circuit and can be ported to the ADC pin as well. It is not shown in the figure below, but it is implemented in the PCB. Because the pin is high impedance, it will not affect these tests connected or disconnected.

TAG B Version 1

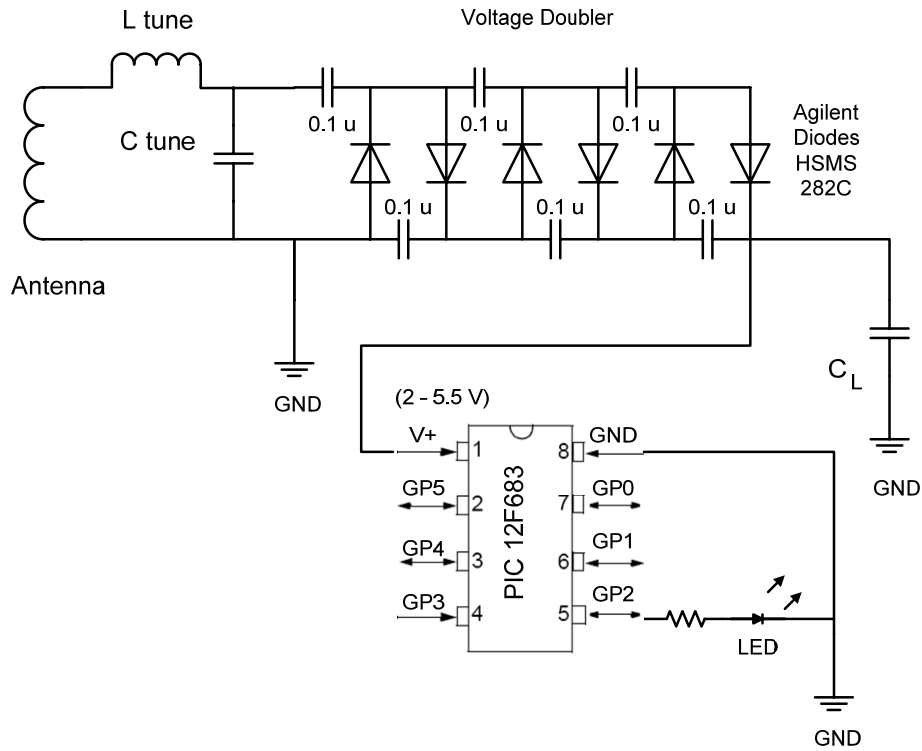


Figure 36: Tag B v1 Circuit Design For RF Powered Tuning.

The PCB layout is shown in Figure 37. The red circles at the corners are holes placed to be able to mount the tag to the testing structure, and are sized for plastic stand offs. At the antenna ends/terminals, surface mount pads (ExpressPCB size 603) are added for the tuning elements. Otherwise, the design is the same as the PCB for the battery powered voltage curve tests.

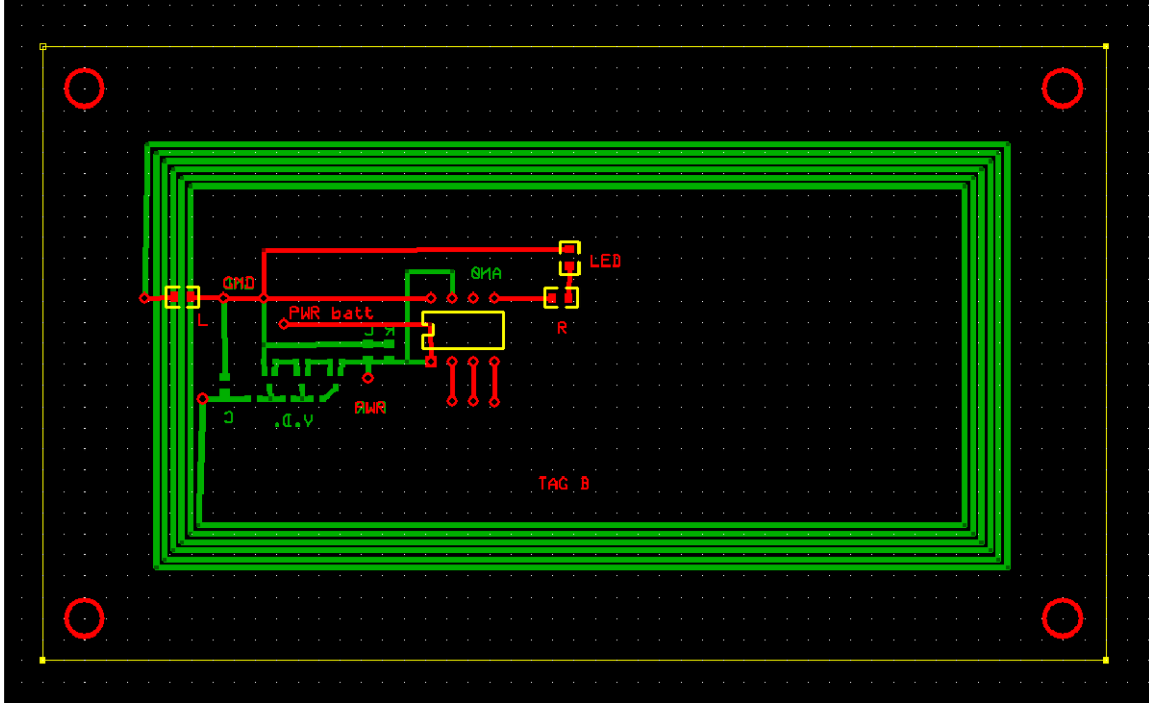


Figure 37: Tag B v1 RF Powered, Tuning PCB Design.

4.2.4 Tag Distance Testing

Table 3 in section 4.2.2 helped identify the starting values to use, and an 8.2 uH inductor (Coilcraft specification) is the first choice. Because the circuit capacitance is not precisely defined yet, a series of capacitors are used to get a sense of their influence. Table 4, in section 4.2.5, lists the tuning set used. Figure 38 shows the test setup. The reader antenna is positioned vertically on its long side, and the tag is positioned at the center and parallel by mounting it to a cardboard box. The box can then be moved back and forth along the marked tape line to determine the operating distance. A hole is cut in the box to be able to observe the performance of the LED. Plastic stand offs are used to mount the tag to the box and not interfere with the RF field.

The progression of tag tuning development is determined based on iterative results, but the initial decision is to try smaller inductor values. This is because a smaller inductor would be better with respect to power consumption due to the resistance of the inductor wire. The actual progression is discussed in the results section, 4.2.5, which is next.

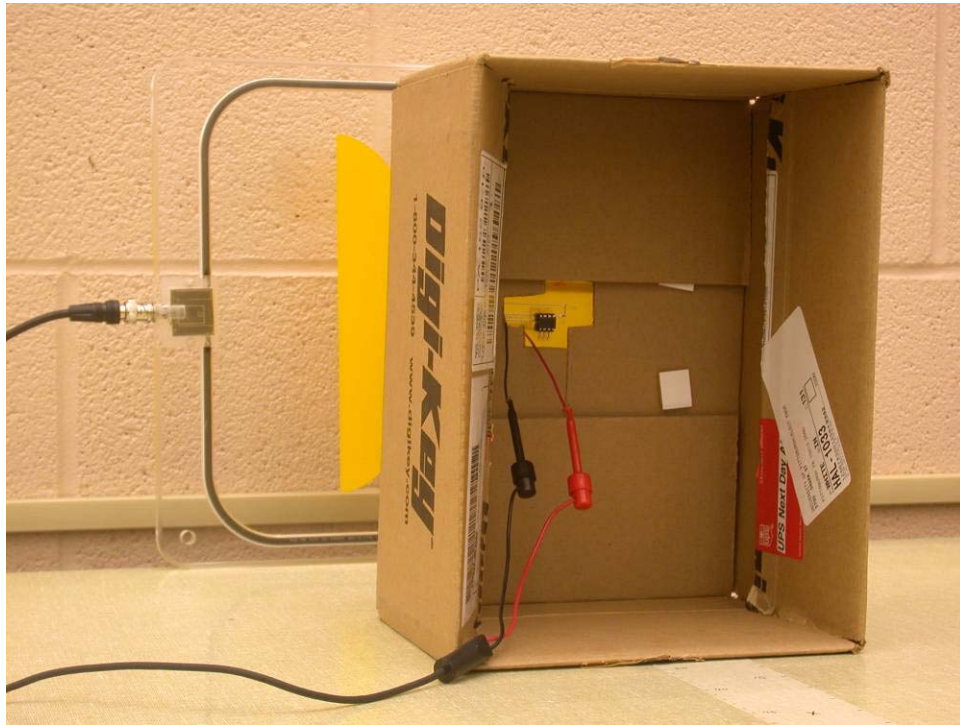


Figure 38: RF Powered Tuning Test Setup.

4.2.5 Tuning Results

Table 4 lists the element sets used for tuning, the blinking LED result, and the distance achieved. It is clear that as the inductance is decreased, the distance improved. It is also clear that the capacitor is helpful in tuning the circuit. Looking at the results while using a 6.8 uH inductor, it is apparent that by adjusting the capacitance values a general “voltage” peak at around the 6 pF value occurs. The final pair of tuning elements chosen is a 1.5 uH inductance with a 2.0 pF capacitance, because this exceeds the 10 inch distance goal. There is room for optimization and improvement, but for the purposes of developing this initial prototype, this set is sufficient. The LED blinked brightly at a distance of 10 inches. The greatest distance observed is 13 inches, but operation is inconsistent. Still it showed the potential for greater obtainable distances.

Table 4: Tag B Tuning Elements and Results

Test Set	Blink	Blink Dist	Test Set	Blink	Blink Dist
8.2uH/2pF	No	-	3.9uH/6pF	Yes	8"
8.2uH/4pF	No	-	3.9uH/8pF	Yes	8"
8.2uH/6pF	No	-	3.9uH/10pF	Yes	8 ½ "
8.2uH/8pF	Yes	5"	3.9uH/12pF	Yes	8"
8.2uH/10pF	Yes	5"	3.9uH/15pF	Yes	8"
8.2uH/12pF	Yes	5"			
8.2uH/15pF	Yes	5"	2.2uH/0pF	Yes	10 in.
8.2uH/18pF	Yes	5"	2.2uH/2pF	Yes	10 in.
			2.2uH/6pF	Yes	10 in.
6.8uH/0pF	Yes	6"	2.2uH/10pF	Yes	10 in.
6.8uH/2pF	Yes	6"	2.2uH/15pF	Yes	10 in.
6.8uH/4pF	Yes	6 ½ "	2.2uH/22pF	Yes	9 ½ in.
6.8uH/6pF	Yes	6 ½ "			
6.8uH/8pF	Yes	6 ½ "	1.5uH/0pF	Yes	11 in.
6.8uH/10pF	Yes	6"	1.5uH/2pF	Yes	11 in.
6.8uH/15pF	Yes	6"	1.5uH/4pF	Yes	10 ½ in.
			1.5uH/10pF	Yes	10 ½ in.

Using the LCR meter inductance measurement for the Tag B spiral antenna, 7.6 uH, and the 1.5 uH inductance added, the total capacitance of the circuit can be calculated. It is

$$[137.759 e^{-18} / (7.6 \text{ uH} + 1.5 \text{ uH})] - 2.0 \text{ pF} = 13.1 \text{ pF}.$$

This is about 7.3 pF greater than the LCR meter measurement of the circuit capacitance, but not an unreasonable value, because there were a few modifications since the circuit was last measured. Also, the nominal Coilcraft inductor value is specified at 7.9 MHz, so the precise inductance at 13.56 MHz is not known, due to component parasitics. Generally the inductance increases with frequency, which would decrease the value of the capacitance calculated.

5.0 STAGE 4: PEAK DETERMINATION ALGORITHM

When contemplating how the tag design might theoretically work, the idea is that the voltage doubler would produce sufficient output voltage to both power the circuitry and create a substantial bell shaped peak. The difference between these two outputs is one of regulation. Components included in the design would require a regulated voltage, while the voltage used to identify the peak should be unregulated to prevent clipping.

Having such a circuit, an algorithm is developed to find the peak voltage of the curve, and prevent any false peaks from occurring. After identifying the peak, the circuit will use RF to communicate the tag identification to the reader. This section discusses the research to create a circuit, develop an algorithm to actually determine the peak voltage, and transmit an 8-bit value to identify the peak.

5.1 COMMUNICATION SOLUTION

The problem of communication is, as noted, that the TI reader is insufficient and is changed to a simple wave generator and amplifier setup. With this came the loss of an RF protocol for transmission back to the reader. A simple amplitude modulation scheme can no longer be employed, without finding another reader unit that has CW operation.

An option available stems from ARS research work at the University of Pittsburgh, where two frequencies are used for power and communication. This solution allows the existing setup to remain as powering to the tag, and new components and devices to be added for tag communication. As an aside, this solution also minimizes the requirement of a lower Q value. Some types of communication protocols require a greater bandwidth and thus, a low Q to operate, but because powering and communication are separate here, Q value can be increased.

5.1.1 Tag Side Communication

The ultimate decision to use any particular communication method is based on the development of a complete system solution, which means that tag solution and reader solution are worked out simultaneously. For ease of discussion, the decisions are treated separately, and the tag is simply defined first.

LINX Technologies makes a variety of RF devices for wireless applications, including transmitters and antennas. For this application, as mentioned, the frequencies used are very important, because they must interact with liquids and metals. The VHF band of frequencies is also acceptable for use in this type of application, although the band is not as globally available. Because the idea is to get an initial product working, the 418 MHz frequency band will be used and the issue of its global regulation explored in Phase II.

The LINX TXM-418-LC transmitter is chosen because of its relatively low power consumption, its compact design, long read range, and single chip solution [18]; No external RF components are needed aside from the antenna. It is also a low cost solution, including PCB integration. A photo of the transmitter setup is shown in section 5.2.3. The antenna chosen is the LINX Splatch antenna. It is a compact planar antenna component suitable for this application, although it does require a very specific ground plane patch. Design issues are discussed in section 5.2.3.

This combination is able to communicate serially using the RS232 communication data protocol at a BAUD rate of 4800. RS232 is chosen for reader side convenience and the BAUD rate is a limitation of the transmitter. Transmission range is up to 300 feet operating at voltage levels between 3 and 5 volts.

5.1.2 Reader Side Communication

The communication system is partially chosen because previous experiments were performed using the LINX components and a customized receiving unit is already available. The device contains a LINX RXM-418-LC receiver, a monopole whip receiving antenna, an RS232 serial port, for connection with a PC, and an integrated power supply. Tag communication is relayed through the receiving chip to the PC, and viewed using the HyperTerminal communication GUI. In this way, the tag ID can be wirelessly transmitted and verified as an ASCII character on the computer screen.

5.2 CIRCUIT DEVELOPMENT

This iteration of circuit design is to incorporate voltage regulation into the circuit, which addresses concerns about high achievable voltage levels, and to add the RF communication components.

5.2.1 Voltage Regulation

Voltage regulation concerns cover two aspects: regulating V_{dd} for the components being used, and developing a way to allow an unregulated voltage to be used by the PIC in determining the peak.

5.2.1.1 The Voltage Regulator

The maximum operating voltage permissible by the PIC 12F683 is 5.5 volts, although it has a slightly higher absolute maximum [15]. A Microchip Technologies regulator, TC1071, is selected to limit the voltage supply to the PIC. It is selected for several reasons: It is thought that integration with a sister component is smoother, it has a low turn on voltage level, its regulated voltage level is adjustable, it is a low drop out regulator (LDO), and it fit the criteria to be used as a voltage reference.

An LDO regulator is chosen because the other varieties all use some sort of switching mechanism to operate and it is considered adverse to the tag [19], as a potential source of noise. The adjustable level of the regulator is convenient, because the circuit is in development and requires design flexibility. The regulator turn on level is critical because the PIC cannot begin running its algorithm until the regulator turns on and supplies power. For this reason, the turn on level and the regulated power supply should be as low as possible. The PIC can operate at 2 volts, so the regulated supply should not be much higher.

Problems arise when considering the unregulated voltage curve. It is desirable to have a voltage that can climb as high as possible in order to observe the peak, but this voltage level can

potentially exceed the regulators maximum operating voltage limits. A regulator that can handle the voltage levels produced is needed, but those levels are not yet known.

Also, in considering the method to input the voltage into the PIC and compare it, there are a few requirements with utilizing the ADC. An ADC uses a reference voltage (V_{ref}) to convert analog values to digital values. By default, the PIC uses V_{dd} as its V_{ref} . While this default condition is convenient in minimizing the complexity, it serves as the highest possible value to compare against and is in opposition to selecting a lower value regulator. A secondary regulating unit for V_{ref} is possible, but to keep complexity and cost low, this direction is not pursued. Instead, a design compromise is developed. The turn on regulation level is chosen to be 2.5 V, which delays operation slightly, but raises the V_{ref} level. This means that the peak voltage could fluctuate between 0 and 2.5 volts. Because higher voltages are possible, a voltage limiting method is needed.

5.2.1.2 The Voltage Divider

The output of the voltage doubler needs to be reduced to levels below that of the voltage reference for proper ADC operation. Again, with the 2.5 volt V_{dd} also being used as the V_{ref} , the design called for a way to limit the voltage but prevent peak clipping. A voltage divider is designed to scale the voltage down below the V_{ref} , but in essence allow it to be unregulated and produce the full voltage curve.

Figure 39 shows the schematic of the solution to this problem and the one additional regulator. The resistors of the regulator voltage divider labeled R3 and R4 are used to adjust the regulated voltage to 2.5 volts. The resistors labeled R1 and R2 define the scaling of the ADC voltage divider. Again, the final values of these resistors depend on the ultimate voltage increase observed. One issue in creating this design is leakage current to ground, resulting in a loss of power. To prevent a significant loss of power, resistor values above 470 k ohm are used in both voltage dividers [20]. Initially, 499 k ohm values are selected for the ADC voltage divider, which results in a halving of the voltage doubler output, and for the regulator.

TAG B Version 3

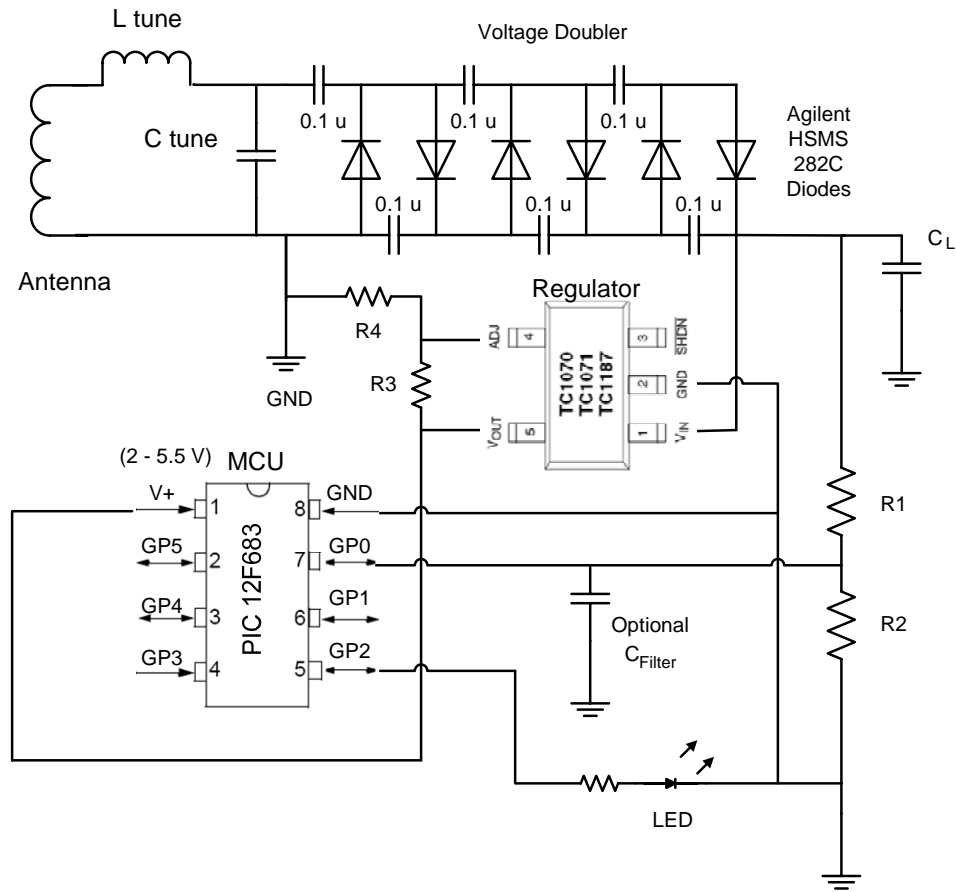


Figure 39: Intermediate Circuit Design Highlighting Regulation.

5.2.2 Transmitter Circuit Design

The most critical redesign effort is to integrate the new transmitter and transmitting antenna into the tag. These two components have very specific design requirements for proper operation [18][21]. The most pertinent being the 1.5 by 3 inch ground plane to which the LINX antenna is optimized. While this may be modifiable, the most efficient transmission is sought so the optimized ground plane is incorporated.

So as not to disturb the electromagnetic field coupling between the spiral antenna and the reader antenna, the ground plane and transmission elements are positioned outside the spiral

antenna. The desired effect is minimal disruption of the electromagnetic flux lines. Figure 40 shows the final circuit, and Figures 41, 42, and 43 show the PCB layout of the design. Photos of the front and back of the Tag B v3 design are also included (Figures 44, 45). A few optional transmitter components can be seen in the detail of the transmitter PCB (Figure 43). These components are part of the optimized design that LINX Technologies suggests and are used to correct noise in the system. In this initial design, these components are not used: a zero ohm, short resistor is used in place of the resistive components, and the capacitor element is simply not included. They are not used initially because they limit the power transfer. One unique requirement is that the port from the transmitter to the antenna needs to be 50 ohms, due to the antenna's design. Because of this, a large trace pad is designed from a LINX model [21]. The distance from the transmitter to the antenna is very short however, which is thought to minimize the criticality of the pad's dimensions.

Powering for the LINX transmitter is provided directly from the voltage doubler. It is designed this way initially because it demands the most power. The absolute maximum operating voltage is 6 volts for the transmitter, and it may have similar issues about the power supply exceeding this level. This problem can be deferred to Phase II. A potential solution is a second regulator. The regulated output of the PIC's regulator is too low for the transmitter to operate, which is why a second regulator is necessary.

The data line to the transmitter is chosen to be GPIO pin 4 of the PIC due to convenient trace positioning and because it is a suitable output port. GPIO pin 3 is not, because it is an input only port. Finally, the grounds are connected so that it would be a common reference for all circuitry.

The LED-resistor series is still part of the design in case the circuit requires visual testing in the future, but it is not used in this stage. An optional noise filter capacitor is included in the design as well, but is not used initially, so that the truest incoming signal can be observed. Several capacitors pads are also designed into the PCB for the regulator. These capacitors, like those elements of the transmitter, can be utilized to reduce noise/interference in the system. They are not used in this design iteration because a clear initial picture of the signal is desired, and minimal delay, associated with additional capacitance, is sought.

As is noted earlier, the voltage divider resistor values for R1 – R2 and R3 – R4 are all initially 499 k ohms. These values cut the output of the voltage doubler in half, and adjust the

regulator to about 2.5 volts, respectively, while minimizing leakage current. The load capacitor remains at its previous value of 0.1 uF.

TAG B Version 3 with Transmitter

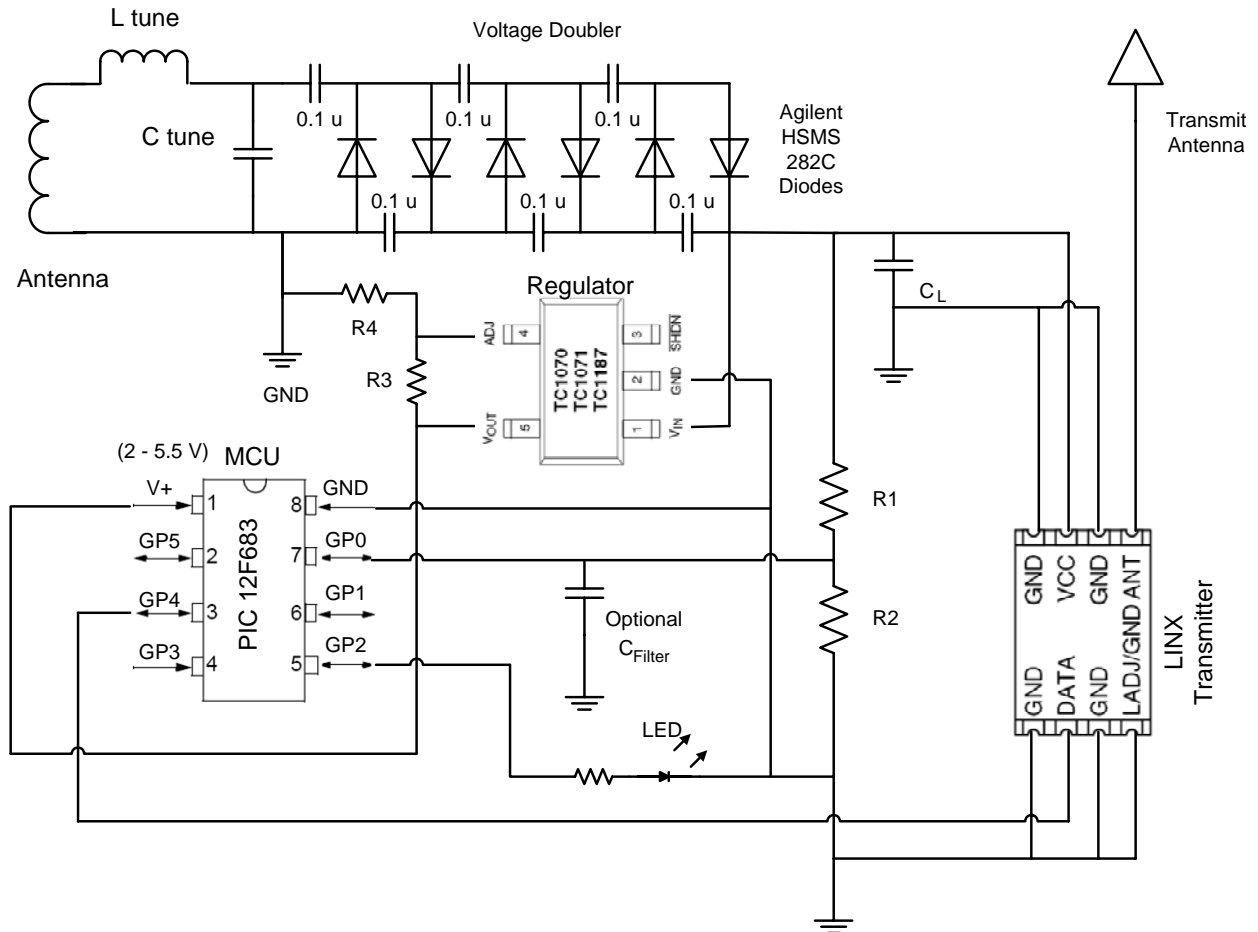


Figure 40: Tag B v3 Circuit Prototype Design For RF Transmission.

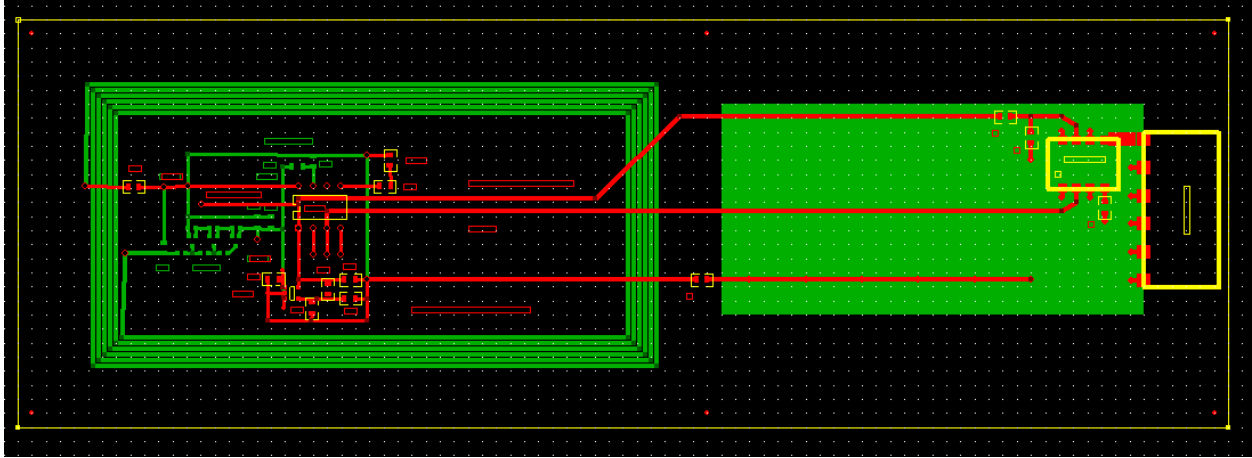


Figure 41: Tag B v3 PCB Design with Transmitter Elements.

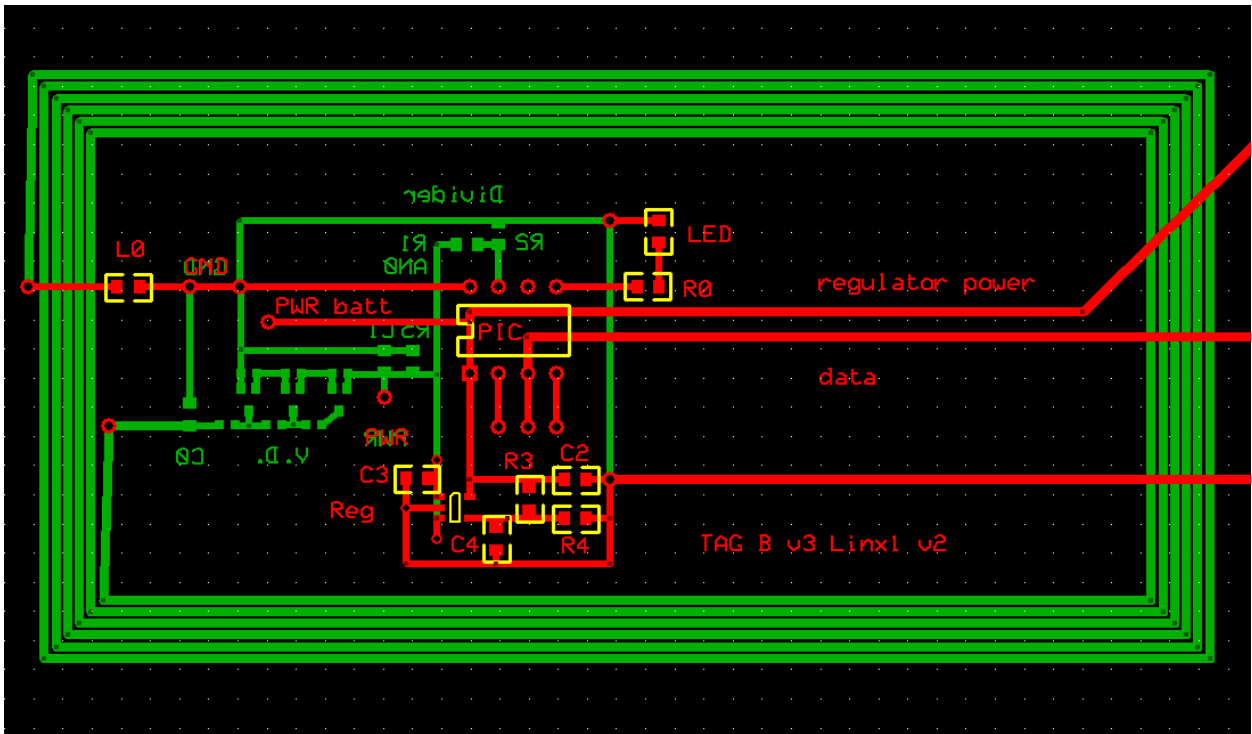


Figure 42: Tag B v3 PCB Design, Regulator Detailed.

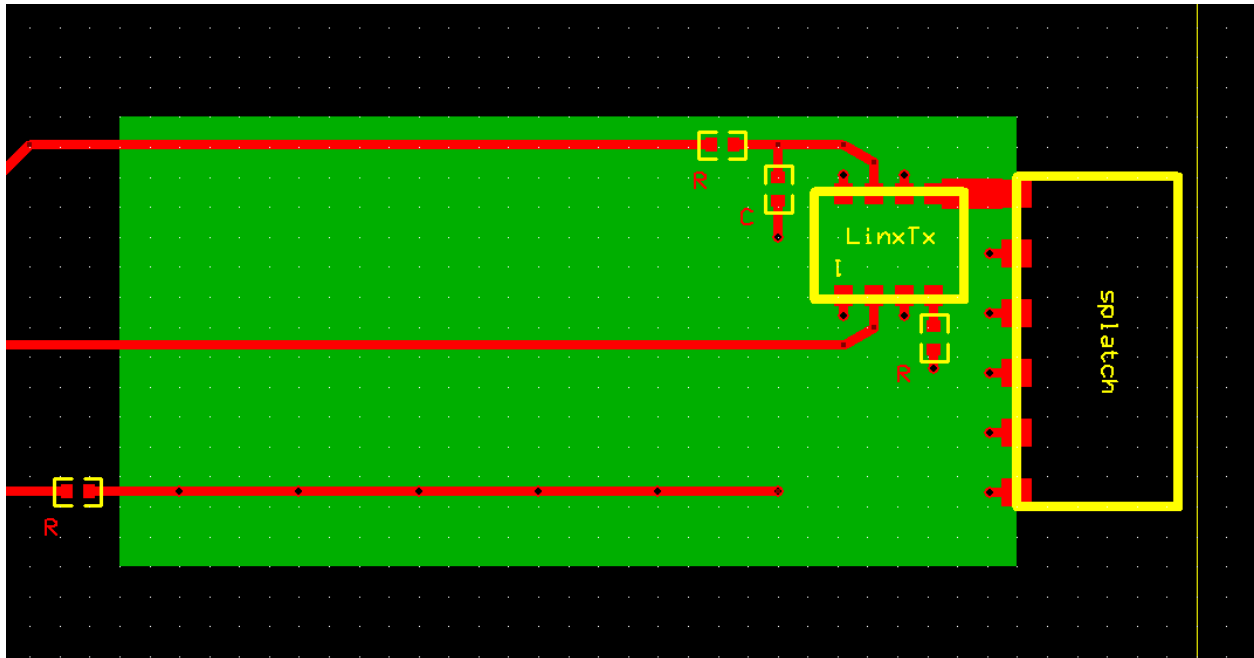


Figure 43: Tag B v3 PCB Design, Transmitter Detailed.

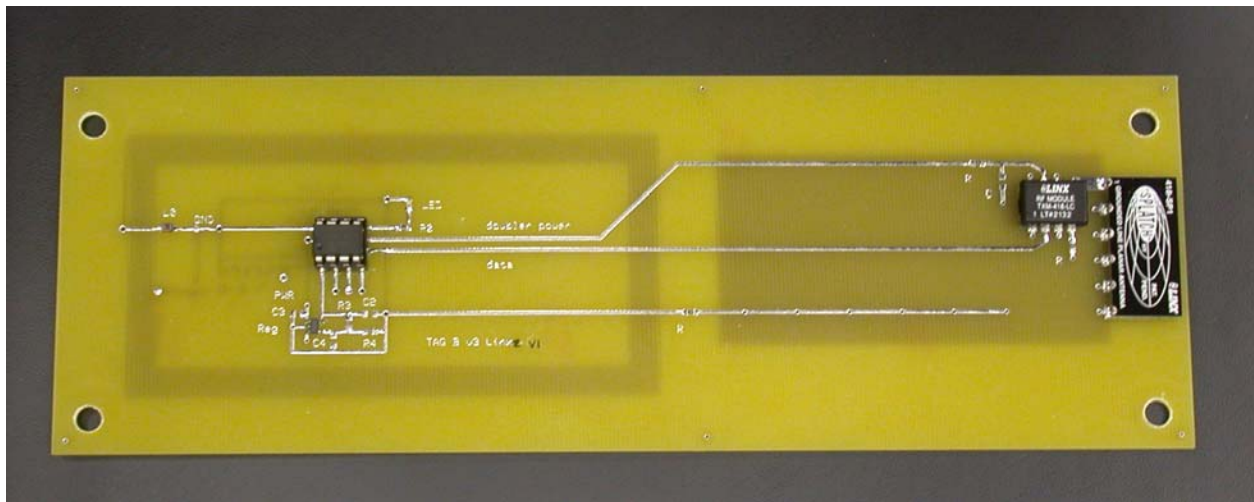


Figure 44: Circuitry Side Photo of Tag B v3 Design.



Figure 45: Spiral Antenna Side Photo of Tag B v3 Design.

5.2.3 Transmitter Testing

Discussion of the peak algorithm and its testing is in section 5.3. This section is concerned with the test setup, focusing on circuitry issues, and explaining the verification method of the transmitter design.

In order to be confident that the transmitter design will work for the RF tests, a battery powered testing board is created. This board (Figure 46) is the same design as the left half of Figure 41, except that a PIC is incorporated to transmit hard coded data. The PIC code will use the predefined RS232 functionality and the `putc()` method of the software to verify the transmission of a character. Figure 47 shows the test setup. The LINX receiving unit is in the foreground of the photo, and the test tag is in the background using a small box to hold it vertical, while being powered by the battery. The receiving unit is connected to the 9 pin serial communication port on a PC, COM1, and HyperTerminal set up to operate at 4800 BAUD through that port. The letter 'A' is used as the hard coded value to transmit.

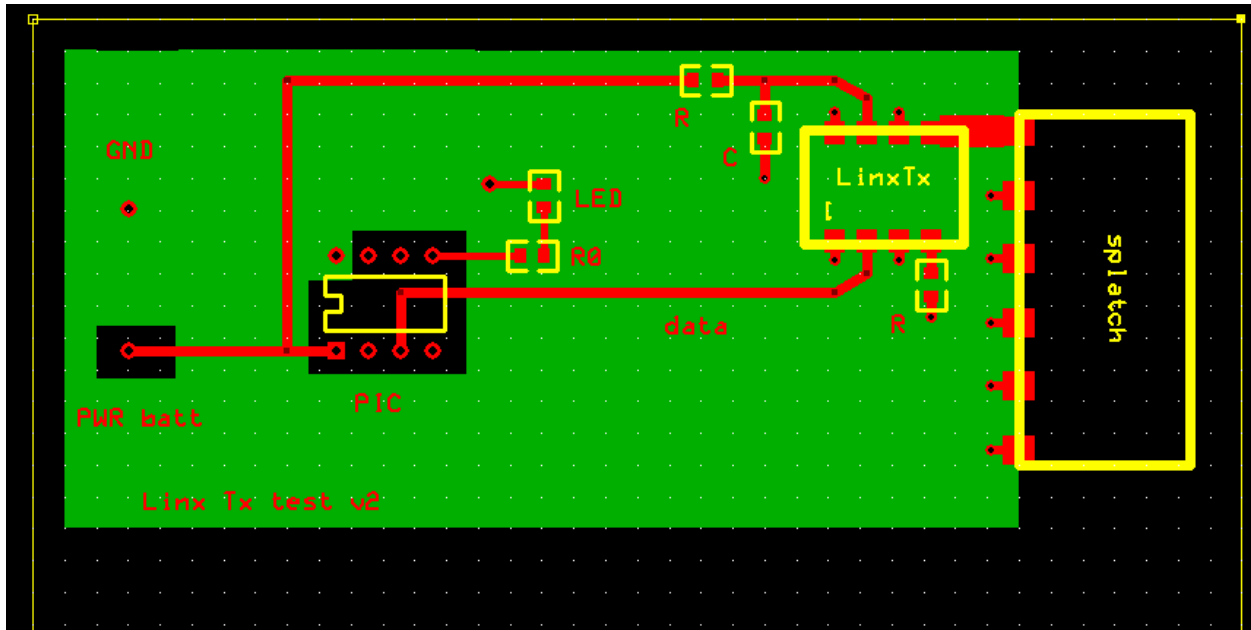


Figure 46: LINX Transmitter Test PCB.

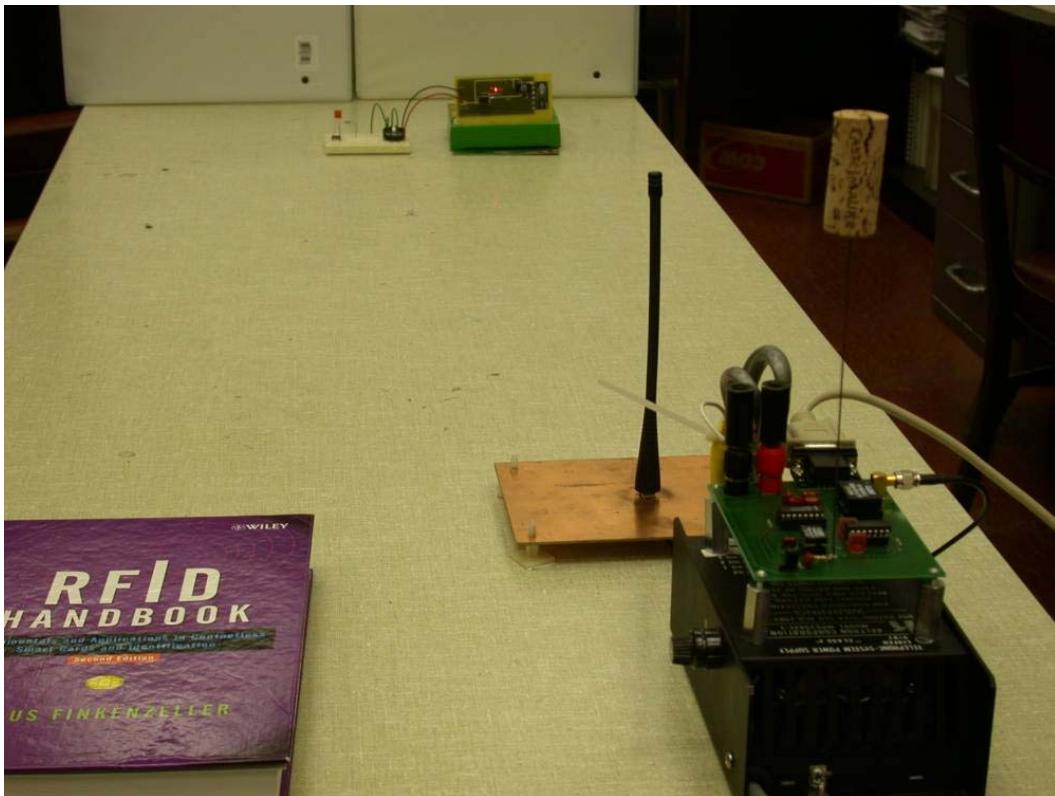


Figure 47: LINX Transmitter Test Setup.

The next set of tests includes positioning Tag B at fixed distances above the reader antenna, and evaluating performance. Figure 48 shows the setup. The tag is positioned over the reader antenna using a cardboard box, and the receiving unit is in the background, about 6 feet away, connected to the computer. Previous tests indicate that the transmitter can successfully transmit at this distance, and it is a convenient distance for existing equipment.



Figure 48: RF Powered, Tag B Transmission Setup.

The testing is designed to first test the read range of the tag, so the tag is placed at 13 inches above the reader antenna and moved closer in 1 inch steps. After the tag is placed at a specific distance, the reader antenna is energized. The initial PIC program for this set of tests simply performs one transmission every 1000ms (Figure 49). This long delay is chosen to reduce the number of variables in the test by eliminating the load capacitor charge time delay from the experiment. The power used is 4 watts.

```

#include <12F683.h>
#device adc=8
#fuses NOWDT,INTRC_IO, NOCPD, NOPROTECT,
NOMCLR, NOPUT, BROWNOUT, IESO, FCMEN
#use delay(clock=4000000)
#use rs232(baud=4800,parity=N, xmit=PIN_A4,rcv=PIN_A1,bits=8,invert)
    // invert required!

void main()
{

    setup_adc_ports(sAN0|VSS_VDD);
    setup_adc(ADC_CLOCK_DIV_8);
    setup_timer_0(RTCC_INTERNAL|RTCC_DIV_1);
    setup_timer_1(T1_DISABLED);
    setup_timer_2(T2_DISABLED,0,1);
    setup_comparator(NC_NC_NC_NC);
    setup_vref(FALSE);

    delay_us(50);

    output_low(PIN_A2);
    output_low(PIN_A4);

    while(TRUE)
    {
        delay_ms(1000);

        putc('U'); // binary 0101 0101
    } //end while
} // end main

```

Figure 49: A PIC Program Written to Transmit a Character.

5.2.4 Transmitter Results

After working out programming issues, the test transmitter device worked very well, transmitting to distances greater than 12 feet. It is determined that the Splatch antenna radiates isotropically, so the antenna works well both vertically and horizontally. One of the programming issues resides with the RS232 C code directive, “#USE RS232”. A parameter exists, called invert, which must be used in order to reverse the polarity of the data bits for proper

RS232 protocol. The RS232 transmission is a 10-bit value including a start bit, 8 data bits sent in LSB to MSB order, and a stop bit.

One issue in this testing is power reserve. The load capacitor is not sufficient in early testing and is increased in sized to be able to successfully transmit a character. Sufficient power existed for the PIC to turn on and operate, but when the program attempted a transmission, the power supply would fall below 2 volts and the PIC would shut off. Figure 50 shows the oscilloscope capture of this action. It shows the first bit of the character transmission is successful (input 1), and the second bit fading from loss of power. It can also be seen that the capacitor is charging back up (input 2). Eventually, the PIC will turn on again and try a second time.

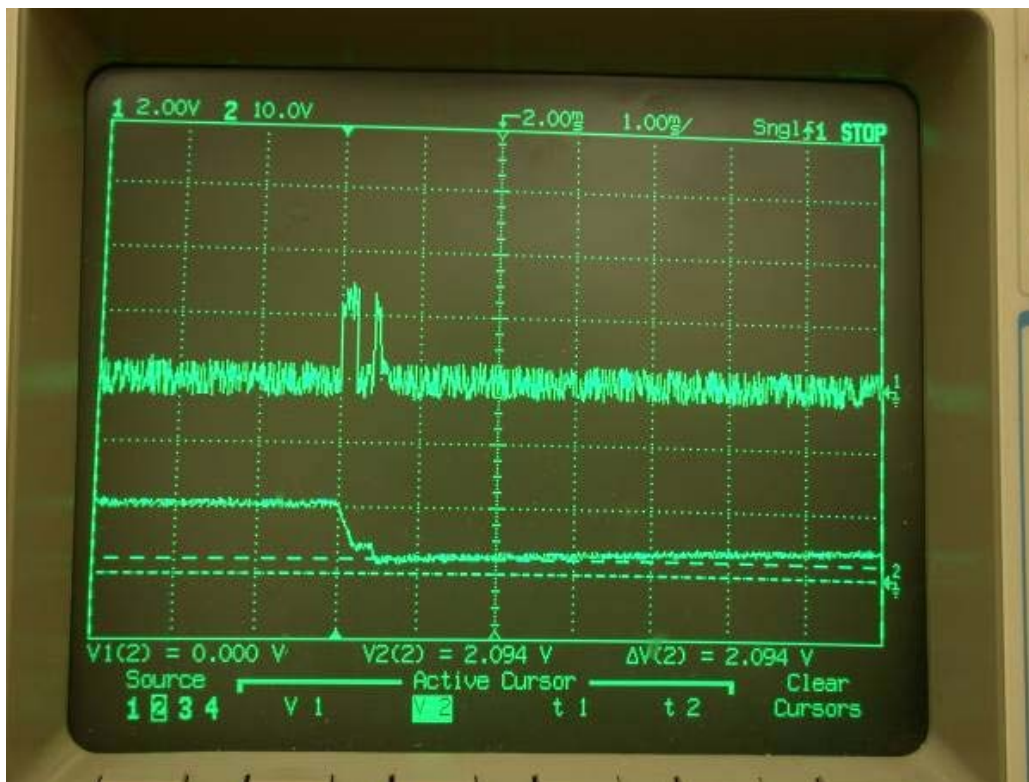


Figure 50: Oscilloscope Capture of Failing RF Transmission.

The load capacitor is eventually increased to 1.2 uF, which is sufficient to sustain a full 10-bit transmission. Figure 51 shows the oscilloscope capture of the successful test. The character used in this test is 'U', because its bit pattern is alternating 1's and 0's. It should be evident from the photo that the voltage increases slightly during a zero bit. This is due to the

simple OOK encoding technique that uses a high voltage to signify a 1 and a low voltage to signify a 0. Because the no power is being used to represent the 0 bits, the load capacitor can accumulate charge. This means that the greater the number of high bits being sent the greater the energy requirement. A character that contains all 1's is also successfully transmitted with a 1.2 uF load capacitor.

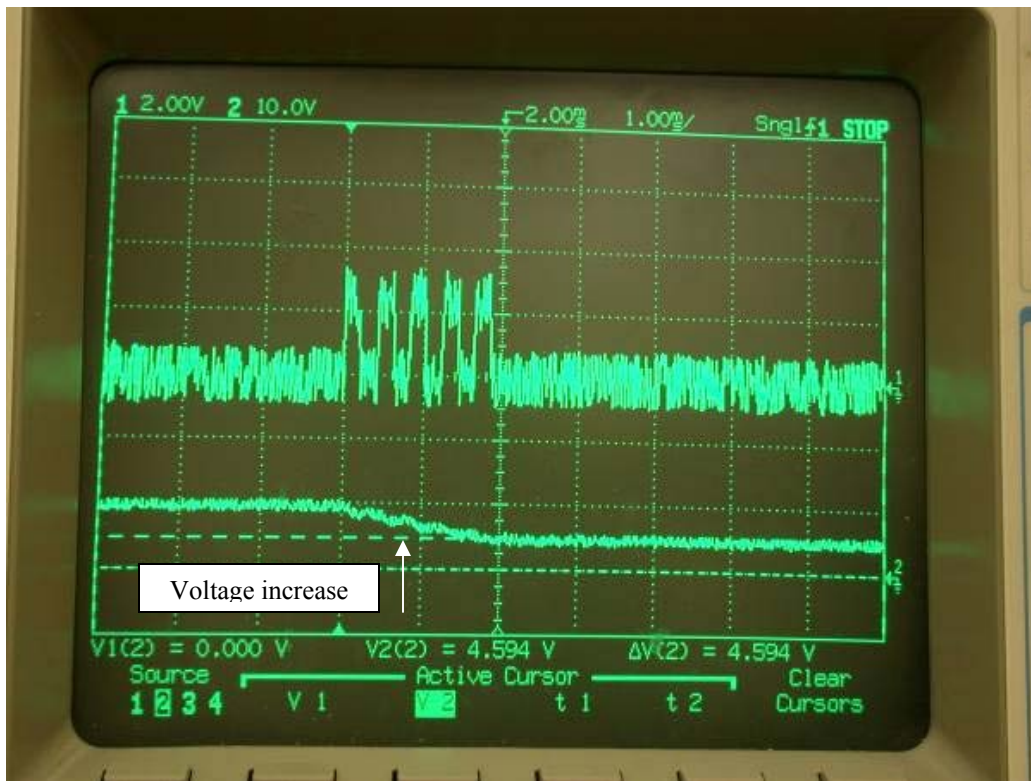


Figure 51: Oscilloscope Capture of Successful RF Transmission.

The program is modified slightly to observe the fastest transmission rate possible. While this is not directly related to the project goals, because only one transmission is actually necessary, it is considered as a second technique in observing the peak voltage response. It did not prove very useful, but clearly shows the transmission characteristic and a limitation of 100 ms between transmissions (Figure 52).

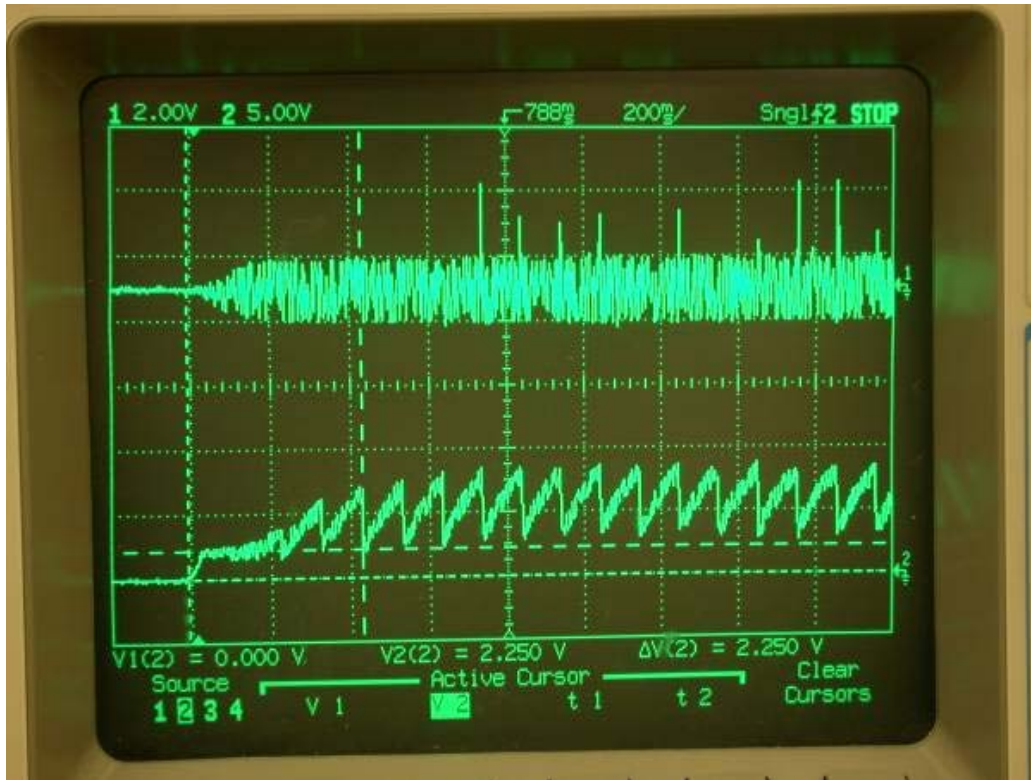


Figure 52: Oscilloscope Capture of a Rapid Succession of RF Transmission.

In this photo, the first three transmissions fail before the charge is sufficient to complete them. This provides a glimpse into the necessity of having adequate charge up time before attempting a transmission. The cut off voltage level for a successful transmission is 2.25 volts. If the load capacitor energy is used to the degree that the voltage falls below this level, the microcontroller shuts off and the transmission ends. The Inputs are reversed in this photo. Input 1 is the transmission output. This signal is not clear because the time division was changed to 200 ms to observe the many transmissions.

5.3 PEAK ALGORITHM SOLUTION

The circuit design at this point is complete, and only the voltage divider resistance values will require some adjustment due to the unknown voltage level that will be reached. Successful RF powered transmission of a character has been proven, so the focus turns to developing an algorithm to identify the peak of the voltage curve. The 1 mph train set will be used to move the tag through the reader antenna field in a consistent testable manner. This section describes the design of the algorithm, verification methods used, pertinent issues, and results.

5.3.1 Peak Algorithm Overview

In order to begin coding, two details are reviewed: the purpose of the algorithm and speculation on the noise previously observed. First, pseudo code is established to clarify the general goal and begin design. Figure 53 contains the pseudo code segment. It is basic, but essentially outlines the problem. There is some initialization required, then the PIC does an ADC read to obtain a new voltage sample, and the sample is compared against the current high value obtained. If the new sample is higher than the saved high value, then the new sample becomes the high value and the voltage is still increasing. If the new sample is lower than the high value, then the high value must be the peak and the tag should transmit its ID.

```
Initialize var high to 0
Read voltage sample
Compare to high
If sample is greater
    save sample as high
Else
    peak found, transmit
End
```

Figure 53: Peak Algorithm Pseudo Code.

This pseudo code is very precise in its peak determination, and the 1 sample delay it takes to identify the peak is fixed so it can be accounted for in calculating the exact position. The 1 sample delay comes from the way the algorithm was created. A peak is identified by the realization that the voltage curve is decreasing, which is the first sample after the peak. The transmission delay is also fixed so this delay can also be calculated, thereby describing the exact distance – position to the train controlling system. Figure 54 shows a high level view of what's happening. The second line down from the voltage peak that extends past the reader antenna is meant to signify extra time available due to the charge accumulated, dX . The tag will be out of the electromagnetic field, but will theoretically still be able to transmit. This is speculative and will end up being a function of the load capacitor size used, the power supplied, and the size of the antenna.

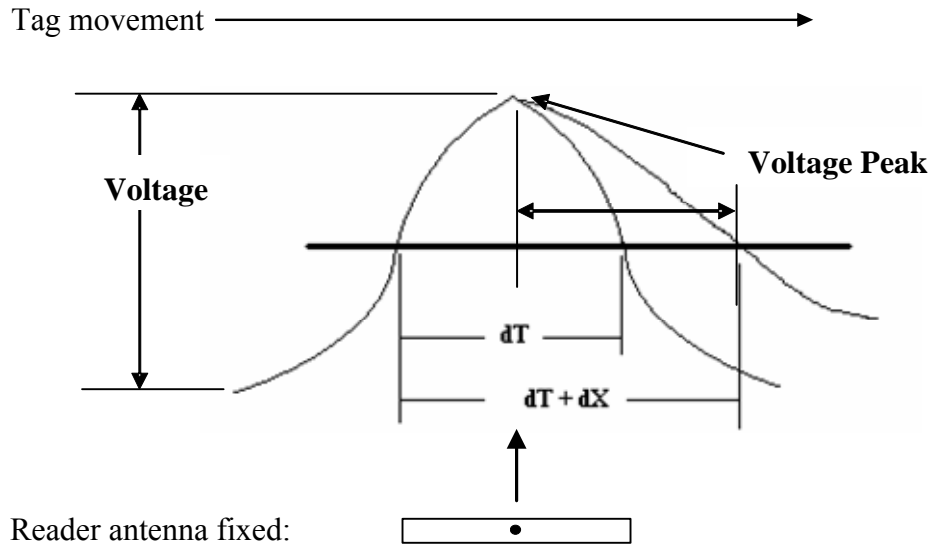


Figure 54: Tag Movement Through Reader Field and the Voltage Curve.

The pseudo code is not realistic, however, and the noise, or interference, in the system must be considered. Figure 55 demonstrates a possible noise scenario. Using the simple pseudo code algorithm, any of the high points in the figure represent a peak, because there is a lower value immediately after it. It is also apparent from the example that it is not just the low points that are a problem, but some of the high points that happen to be lower than a previous noise spike. Though the peak voltage is still climbing, *noise sag* can make the algorithm falsely determine that it has found the peak. A method to eliminate this *noise sag* is therefore required. A simple algorithm solution is sought, but a software or hardware filter is also considered. Hypothetically, if a filter is used the voltage curve shown in Figure 54 will be representative of the actual curve and the pseudo code algorithm is sufficient. Any solution represents transmission delay, however, and must be explored.

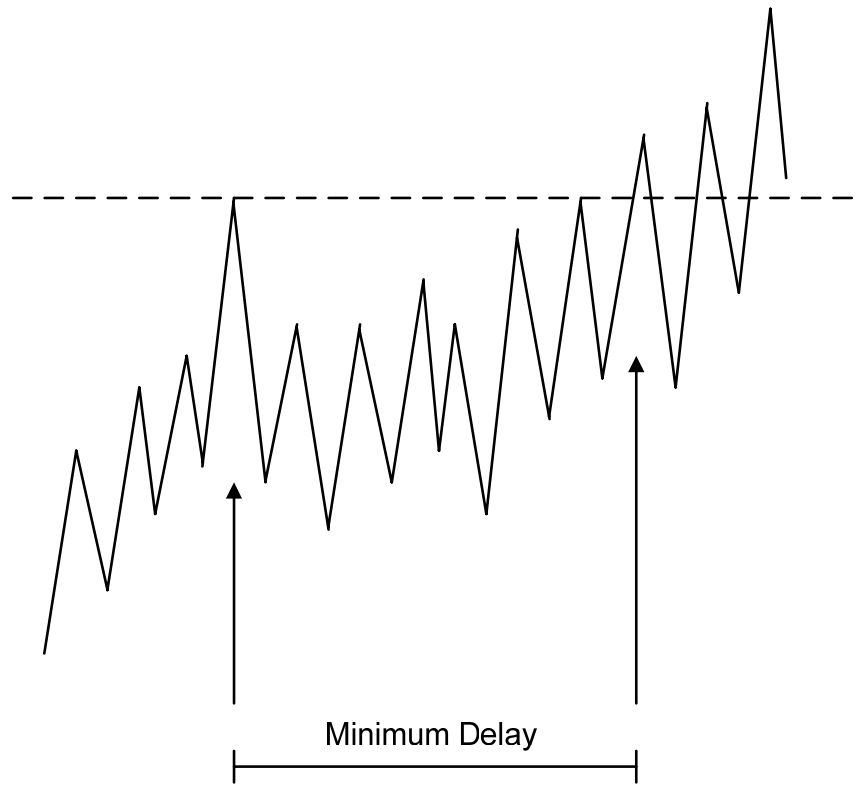


Figure 55: Noise Example with Inherent Delay.

5.3.2 Peak Algorithm Design

Researching the problem, three issues are identified and addressed: the peak is related to speed moving through the field, there is noise variation within the curve, and only one transmission should occur. The voltage curve is captured on an oscilloscope and provides insight into these concerns. Figure 56 presents the curve at 1 mph. It is clear from the photo that a voltage plateau exists before the voltage begins to steadily increase toward the peak. If the peak algorithm is started before the voltage is rising, it will falsely determine a peak and can be nearly 8 inches off center. Also, more noise exists at the start of the bell shape than during the sharper voltage increase.

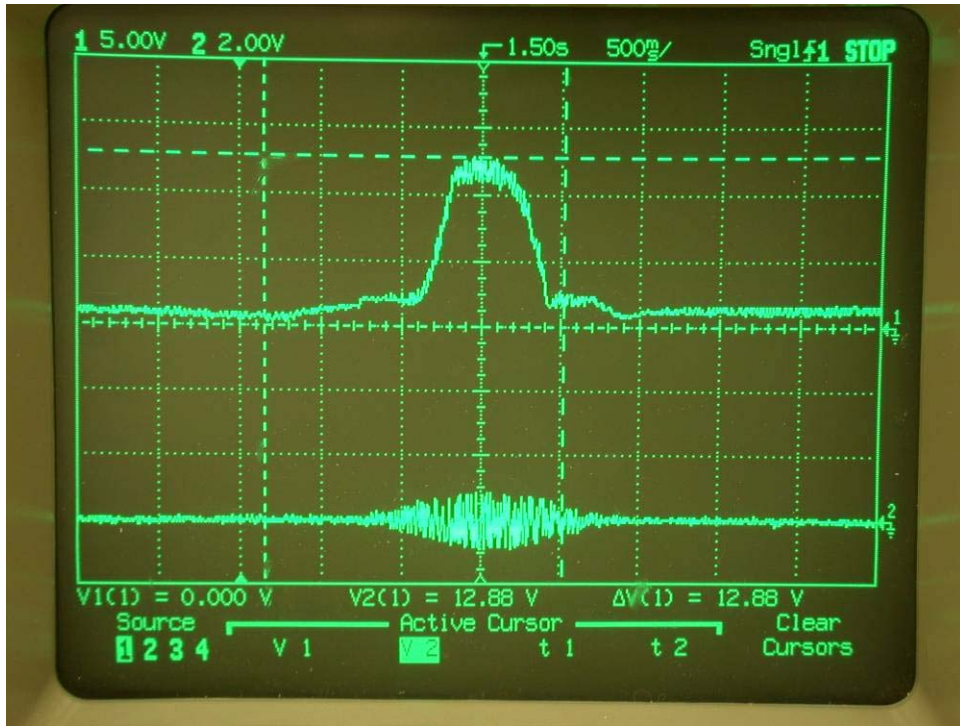


Figure 56: Full Voltage Curve Oscilloscope Capture at 1 mph.

A single solution is found to handle the plateau and noise variation issues. The peak transmission algorithm is only allowed to begin when a significant voltage increase towards the peak occurs. Figure 57 shows the program flow. The voltage division in the above photo is 5 volts, and the plateau determined to be about 2.5 volts plus noise. It is estimated that if the voltage is beyond 3 volts, the voltage will be increasing sufficiently, so this is used as a starting threshold.

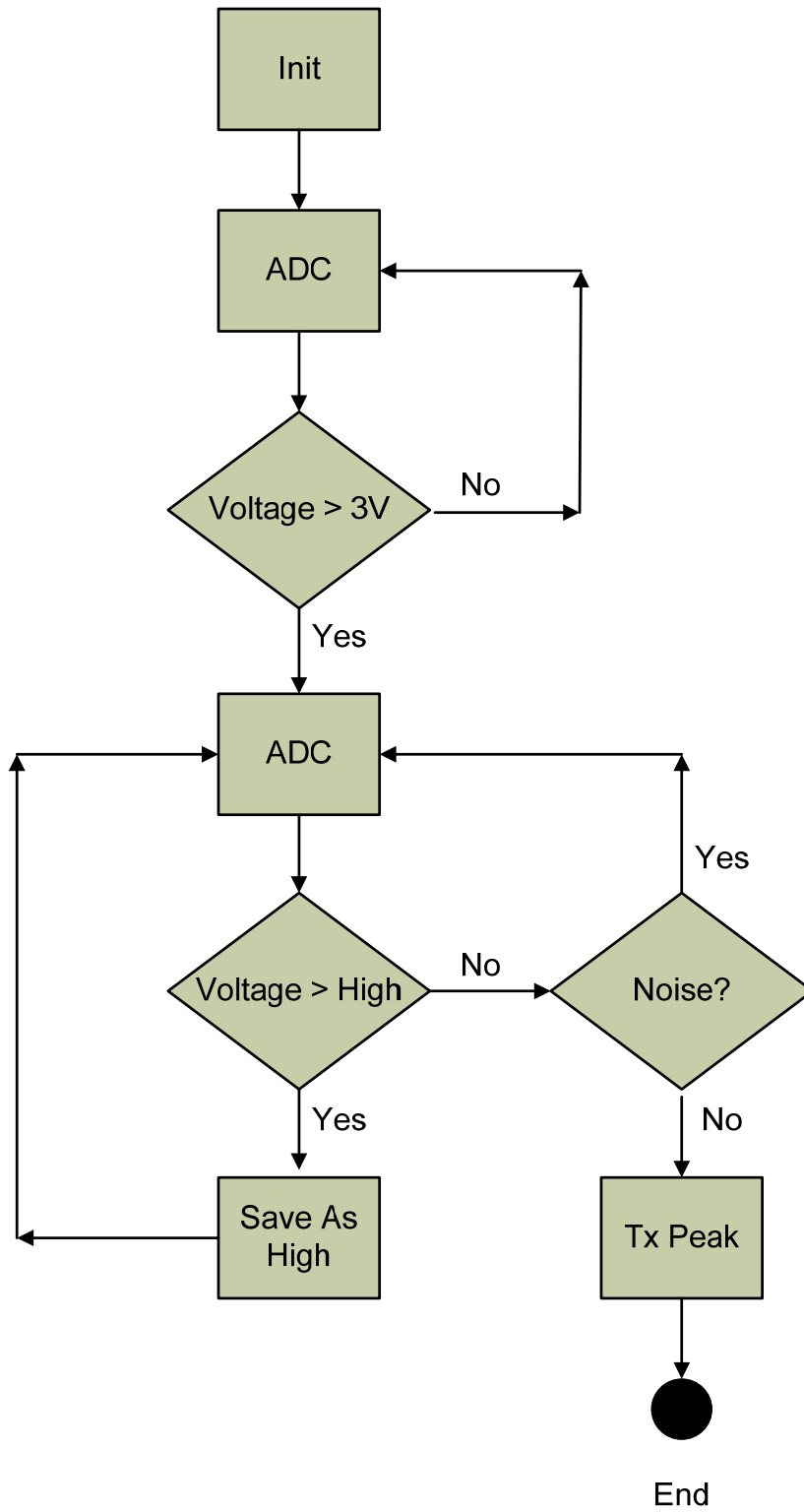


Figure 57: Peak Algorithm Program Flow Chart.

In order to explicitly control the PIC operation and permit only a single transmission, a loop is inserted directly after the transmission occurs. The program will essentially end, but be executing known code. This is useful to gauge power usage issues, and will likely be valuable to Phase II research.

Figure 58 displays the algorithm developed. There are two outer loops; one that prevents the peak detection algorithm from starting until a specified voltage threshold is reached, and one that continuously samples the voltage level after starting. As mentioned, the initial voltage level is chosen to be 3 volts. Because the PIC performs an ADC, the voltage is converted to a decimal value. Therefore, the 3 volt value is represented by its decimal equivalent and is used to compare with the current voltage sample.

Once the peak detection algorithm is started, it must continually loop and sample the voltage, comparing it to the high value as described previously. The process is complicated by the noise in the system and so the samples are additionally checked to be noise or not.

Noise is handled by using a variable to essentially delay the decision of whether the peak is found or if *noise sag* is occurring. The noise variable is called *sampleNoise* in the peak algorithm code, but will be referred to as NVar. Referring to Figure 55, if the algorithm waits the length of this delay and samples again, a voltage higher than the saved high will be obtained thereby identifying the previous values to be *noise sag* instead of the peak. Upon finding the peak, the transmission will have also been delayed this length of time. This delay negatively impacts the speed that the tag can achieve because at higher speeds delay means that the tag has moved out of the electromagnetic field and must rely solely on its energy reserve. For this reason, future tag designs will be optimized for noise reduction in the system. Another option is to use filtering, and is explored in section 5.3.4.

```

while(TRUE) //0 loop until time to start
{
    voltage = read_adc(); // get sample
    delay_us(50);

    if(voltage > 73) //0 start peak algorithm past 3.5V threshold
    {
        while(TRUE) //1 loop until peak identified
        {
            voltage = read_adc(); // get sample
            delay_us(50);

            if( voltage > high ) //1 compare sample to high value
            {
                high = voltage; // if higher, save new high
                sampleNoise = 0; // reset noise variable
            } // end if1
            else //1
            {
                if( voltage <= high ) //2, peak decreasing or noise
                {
                    if( sampleNoise == 129 ) //3
                    { // 130th time voltage is still decreasing = peak

                        voltTx = (char)high; // conversion for transmission
                        putc(voltTx); // transmit peak

                        while(TRUE) // end - loop until out of field
                        {
                            delay_ms(100);
                        }
                    } //end if3
                    else //3, possible noise sag; increment
                    {
                        sampleNoise = sampleNoise + 1;
                    } //end else3
                } //end if2

                else //2, error
                {
                    putc('X'); // error
                } //end else2
            } // end else1
        } //end while1
    } //end if0

    delay_us(150); // approximate inner cycle
} //end while0

```

Figure 58: The PIC Program Written to Transmit the Voltage Peak.

5.3.3 Algorithm Testing Method

The train setup is again used to test the tag at 1 mph (Figure 59). The train carries Tag B completely through the reader antenna field enabling the entire process cycle. An oscilloscope and 10x sensitivity probes are used to observe the voltage curve and identify the RF peak transmission. Three 22 AWG wire segments are soldered to the tag: one at the voltage doubler output point to record the unregulated voltage, one at ground, and one at the transmission output pin of the PIC. These wires allow the voltage to be monitored on the oscilloscope.

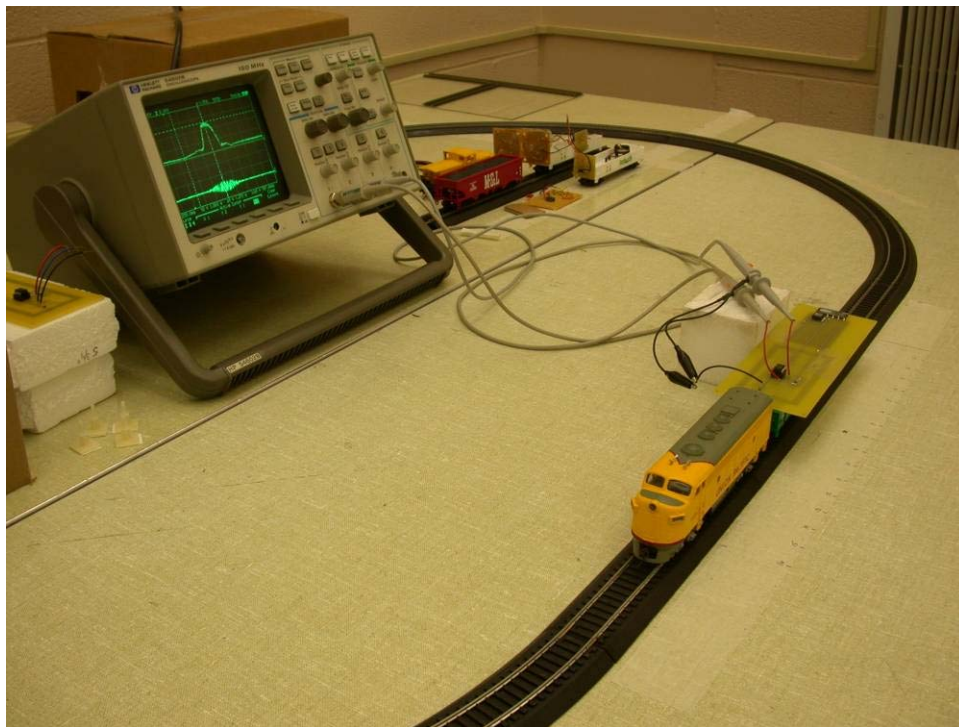


Figure 59: 1 mph Tag B Peak Determination Test Setup.

Figure 60 shows the complete test setup with the reader antenna 10 inches under the table, the LINX receiver at the edge of the table about 2 feet from the tag, the PC connected to the receiver with the serial connector cable, and the HyperTerminal GUI running. All of the equipment is turned on, the train carries the tag through the field, and the PIC is powered up, determines the peak, and then transmits the peak voltage. The peak voltage is sent instead of an

arbitrary ID, to be able to verify the voltage level chosen as the peak. The receiver will then pick up the transmission, relay it to the PC, and HyperTerminal will show the respective ASCII character. This character will then be translated to a decimal value, which can be converted back to a voltage. Appendix B contains the ASCII tables used. The conversion process is a decimal value multiplied by the voltage step divided by the voltage divider used. As an example, the threshold voltage, DEC 73, from the peak algorithm conversion is,

$$(73 * (2.45/256)) / (499 \text{ k} / (2 \text{ M} + 499 \text{ k})) = 3.5.$$

This formula shows that DEC 73 is the voltage equivalent of 3.5 volts, which is the value at which the peak algorithm should start up. It also shows a change in the voltage divider, reducing the voltage to the ADC even further by using a 2 Megaohm value for R1.



Figure 60: 1 mph Tag B Peak Transmission Test Setup.

The same operation will be performed on the peak value transmitted, which would then be compared with the voltage level shown on the oscilloscope for verification. This process is performed using different tag to reader antenna distances and various tag to LINX receiver distances.

5.3.4 Signal Noise Analysis

Signal noise is a great concern. Because it impacts achievable speed, an analysis is performed to better understand its affect. An FFT is run on peak voltage curve data to identify other frequency components in the signal, determine the origins if possible, and determine if they can be removed. This is done in two ways: first, the data is captured using a different oscilloscope that is able to save the data in CVS format and then the data is imported into MATLAB, and second, an FFT Analyzer is used directly with the voltage signal as input. Next, a filter design simulation is performed to determine the viability of using a digital filter.

A voltage curve is obtained using the peak detection algorithm with the transmit line commented out. That way, the curve would be the same exact curve that the PIC ADC is seeing. The figure below shows the series of data import-exports necessary. The data collected is in CVS format, which is a comma delimited format. This file is imported into Excel and separated into its voltage and time components. A chart is created to confirm the voltage curve at this step. Then the data can be copied into MATLAB as vectors for analysis. The curve is then plotted once again to verify translation. Once the data is entered into MATLAB, an FFT can be performed (Figure 62). It is determined in Excel that the oscilloscope is able to save the full curve using a sampling rate of 500 us. The cycle of the peak algorithm comparison is about 138 us. While the oscilloscope's sampling rate is nearly 4x lower than that of the actual signal, the simulations are adequate for analysis.

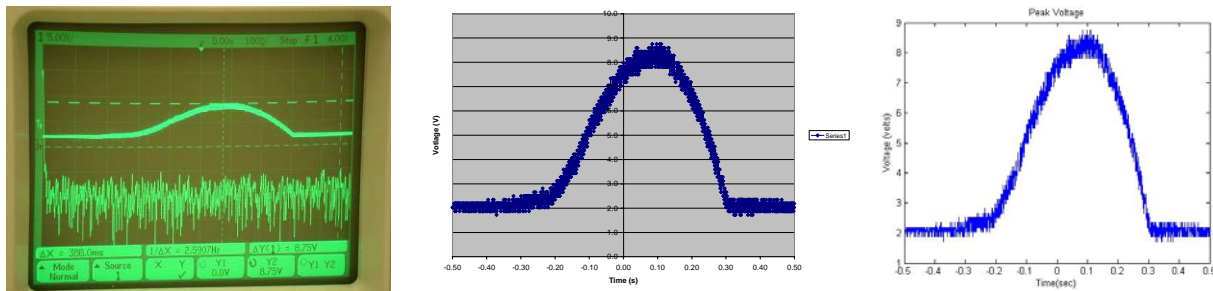


Figure 61: Porting a Voltage Curve from Scope to Excel to MATLAB.

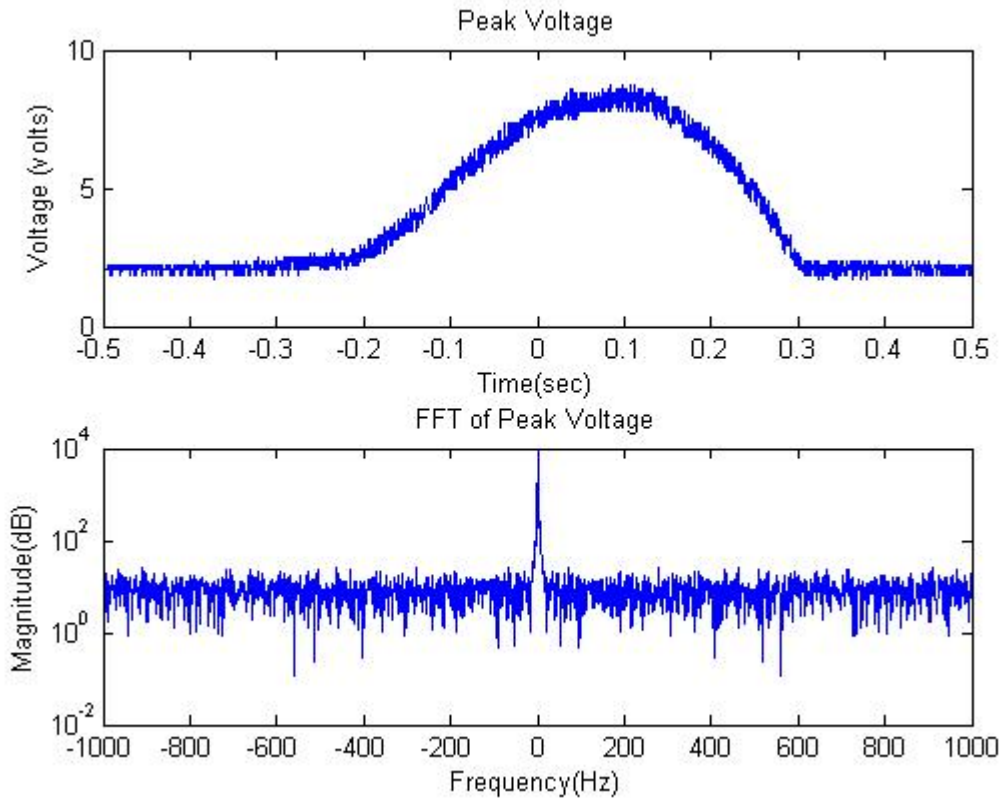


Figure 62: MATLAB 1 mph Voltage Curve FFT Analysis.

The other method used to perform an FFT analysis on the voltage curve data is to directly connect an FFT Analyzer, made by HP called a Dynamic Signal Analyzer, to the tag. This piece of equipment is loaned to us from US&S, and the analysis performed together with Mr. Joe Schaad. This machine can perform a *waterfall save* in which several FFTs can be run and saved in 100 ms intervals as the tag moves through the electromagnetic field. Figure 63 shows two photos of the analysis. It is much clearer in these photos, that some other frequency components do exist and that filtering can be useful. The components identified from this testing are frequencies at 2.1 kHz and 4.2 kHz, and their harmonics.

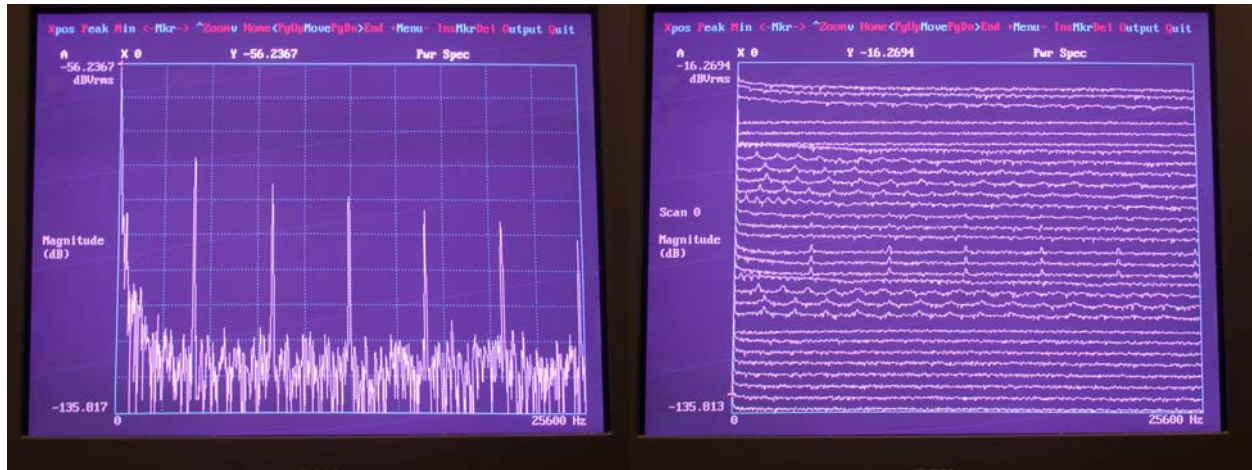


Figure 63: FFT Analyzer Images of the Voltage Curve.

An IIR (infinite impulse response) digital filter is then designed to filter out frequencies above 1 kHz. A Butterworth filter is used because of its simplicity. During testing the order of the filter is kept as low as possible to reduce delay. The higher the order the more data points are required to do the filtering. With more points comes the delay time needed to obtain them and the more complex the calculation, which is additional delay. Only a basic analysis was performed, but it seems likely that a 1 order filter is possible keeping complexity to a minimum. In this simulation an order 2 filter is created, which smoothed out the voltage curve very nicely. Figure 64 shows the comparison between filtered and unfiltered data. This basic analysis and simulation also allows the filtered signal peak algorithm detection to be compared with NVar noise handling.

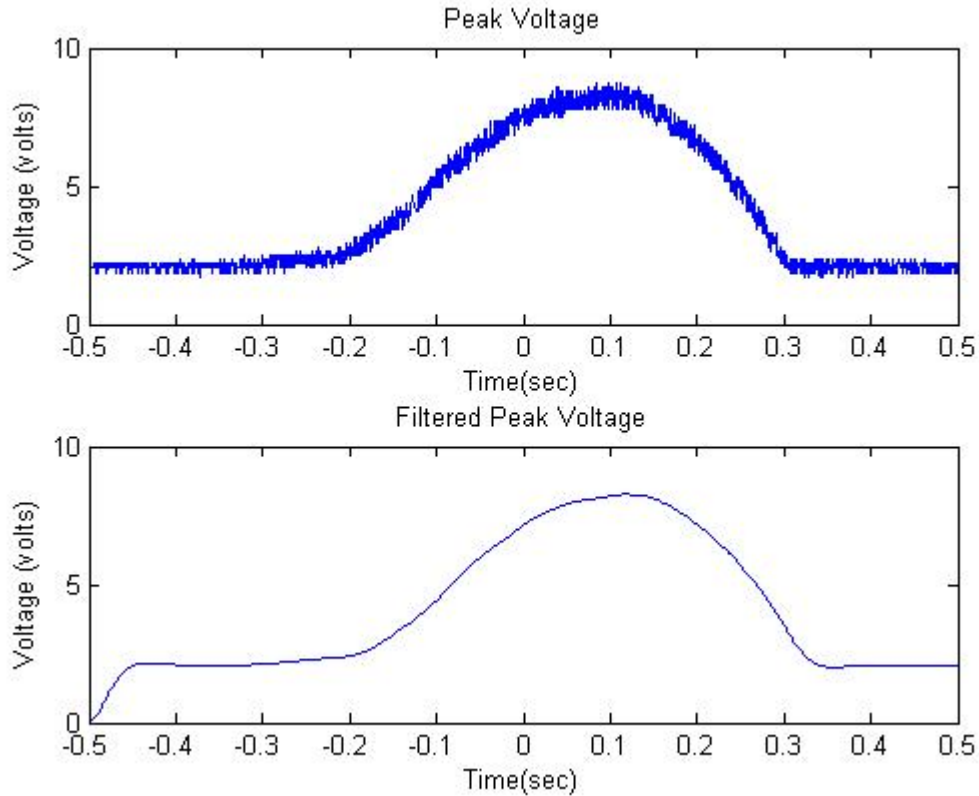


Figure 64: MATLAB 1 mph Voltage Curve Butterworth Order 2 Filter.

5.3.5 Algorithm Simulation

Having the peak voltage curve data in MATLAB, a script is written to allow simulation of the peak algorithm. The noise variable value required in the algorithm can be quickly found using this method of testing, and trial and error time is reduced. The filtered data can also be tested, verifying that it eliminates the need for the noise variable. This will allow the filtered data to be compared to the unfiltered data. The following code segment (Figure 65) is the MATLAB equivalent of the peak algorithm. The main difference from the original is that a *for* loop is used with the imported data because it is finite. This particular code segment is modified to use filtered data. The first two lines can be commented out to use it on unfiltered data.

```

[B,A]=butter(2,10/1000); % determine coefficients

filt_volt=filter(B,A,volt);

high = 0;
sampleNoise = 0;
done = 0;
threshold = 3.5; % algorithm start voltage

for i=1:size(filt_volt,1)

    x(i) = i;

    if( filt_volt(i) > threshold ) %00

        if( done == 0 ) %0

            if( filt_volt(i) > high ) %1
                high = filt_volt(i);
                highIndex = i;
                %save index??
                sampleNoise = 0;
            else
                if( filt_volt(i) <= high ) %2

                    if( sampleNoise == 0 ) %3
                        fprintf('high voltage = %f\n', high);
                        fprintf('send voltage = %f\n\n', filt_volt(i));

                        sampleNoise = 0;
                        transIndex = i;
                        done = 1;
                    else
                        sampleNoise = sampleNoise + 1;
                    end %if3
                else
                    fprintf('error\n');
                end %if2
            end %if1
        end %if0
    end %if00
end %for loop

```

Figure 65: MATLAB Script Segment For Algorithm Simulation.

5.3.6 Algorithm Design Results

5.3.6.1 Peak Algorithm Results

Tag B successfully transmitted the peak using RF power, RF transmission, and the peak determining algorithm developed. It is able to do this 100 % of the time using an NVar of 130 and a power of approximately 3.6 watts. The distance between tag and reader antenna is 10 inches, and had a maximum of ± 1 inch tolerance. The RF communication distance between the tag and the LINX receiver is 2 feet, and is a strong signal. The load capacitor used is 1.2 uF, and the ADC voltage divider reduced the maximum voltage by 20 % using a 2 M ohm value for R1 and a 499 k ohm value for R2. This change is required because the peak voltage is found to exceed 10 volts. Figure 66 shows the oscilloscope capture of the transmission. It is clear that the curve is entering the peak when the transmission occurs. The power decreases because of it, and then the system begins to charge back up before leaving the electromagnetic field.

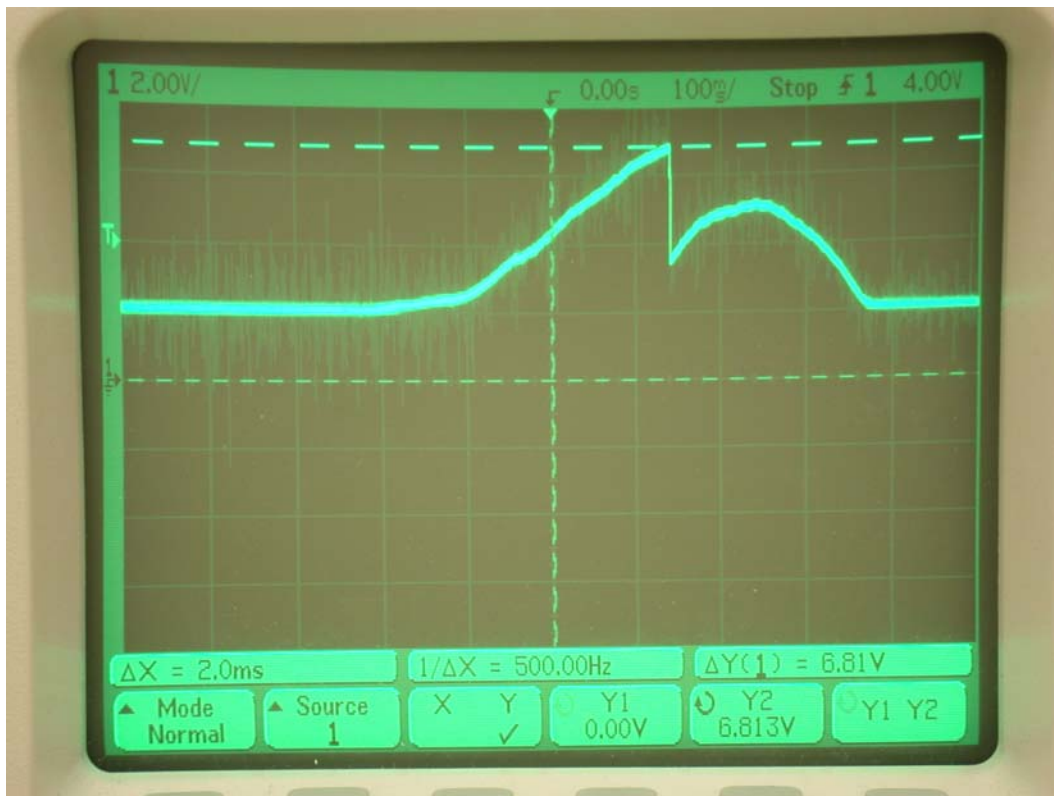


Figure 66: Oscilloscope Capture of a Peak Transmission.

During testing, the tag is made operational, but stopped working at one point. It is determined that the voltage had exceeded the maximum operating levels of some of the components. The voltage regulator, in particular, failed during a test where the voltage went to 13 volts. It subsequently destroyed the PIC, and functionality ceased. A new regulator was found, the Micrel mic5207 that can work to a maximum of 16 volts, but is not used in this prototype. The LINX transmitter is directly attached to the voltage doubler output, and it too has a limitation. A second regulator is probably required in the next prototype. In order to continue testing, the power is decreased on the signal generator to lower the peak voltage level. A setting of 1 dBm provides about 4 watts of power, and a setting of 0 dBm provides about 3.3 watts of power. In the final rounds of testing, the power setting used is between 0 and 0.5 dBm. This is a positive statement that implies all future results can be improved by simply adding a second regulator.

The peak algorithm works well with one main issue to be resolve. The initial algorithm start threshold chosen is too low. While the voltage plateau had been identified, which occurs at about 2.25 volts, the noise in the signal is higher. At times, the noise at the start of the peak is much greater than anticipated. Increasing the threshold to 3.5 volts solved this problem, and allowed for a reduced NVar. The NVar that guaranteed successful transmission is 130 and this is greater delay than was expected. This value is equivalent to about 18 ms, which is significant to speed.

The next issue is evaluating performance at greater speeds, and special considerations include NVar issues, transmission distance issues, and precision tolerance issues.

5.3.6.2 Signal Analysis Results

The signal analysis showed that there are frequency components of 2.1 kHz and 4.2 kHz and their harmonics, which can be eliminated. The question is with what delay. The number of actual code lines to perform the filtering in the PIC is not known, so while delay will increase, it cannot currently be calculated. The delay, or phase shift, due to the filter can be obtained. Figure 67 shows the filtered signal plotted against the original noisy data. The delay is determined to be 25 ms. This is fairly significant, and would limit this particular tag's speed to about 25 mph. As mentioned, a larger tag antenna can be created, and using a larger antenna would minimize the impact of this delay. Again, this is an optimization to consider in Phase II.

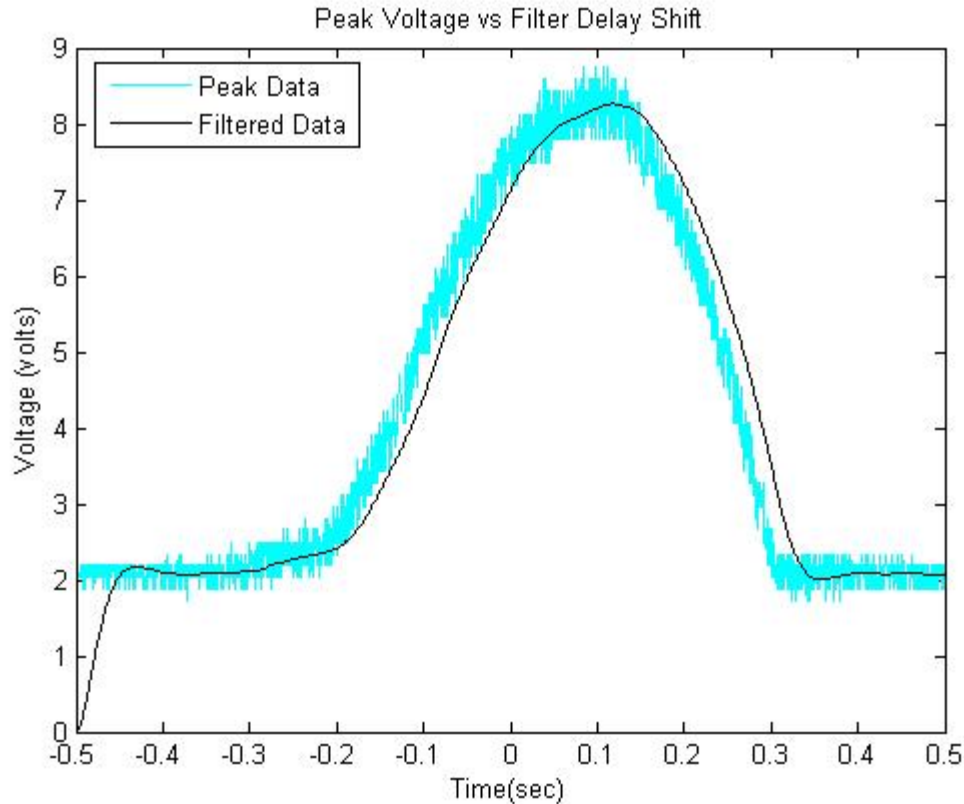


Figure 67: MATLAB 1 mph Voltage Curve Filter Delay Comparison.

5.3.6.3 Algorithm Simulation Results

Using the 1 mph data collected, the peak algorithm is simulated. The result is a secondary verification that it does indeed find the peak. Tests are performed with an NVar ranging from 5 to 130. The tests using 35, 45, and 95 show a clear picture of NVar performance. Figures 68, 69, and 70 show that progression respectively. Two asterisks are shown on each of these curves. The first identifies the value that the algorithm determines is the peak, and the second identifies the point at which the transmission occurs. The distance between them is the delay of the algorithm. Again, this is desired to be as small as possible. It is clear that NVar 45 is the value that first finds the peak, even though it is “early” in the peak. This is because the peak at 1 mph is more gradual, i.e. not as sharp. This is simply the tolerance of the system. At 1 mph and a 500 us sample rate, the delay is 22.5 ms. The tolerance is calculated to be ± 0.4 inches; a very precise identification. Only one case is simulated, so this is not representative of

all possibilities. Compared to the physical test results and an NVar 130, the simulation seems a bit ideal. The results indicate that NVar falls within this range, and improvement is possible. Also, research must be done to determine what kind of error tolerance can be handled. That is, the NVar in physical testing went to 130 in order to always transmit the peak. If the noise happens to spike high 1 % of the time, and NVar can be reduced to 45 if that 1 % is not critical, then the system would be improved. Because control is vital on transit systems this may not be possible, but could be an option depending on the number of tags used to slow a train. The possibility of skipping one reading is a subject for future consideration.

With respect to the design, it is believed that circuit design can be optimized for noise reduction thus improving delay and tolerance. One known negative factor is that the antenna metal trace was cut in one place to test it on the LCR meter. A zero ohm, shorting resistor element is used to reconnect the trace lines. It is believed that this is possibly increasing the noise in the circuit. Two identical circuits are used to perform peak testing, with the exception of the cut trace, and the first tag built had an NVar of 75. It died later due to the high power that was used initially, but supports the redesign statement. It also suggests tag improvement and noise reduction are possible using higher power.

Figure 71, on the other hand, shows the peak algorithm simulation results using the filtered data. In this figure the second asterisks is over top of the first asterisk because the algorithm did not require an NVar. That is to say, the noise is eliminated from the curve, so the first voltage sample lower than the saved high is the real peak. Again, the delay determined for filtering is 25 ms, which does not include the PIC instruction processing delay. It is similar to the delay result of the NVar solution and is very precise as well. Depending on the direction chosen in regards to antenna design, power, and certain other factors, this appears to be a viable method to use.

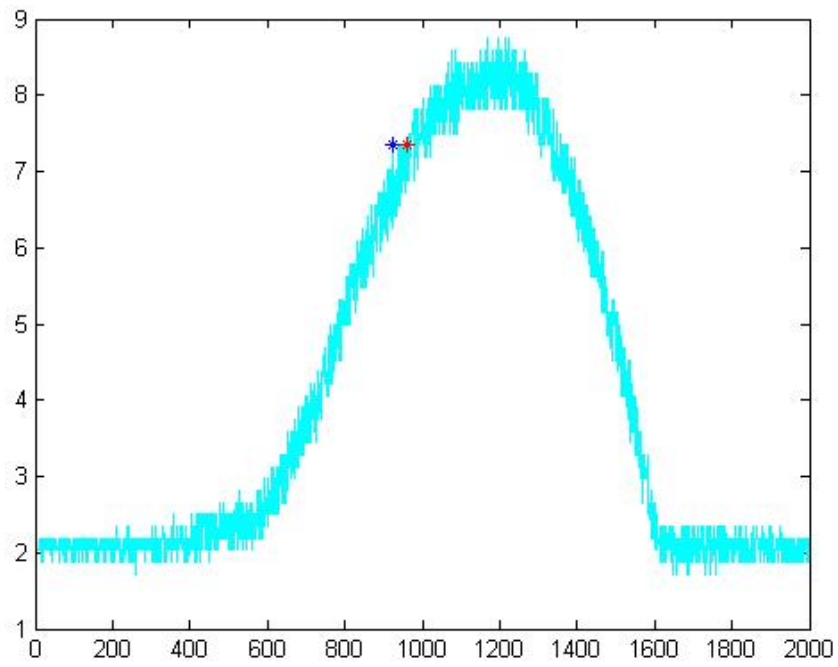


Figure 68: Noisy Voltage Curve Peak Algorithm Simulation, NVar 35.

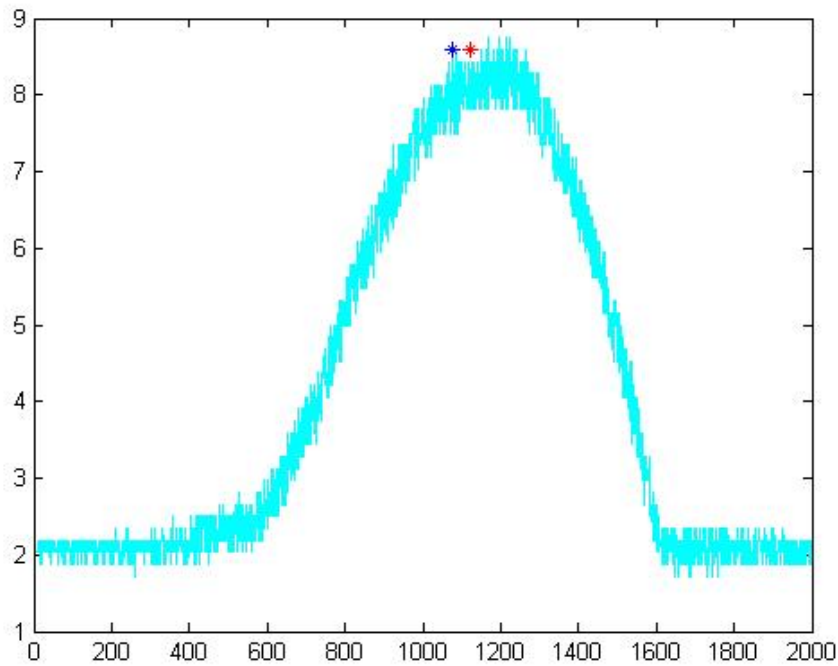


Figure 69: MATLAB Noisy Voltage Curve Peak Algorithm Simulation, NVar 45.

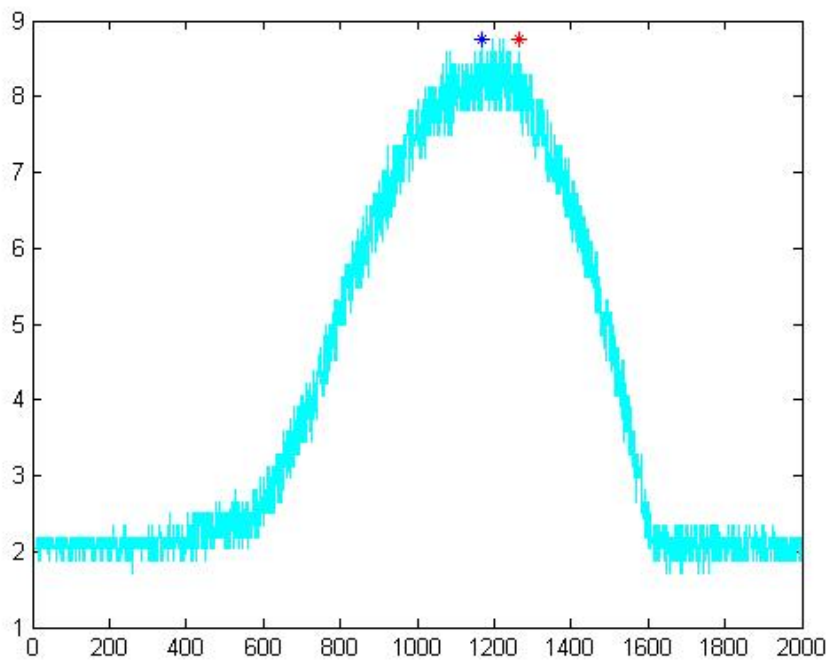


Figure 70: MATLAB Noisy Voltage Curve Peak Algorithm Simulation, NVar 95.

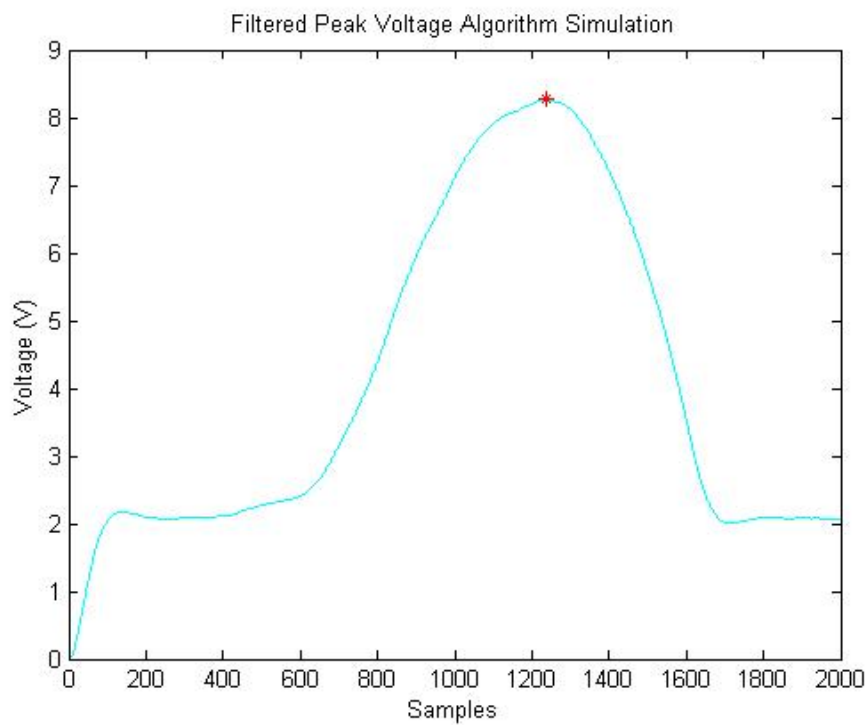


Figure 71: MATLAB 1 mph Voltage Curve, Filtered Data, Peak Algorithm Simulation.

6.0 STAGE 5: SPEED INCREASE

In order to test the tag at higher speeds, a separate system is designed that can move a tag through the reader field in a stable and consistent manner. It is designed to allow speed adjustment from 1 to 80 mph, and it accommodates the need to adjust the tag and reader antenna distances from between 6 and 24 inches. It is referred to as the HSPO System, the high speed pass over system. The task of designing and building the HSPO system is developed into an undergraduate project for Mr. Vu Nguyen. While advising on the systems requirements and specifications, this system is developed in parallel with the tag. With the HSPO completed, speed testing commenced.

6.1 HIGH SPEED PASS OVER SYSTEM

Conceptually, the system is envisioned using a cable to hold the tag, CO₂ to propel the tag, and IR sensors to measure the speed. This system does not have enough stability, however, and methods using a track are explored. When the HSPO system was developed into the undergraduate project, Mr. Nguyen improved the cable design by using a two wire system that is powered by a paintball gun. Paintball guns use CO₂ to propel the paintballs and have 10 inch barrels. Both of these aspects fit conveniently into its development, because a method to push the tag, not hit the tag, is desired. Figure 72 shows the whole system.



Figure 72: The HSPO System Design.

The section jutting out is a reader antenna holder and allows for adjustable distance. The whole design revolves around how the antenna is positioned here. Two wires stretch the length of the structure. They are fixed at the gun end and ratchet tightly at the far end. These wires are precisely leveled so that the tag passes across the center of the reader antenna. The gun is also precisely placed, because the gun barrel will stick through in the middle of the wires where it is used to push the tag. The open box like structure is designed to hold the sensors that measure the speed. These sensors need to be placed outside of the electromagnetic field to prevent interference, but as close as possible in order to determine the speed accurately. The structure is raised because stiffeners had to be added to the bottom to prevent the frame from bowing. When the wires are ratcheted tight, without stiffeners the ends actually lift off the ground.

The system is RF friendly in that it contains very little metal. The design is wood, plastic, and Kevlar wire. Even the method of building the structure is important, and dowels are used to glue the boards together (Figure 73).

A plastic tag base is developed to carry the tag through the electromagnetic field. It is made of an epoxy resin (plastic) to be strong but light. As it happens, the tag holder design is too heavy and had to go through several iterations to lighten it. It is first perforated, and then shaved down. Finally, the ends are cut away and used by themselves. The two ends are cut off and

holes drilled into them so that the tag can be mounted to it and act as the main support. This reduces the weight significantly. The system is not powerful enough yet to meet the goal of 80 mph, but can reach speeds of 25 mph, which is sufficient for Phase I testing. The tag is pushed by a “plug” that is inserted down the barrel and is forced out from the CO₂ pressure, which is stated to be between 750 and 800 psi. The plug is prevented from ejecting by a plastic barrier added for safety.

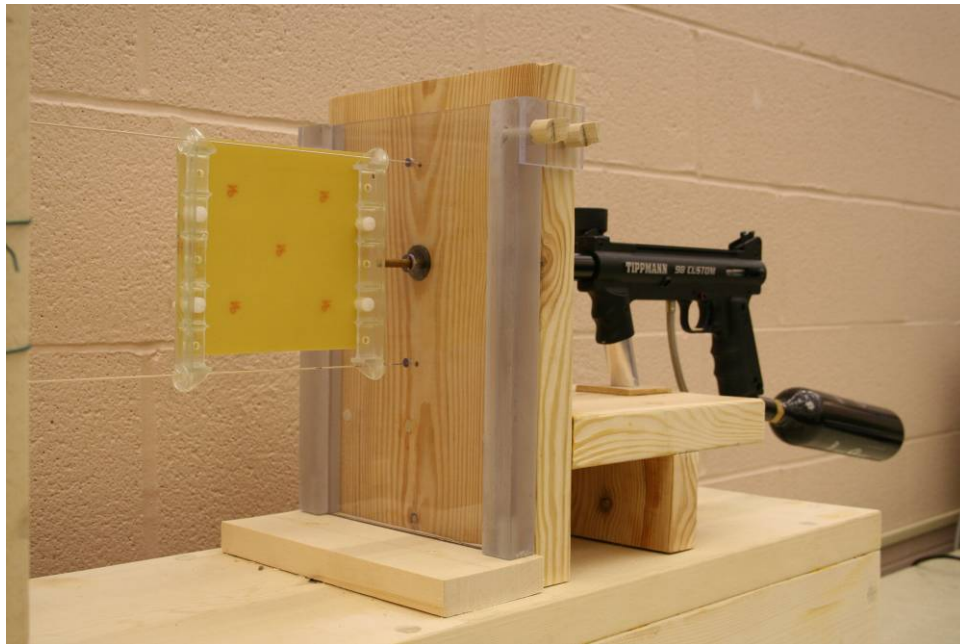


Figure 73: The Tag Base Assembly with PCB Structure.

The IR sensors proved unsatisfactory and were only able to measure speeds under 15 mph. The sensors would simply not trip due to the speed of the tag. A radar gun, and laser sensors are both tried as improvements. The laser sensors work well, and have accurately measured speeds up to 27 mph thus far.

Options to improve the system speed include a nitrogen powering solution, thoughts on adding an incline, and a 22 caliber bullet nail gun solution. Replacing CO₂ with nitrogen is expected to provide more power, better regulation, and more consistent performance. Inclining the system by putting the gun end in the air should reduce friction between the tag and the wires improving speed. And, if those solutions do not work, a different gun with more thrust could be used to propel the plug. Mr. Nguyen’s final report contains the design detail.

6.2 TAG DESIGN CONSIDERATIONS

The tag design is not altered from previous testing except to drill holes for mounting it to the HSPO system. This section discusses the power and energy constraints of the final prototype design.

As noted, the design uses a 1.2 pF load capacitor to store charge. Some calculations on power, energy, and the load capacitance are done to gain insight into the circuit's ability. Two approaches are taken. One, based on the oscilloscope values observed and the capacitance used, and two, estimating the current consumed. Using the formula $W = \frac{1}{2} C V^2$, with a capacitance of 1.2 uF, and a voltage of 10 volts (oscilloscope high voltage), the energy available is 60 uJ. Using a transmission time of 1.83 ms, also measured from the oscilloscope, the power ($W = P \cdot t$) to transmit nine high bits is estimated to be 32.8 mW.

For comparison, the formula $P = I \cdot V$ is used, and the current is estimated. The LINX transmitter uses 3 mA typically, the PIC uses approximately 200 uA, and the regulator uses about 200 uA, because it is based on the load of the PIC. Estimating the current to be 3.5 mA, and using the same voltage as before, 10 volts, the power ($P = I \cdot V$) usage is 35 mW. Again using a transmission time of 1.83 ms, the available energy is 64.05 uJ. These are fairly similar results, and seem to be accurate. The capacitance, using the formula $C = (2 W) / V^2$, is then calculated to be 1.281 uF, a value that fits the profile. Recall that the required LED power is estimated to be 34 mW, which also supports the calculations, and happens to be a very good choice for representing the load.

Finally, charge time can be estimated using the formula $\tau = RC$, which is the time constant. We know C to be 1.2 uF, but resistance of the circuit is estimated through antenna measurements. Because a resonant tag is balanced and the antenna is the conjugate of the circuitry, the resistance of the circuitry should be equal to the resistance of the antenna. The antenna is measured on the LCR meter and found to be about 14 k ohm. Using these values, the product is 16.8 ms. This seems rather large, but is consistent with the other results. With this delay, the maximum speed obtainable with the current solution is about 27 mph. This is also consistent with previous calculations.

Based on capacitance alone, to reach speeds of 80 mph the load capacitor cannot exceed 0.4 uF. This reduces the charge up delay and allows the tag sufficient time to transmit. It is clear that to reach higher speeds, the tag must be optimized, and/or redesigned. Again, some of the positive points are that there is ample room to increase the antenna size and to increase the power supplied to it.

At 80 mph, a tag can traverse the 16 inch reader antenna field in 11.4 ms. The transmission time available is only half that, about 5.6 ms, because the transmission must occur before the edge of the antenna, 8 inches from the center. For the 10 bits to be successfully sent in this time frame, the BAUD rate must be at least 1785. The current BAUD rate is 4800, which is a limitation of the LINX transmitter, but this is more than sufficient. Theoretically, at this rate, 26 bits can be sent at 80 mph.

6.3 SPEED TESTING

Figure 74 below shows the setup used to perform higher speed tests. The HSPO system is equipped with the sensors to calculate speed using an oscilloscope, the reader antenna to create the electromagnetic field, and a near field probe (top) to capture the transmissions using a secondary Tektronix spectrum analyzer. In the front, slightly right, the LINX receiving unit and antenna are positioned to be about 18 inches away. Once everything is powered, the paintball gun propels the tag through the field.

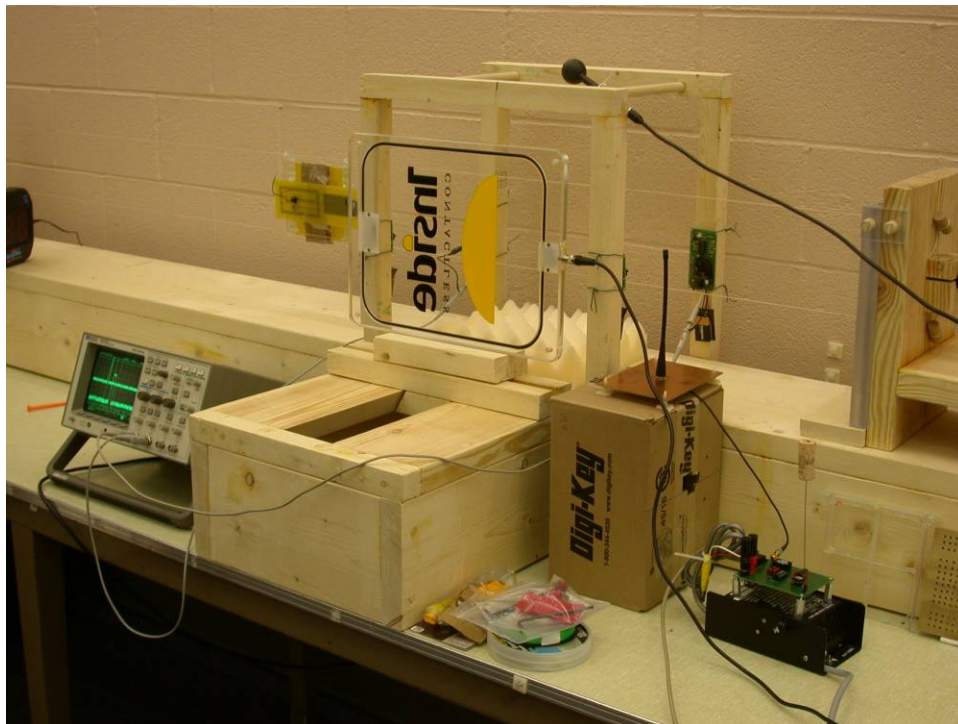


Figure 74: High Speed Test Setup.

6.4 SPEED RESULTS

As an example, Figure 75 shows an oscilloscope capture of the IR sensors being tripped by the tag as it travels passed them. The time delay between them is 194 ms. Using the formula

$$(\text{scope delay} * 5280 \text{ feet} * 12 \text{ inches}) / (3600 \text{ seconds}),$$

the speed is calculated to be 3.4 mph in this example.

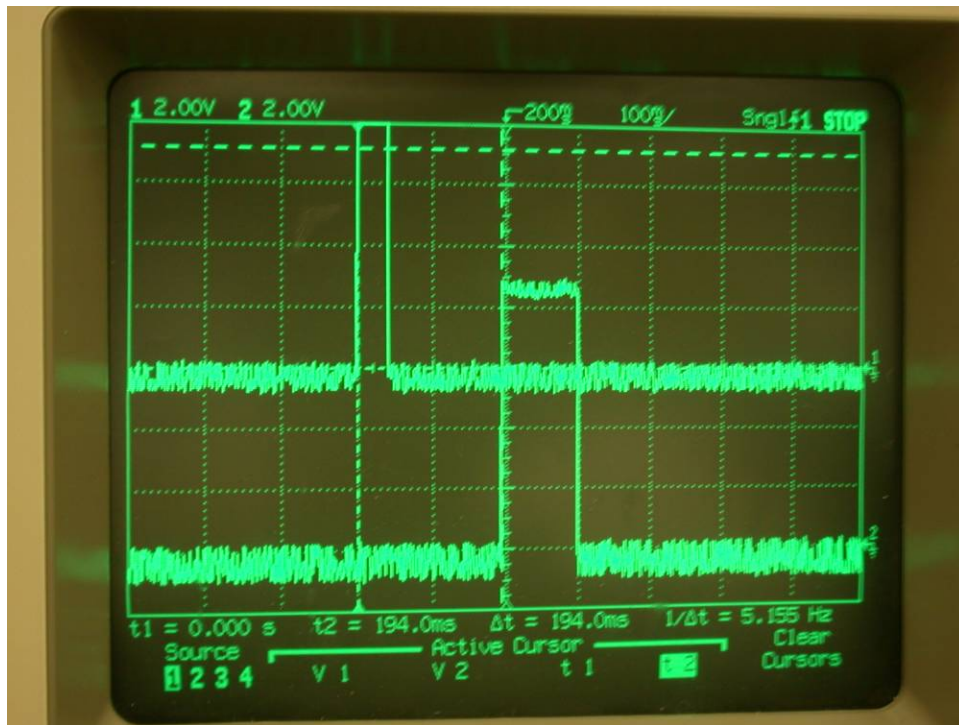


Figure 75: Oscilloscope Capture of Tripped IR Sensors.

Another example of the transmission is shown in Figure 76. In the upper left hand corner, the actual character bits are captured. The bit pattern is 1011000010. The first and last bits are the start and stop bits so these are removed leaving 01100001. In RS232, the bits are sent inverted and reversed, and so we see 1001 1110 and 0111 1001 respectively. Converting this into decimal, hex, and a char we see 121, 79, and 'y' respectively. This is the same character that is observed in the HyperTerminal GUI verifying earlier results. This translates to 5.6 volts using

the calculation described earlier and is accurate because the power is temporarily low. The voltage curves observed during high speed testing are all slightly lower than those of the 1 mph tests. This is probably due to the size of the load capacitor, and falls under the statements made about optimizing.

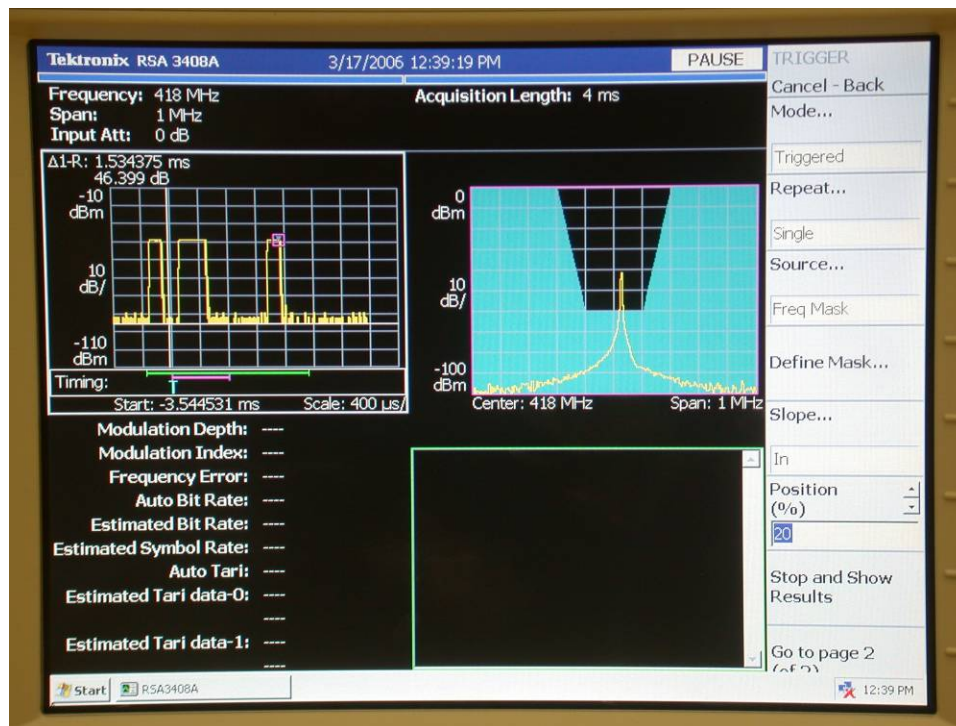


Figure 76: RF Transmission Captured by Tektronix Spectrum Analyzer.

To ensure 100 % accuracy in RF transmission, the NVar is set to the previous result of 130. With the power output at 0 dBm, 3.3 watts, the tag's obtainable high speed is about 10 mph. Note, an NVar of 130 at a sampling rate of 138 us equates to a time of about 18 ms. Because transmission is more likely to be successful while being energized in the reader field, there is a limited amount of time available. The tag will be in the reader field for 18 ms if the speed is limited to about 25 mph. If transmission occurs beyond 18 ms, the tag must rely on the energy stored on the load capacitor, which might not be sufficient. Finally, lower power means lower induced current and slower charging time. With the regulators replaced, the power increased, and tag design noise reduction techniques employed, the tag should be able to reach 20 to 25 mph. Higher speeds call for some redesign adjustments, such as a larger antenna.

7.0 CONCLUSION

The task to develop a proof of concept design for precise single dimension position determination using RFID technology has been accomplished. The system works. All the components have been verified. And achieving the long term goals appears feasible.

The theoretical bell shaped voltage curve is shown to exist. An antenna is designed that allowed a circuit to be passively powered at a distance of 10 inches. A method is created for determining the peak of the voltage curve, and it is shown to translate into a precisely defined position, with a tolerance of ± 0.4 inch at slower speeds. Finally, a system to test the device at higher speeds is developed and used to verify operation at speeds between 1 mph and 10 mph.

The prototype has been shown to be viable. Indications point to achieving 25 mph operation, through only a minimal optimization of the existing tag. Factors that support this statement include: a temporarily reduced power supply due to voltage regulation issues, a high load capacitance due to the heavy demands from the off the shelf transmitter, and an increased noise level due to rapid prototyping design. The greatest factor is the load capacitance. The 1.2 pF value, used in the time constant formula $\tau = RC$ with the measured 14 k Ohm resistance, give a ramp up delay of 16.8 ms. For transmission to occur while being energized by the reader field, the speed cannot exceed 27 mph. With these factors corrected, higher speeds are likely.

Several enhancements further support the feasibility of the product including: larger antenna design that would couple more efficiently with the reader antenna and harvest more energy, tuning research ensuring maximum power transfer through resonance, the ability to utilize techniques based on pulsed power increase, but not average power (EIRP) increase, and finally, developing filtering designs to handle noise in a different manner.

The four main considerations for improvement are power, antenna design, transmitter design, and noise handling. The results of the current research suggest that the 18 inch, 80 mph position determination appears to be reasonable.

7.1 PHASE II OPTIMIZATIONS

In no particular order, this section lists aspects of the tag device that should be considered when designing prototype 2. These considerations are in addition to the optimizations mentioned in the paper.

An external oscillator might be desirable, because internal RC type oscillators are not recommended for time critical applications. The opposing fact is that more complexity is created, a higher drive current is required, and it will cost more.

Spiral antenna resistance should be kept low to facilitate current flow. It is believed that one of the reasons the 4x2 inch antenna works well is that its resistance is measured to be about 30 ohms. The spiral inductance should also be examined, because inductance is directly linked to induced current. A higher inductance typically means better resonance.

Tag transmitter power should be reduced. Reduction means less voltage required, a lower value capacitor needed, less delay, more distance, and higher speeds. A custom loop antenna design was considered, but initial designs were too involved for Phase I and it was not continued. If this transmitter can be developed, a big step forward would be achieved for power consumption, and it could potentially be moved inside the spiral antenna to reduce the overall passive device size.

The voltage doubler should be reconsidered, and the number of stages explored. Some delay exists because of the capacitors internal to the voltage doubler. Choosing differently sized elements could positively affect charge up time and lead to a speed increase.

Finally, an impedance matching technique should be applied to the design's bandwidth versus maximum power transfer issue. The system needs to be tolerant of metal, and must not become easily detuned. This aspect also relates to flexibility in read distance. Because a train's wheel diameter can change by as much as 2 inches, the design must be able to operate at a ± 1 inch read range, which the current tag can likely handle.

7.2 PHASE II CONSIDERATIONS

All of the optimizations mentioned are important to Phase II. However, creating and using a larger antenna has been proven to increase range and voltage. The 4x2 inch antenna doubled the distance and voltage over the 1x1 inch antenna. To meet the goals of an 18 inch read range at 80 mph speeds, a larger antenna design should be a primary focus. Along with generating a stronger field, this will certainly allow for increased speeds. The larger design should allow for more flexibility in designing for distance, and translate into a wider read range operation.

A dynamic noise variable can be considered as well. Because the tag will have an ID that is linked to a specified distance from a station platform, this ID can be used to dynamically adjust the NVar value for the speed at that distance. This is beneficial because at higher speeds the voltage change is more rapid and requires less noise variable delay. If the delay can be reduced, higher speeds are achievable.

7.3 FUTURE CONSIDERATIONS

A multiple tag device system, say three, should be explored where the antenna size of the tag is changed relative to speed. This system should be considered because of the precision desired. At slower speeds for instance, a smaller antenna will provide a sharp voltage curve where a larger antenna will have a plateau shape, essentially a clipped voltage, or even a malformed shape with a dip in the middle. Conversely, at higher speeds, the smaller antenna will not have a sufficient voltage curve to sustain an RF transmission, while the larger antenna would. If two or three tag designs are developed, then they can be placed decreasing in size at corresponding speed locations.

Another idea is to turn the system into a semi-active tag system, and combine it with the University of Pittsburgh's battery saving methods. In this way, the matter of storing enough energy is removed, the load capacitor can be decreased, and the speed of the system drastically increased. A semi-active tag uses a battery to aid RF transmission, but not to power the tag. Using the battery saving methods, the tag could last up to 100 years, depending upon usage.

APPENDIX A

SOURCE CODE

```
// Program: PeakDetectionAlgorithm.c
// Author:  Tim Carey
// Date:    3/23/2006

// Chip:    PIC "OP" (back)

// Program: read voltage doubler voltage to find peak voltage
//           If voltage higher than 2.5 volts then start peak algorithm
//           Read voltage doubler voltage to find peak voltage
//           Perform ADC and compare with highest voltage
//           If higher peak still rising, save as highest volt
//           If lower, could be a noise sag or the peak
//           If tenth lower voltage, Tx peak voltage (high)
//           If not increment sample counter
//           Repeat

// voltage scale: 7 V peak *(499k/(2M+499k)) = 1.40 V ADCpeak
//                (2.45ref/256resolution)= 0.00957 Vstep
//                1.4 V/0.00957 Vstep = 146 DEC
//                2.5 Vplateau => 0.5 V ADCplateau
//                0.5 V/0.00957 Vstep = 52 DEC

#include <12F683.h>
#define adc=8
#define fuses NOWDT,INTRC_IO, NOCPD, NOPROTECT, NOMCLR, NOPUT, BROWNOUT, IESO, FCMEN
#define use delay(clock=4000000)
#define use rs232(baud=4800,parity=N,xmit=PIN_A4,rcv=PIN_A1,bits=8,invert)
// invert required!

int voltage = 0; // variable to store new voltage sample
int high = 0; // variable to store current high value
int sampleNoise = 0; // variable to prevent false peak identification

char voltTx; // variable to transmit voltage
```

```

void main()
{
    setup_adc_ports(sAN0|VSS_VDD); // PIC initialization
    setup_adc(ADC_CLOCK_DIV_8);
    setup_timer_0(RTCC_INTERNAL|RTCC_DIV_1);
    setup_timer_1(T1_DISABLED);
    setup_timer_2(T2_DISABLED,0,1);
    setup_comparator(NC_NC_NC_NC);
    setup_vref(FALSE);

    output_low(PIN_A2); // ensure output is low
    output_low(PIN_A4);

while(TRUE) //0 loop until time to start
    {
        voltage = read_adc(); // get sample
        delay_us(50);

        if(voltage > 73) //0 start peak algorithm past 3.5V threshold
            {
                while(TRUE) //1 loop until peak identified
                    {
                        voltage = read_adc(); // get sample
                        delay_us(50);

                        if( voltage > high ) //1 compare sample to high value
                            {
                                high = voltage; // if higher, save new high
                                sampleNoise = 0; // reset noise variable
                            } // end if1
                        else //1
                            {
                                if( voltage <= high ) //2, peak decreasing or noise
                                    {
                                        if( sampleNoise == 129 ) //3
                                            { // 130th time voltage is still decreasing = peak

                                                voltTx = (char)high; // conversion for transmission
                                                putc(voltTx); // transmit peak

                                                while(TRUE) // end - loop until out of field
                                                    {
                                                        delay_ms(100);
                                                    }
                                            } //end if3
                                        else //3, possible noise sag; increment
                                            {
                                                sampleNoise = sampleNoise + 1;
                                            } //end else3
                                    } //end if2
                            }
            }
    }

```

```
        else //2, error
        {
            putc('X'); // error

        } //end else2
    } // end else1
} //end while1
} //end if0

delay_us(150); // approximate inner cycle

} //end while0
} // end main
```

APPENDIX B

B.1 STANDARD ASCII TABLE

ASCII	Hex	Symbol	ASCII	Hex	Symbol	ASCII	Hex	Symbol	ASCII	Hex	Symbol
0	0	NUL	32	20	space	64	40	@	96	60	`
1	1	SOH	33	21	!	65	41	A	97	61	a
2	2	STX	34	22	"	66	42	B	98	62	b
3	3	ETX	35	23	#	67	43	C	99	63	c
4	4	EOT	36	24	\$	68	44	D	100	64	d
5	5	ENQ	37	25	%	69	45	E	101	65	e
6	6	ACK	38	26	&	70	46	F	102	66	f
7	7	BEL	39	27	'	71	47	G	103	67	g
8	8	BS	40	28	(72	48	H	104	68	h
9	9	TAB	41	29)	73	49	I	105	69	i
10	A	LF	42	2A	*	74	4A	J	106	6A	j
11	B	VT	43	2B	+	75	4B	K	107	6B	k
12	C	FF	44	2C	,	76	4C	L	108	6C	l
13	D	CR	45	2D	-	77	4D	M	109	6D	m
14	E	SO	46	2E	.	78	4E	N	110	6E	n
15	F	SI	47	2F	/	79	4F	O	111	6F	o
16	10	DLE	48	30	0	80	50	P	112	70	p
17	11	DC1	49	31	1	81	51	Q	113	71	q
18	12	DC2	50	32	2	82	52	R	114	72	r
19	13	DC3	51	33	3	83	53	S	115	73	s
20	14	DC4	52	34	4	84	54	T	116	74	t
21	15	NAK	53	35	5	85	55	U	117	75	u
22	16	SYN	54	36	6	86	56	V	118	76	v
23	17	ETB	55	37	7	87	57	W	119	77	w
24	18	CAN	56	38	8	88	58	X	120	78	x
25	19	EM	57	39	9	89	59	Y	121	79	y
26	1A	SUB	58	3A	:	90	5A	Z	122	7A	z
27	1B	ESC	59	3B	;	91	5B	[123	7B	{
28	1C	FS	60	3C	<	92	5C	\	124	7C	
29	1D	GS	61	3D	=	93	5D]	125	7D	}
30	1E	RS	62	3E	>	94	5E	^	126	7E	~
31	1F	US	63	3F	?	95	5F	_	127	7F	~

B.2 EXTENDED ASCII TABLE

ASCII	Hex	Symbol	ASCII	Hex	Symbol	ASCII	Hex	Symbol	ASCII	Hex	Symbol
128	80	Ç	160	A0	á	192	C0	?	224	E0	α
129	81	ü	161	A1	í	193	C1	?	225	E1	β
130	82	é	162	A2	ó	194	C2	?	226	E2	Γ
131	83	â	163	A3	ú	195	C3	?	227	E3	π
132	84	ä	164	A4	ñ	196	C4	?	228	E4	Σ
133	85	à	165	A5	Ñ	197	C5	?	229	E5	σ
134	86	â	166	A6	a	198	C6	?	230	E6	μ
135	87	ç	167	A7	o	199	C7	?	231	E7	τ
136	88	ê	168	A8	ç	200	C8	?	232	E8	Φ
137	89	ë	169	A9	?	201	C9	?	233	E9	Θ
138	8A	è	170	AA	¬	202	CA	?	234	EA	Ω
139	8B	ï	171	AB	½	203	CB	?	235	EB	δ
140	8C	î	172	AC	¼	204	CC	?	236	EC	?
141	8D	ì	173	AD	ì	205	CD	?	237	ED	φ
142	8E	Ä	174	AE	«	206	CE	?	238	EE	ε
143	8F	Å	175	AF	»	207	CF	?	239	EF	?
144	90	É	176	B0	?	208	D0	?	240	F0	?
145	91	æ	177	B1	?	209	D1	?	241	F1	±
146	92	Æ	178	B2	?	210	D2	?	242	F2	?
147	93	ô	179	B3	?	211	D3	?	243	F3	?
148	94	ö	180	B4	?	212	D4	Ö	244	F4	?
149	95	ò	181	B5	?	213	D5	?	245	F5	?
150	96	û	182	B6	?	214	D6	?	246	F6	÷
151	97	ù	183	B7	?	215	D7	?	247	F7	?
152	98	ÿ	184	B8	?	216	D8	?	248	F8	?
153	99	Û	185	B9	?	217	D9	?	249	F9	?
154	9A	Ü	186	BA	?	218	DA	?	250	FA	·
155	9B	ç	187	BB	?	219	DB	?	251	FB	?
156	9C	£	188	BC	?	220	DC	?	252	FC	?
157	9D	¥	189	BD	?	221	DD	?	253	FD	²
158	9E	?	190	BE	?	222	DE	?	254	FE	?
159	9F	f	191	BF	?	223	DF	?	255	FF	

APPENDIX C

MATLAB FILTERING SCRIPT

```
% Program: FilterPeakSim.m
% Author:  Tim Carey
% Date:    4/18/2006

% *****
%
% This program simulates a voltage curve peak detection
% algorithm. It requires a vector of voltages entered
% into MATLAB prior to running. (such as saved data
% from an oscilloscope) It performs a Butterworth filter
% on the voltage data, and then runs the algorithm.
% The filter is order 2 with a 1 kHz cut off (low pass).
% It then plots the result.
%
% Removing the filter, the algorithm can find the peak
% of a noisy signal by increasing the value that the
% sampleNoise variable is compared to.
% ex. ( sampleNoise == 45 )
%
% *****

%Enter variables first in MATLAB command interface (vectors)
%volt=;    %voltage in volts
%time=;    %time in seconds

[B,A]=butter(2,10/1000); % determine coefficients

filt_volt=filter(B,A,volt);

high = 0;
sampleNoise = 0;
done = 0;
threshold = 3.5; % algorithm start voltage
```

```

for i=1:size(filt_volt,1)

    x(i) = i;

    if( filt_volt(i) > threshold ) %00

        if( done == 0 ) %0

            if( filt_volt(i) > high ) %1
                high = filt_volt(i);
                highIndex = i;
                sampleNoise = 0;

            else

                if( filt_volt(i) <= high ) %2

                    if( sampleNoise == 0 ) %3
                        fprintf('high voltage = %f\n', high);
                        fprintf('send voltage = %f\n\n', filt_volt(i));

                        sampleNoise = 0;
                        transIndex = i;
                        done = 1;
                    else
                        sampleNoise = sampleNoise + 1;
                    end %if3

                else
                    fprintf('error\n');
                end %if2

            end %if1

        end %if0

    end %if00

end %for loop

plot(x,filt_volt,'c-',highIndex,high,'b*',transIndex,high,'r*')

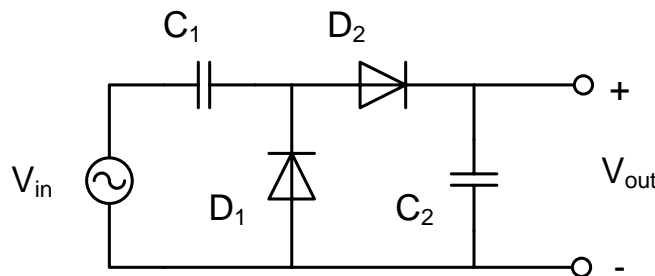
title('Filtered Peak Voltage Algorithm Simulation')
xlabel('Samples')
ylabel('Voltage (V)')

```

APPENDIX D

SINGLE STAGE VOLTAGE DOUBLER OPERATION

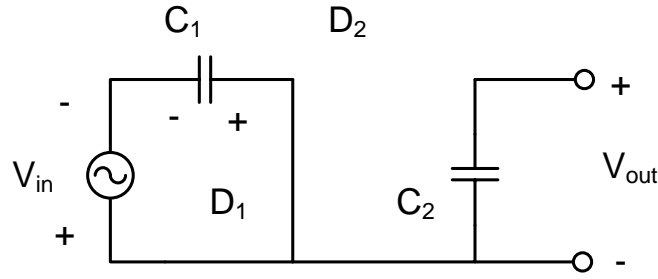
Also referred to as a multiplier circuit or charge pump, operation is based on the cycle of a sine wave. Functionality of the voltage doubler is two fold: it rectifies the AC signal into a DC voltage and it increases the input voltage. The circuit is shown below. It is comprised of diodes and capacitors. The diodes control the current flow and the capacitors store the charge.



Single Stage Voltage Doubler

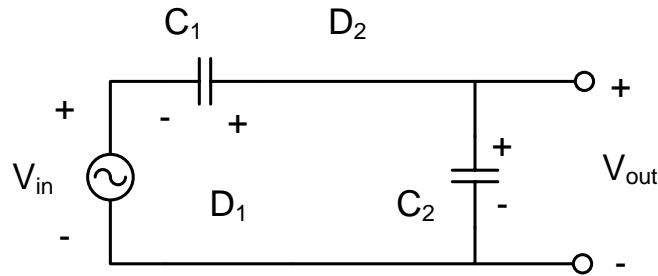
V_{out} voltage is increased at the rate of $2n * V_{in}$, where n is the number of stages. In this case n is one so the output voltage is $2 * 1 * V_{in}$, which demonstrates the doubling. Because it operates on an AC sine wave, the circuit is analyzed by examining two sections, the positive half of the sine wave and the negative half of the sine wave.

During the negative half of the sine wave, C_1 is charging because D_1 is on and allowing current to flow but D_2 is off and acting as an open switch. The circuit below is a representation of this action. At the end of the half cycle, C_1 has fully charged and is ideally equal to V_{in} .



Negative Half Cycle

During the positive half of the sine wave, D_2 is on and allowing current to flow, while D_1 is off and acting as an open switch. The circuit below is representative of this action. In this half of the cycle, C_2 will charge to the voltage of V_{in} as C_1 did. Because C_1 had fully charged the half cycle before, C_2 is also charged by C_1 (equal to V_{in}) and is therefore charged to $2V_{in}$. The circuit has ideally produced double the voltage of V_{in} at the end of the cycle.



Positive Half Cycle

Multiple stages can be connected to further increase the voltage, as was done in the tag designed in this research. This is typically done in energy harvesting circuits where the amount of voltage obtained is insufficient to operate the circuitry components. The doubling discussed is ideal and unrealistic though. The diodes and capacitors both experience leakage current that prevents full charge transfer. The diodes are also non-linear devices that change their operating characteristic depending on the voltage available. On average the voltage increase is about 80% that of the theoretical, but this is an adequate representation.

BIBLIOGRAPHY

- [1] Patrick J. Sweeney II, *RFID for Dummies*. Hoboken: Wiley Publishing, 2005.
- [2] Correspondence with Joe Schaad, Union Switch & Signal.
- [3] Mike Dempsey, RFID Positioning Systems.
<http://www.radianse.com/download/news-bit-2004.pdf>
- [4] Transcore Product Brief:
<http://www.transcore.com/technology/techapps.htm>
- [5] Siemens DIGILOC® Technical Characteristics Document:
http://www.transportation.siemens.com/ts/en/pub/products/ra/products/train_control/digiloc.htm
- [6] Union Switch and Signal Systems Bio:
<http://www.switch.com/railtransit.html>
- [7] Youbok Lee, Microchip Technology, *AN710: Antenna Circuit Design for RFID Applications*, 2003.
- [8] Sedra/Smith, *Microelectronic Circuits*, 4th edition. New York, Oxford University Press, 1998.
- [9] Klaus Finkenzeller, *RFID Handbook: Fundamentals and Applications in Contactless Smart Cards and Identification*. Hoboken: Wiley Publishing, 2003.
- [10] UPM, *Tutorial Overview of Inductively Coupled RFID Systems*. UPM Rafsec, May 2003.
<http://www.rafsec.com/rfidsystems.pdf>
- [11] Steven A. Hackworth, MS Thesis, *Proof of Concept Design for a Remotely Powered Deep Brain Stimulation Device*. University of Pittsburgh, 2004.
- [12] Agilent Technologies, HSMS 2822 Diode Datasheet, 2004.
<http://www.avagotech.com/pc/downloadDocument.do?id=5367>
- [13] Custom Computer Services (CCS), *PIC MCU C Compiler Reference Manual*, 2005.

- [14] Stanley, *BR1111C Series Ultra Compact SMT (Red) LED Product Guide*, 2004.
http://www.stanley-components.com/en/search/search_product.cfm#FFFFFF
- [15] Microchip Technologies, *PIC12F683 Data Sheet: 8-pin Flash Based, 8-bit CMOS Microcontrollers with nanoWatt Technology*, 2004.
- [16] Coilcraft, *Chip Inductors: 0805LS Series (2012) Data Sheet*, 2005.
<http://www.coilcraft.com/pdfs/0805ls.pdf>
- [17] Panasonic, *Multilayer Ceramic Capacitors Data Sheet*, 2006.
<http://industrial.panasonic.com/www-data/pdf/ABJ0000/ABJ0000CE1.pdf>
- [18] LINX Technologies, *LC Series Transmitter Module Data Guide*, 2005.
http://www.linxtechnologies.com/documents/TXM-xxx-LC_Manual.pdf
- [19] Chester Simpson, National Semiconductor, *Linear and Switching Voltage Regulator Fundamentals*. <http://www.national.com/appinfo/power/files/f4.pdf>
- [20] Microchip Technologies, *TC1070/TC1071/TC1187 50mA, 100mA and 150mA Adjustable CMOS LDOs with Shutdown Data Sheet*, 2002.
- [21] LINX Technologies, *Data Guide "Splatch" Planar Antenna*, 2004.
http://www.simplesolutions-uk.com/pdfs/ANT_SP.pdf